Investigating the interplay between DNA replication and meiotic recombination

Lilian Lanteri

ANNÉE 2018

UNIVERSITÉ DE RENNES 1

UNIVERSITE BRETAGNE LOIRE

THÈSE / UNIVERSITÉ DE RENNES 1
sous le sceau de l'Université Bretagne Loire

pour le grade de

DOCTEUR DE L'UNIVERSITÉ DE RENNES 1

Mention : Génétique Génomique Bioinformatique

Ecole doctorale Biologie – Santé

présentée par

Lilian LANTERI

Préparée à l'unité de recherche UMR6290 CNRS-UR1
Institut de Génétique et Développement de Rennes
Composante universitaire Science de la Vie et de l'Environnement

---

Investigating the interplay between DNA replication and meiotic recombination

Thèse soutenue à Rennes
le 19 Janvier 2018

devant le jury composé de :

Dr Daniel FISHER
Directeur de recherche / Institut de Génétique Moléculaire de Montpellier (IGMM) / Rapporteur

Dr Benoit ARCANGIOLI
Directeur de recherche / Institut Pasteur / Rapporteur

Dr Gilles SALBERT
Professeur des Universités / Institut de Génétique et Développement de Rennes (IGDR) / Président du Jury

Dr Pei-Yun Jenny WU
Chargée de recherche / Institut de Génétique et Développement de Rennes (IGDR) / Directeur de thèse

ABSTRACT

DNA replication is a highly conserved and regulated step of the cell cycle. Defects in genome duplication have severe consequences for cell proliferation and have been linked to different pathologies, including cancer. Replication initiates at discrete sites along the chromosomes known as origins. For a population of cells, the program of replication is defined by the distribution and activation of origins across the genome. However, cells within the same population display plasticity in origin usage, and the subset of origins activated during S-phase varies from one cell cycle to the next. While changes in the replication program have been observed during development and differentiation as well as in cancer, the functional importance of these alterations remained unknown. Our laboratory previously demonstrated in the fission yeast that the program of origin selection during pre-meiotic S phase regulates the sites of double-strand break (DSB) formation during meiosis, providing the first evidence for the functional consequences of genome-wide changes in origin usage. Building on this work, my thesis takes two approaches to investigate the crosstalk between genome duplication and meiotic recombination, using the fission yeast *Schizosaccharomyces pombe* as a model system.

First, we explored the impact of chromosomal organization on the program of DNA replication and meiotic recombination. To this end, we engineered chromosomal rearrangements that exchange the positions of replication domains with different efficiency and timing characteristics. Our results demonstrated that this induced local changes in origin efficiency near the endpoints of the rearranged region during both mitotic and pre-meiotic S phase. Interestingly, while genome-wide analysis of the DSB profile showed alterations near the rearranged ends, these differences did not reflect the changes in origin usage. This unexpected finding suggests a complex regulation of DSB formation during meiosis that hints at a potential role for chromosomal context in this process.

In addition, we aimed to investigate the steps in DNA replication that are important for promoting DSB formation. Specifically, we focused on evaluating whether the replication machinery must progress through a DSB site before breaks are formed or whether origin activation is sufficient to induce nearby DSBs. For these studies, we constructed and characterized a system for inducing a replication fork barrier during pre-meiotic S phase.

Taken together, my thesis work provides new directions for investigating the interplay between chromosomal organization, DNA replication and meiotic recombination.

RÉSUMÉ

La réplication de l'ADN est une étape essentielle du cycle cellulaire et les étapes qui la composent sont fortement conservées et régulées. Des erreurs dans la duplication du génome peuvent avoir de graves conséquences sur la prolifération cellulaire et ont été liées à différentes pathologies telles que le cancer. La duplication du génome commence à partir de sites distribués tout au long du génome appelés origines de réplication. Cette duplication est réalisée suivant un programme de réplication précis qui est défini, pour une population de cellules, par la distribution et l'activation de ses origines le long du génome. Toutefois, les cellules au sein d'une même population font preuve d'une certaine plasticité quant à l'utilisation de ces origines. Par exemple, l'ensemble des origines activées varie d'une phase S à une autre ainsi que d'une cellule à une autre. Bien que ces changements du programme de réplication aient été observés durant le développement, la différenciation cellulaire ainsi que dans les cancers, l'importance de ces changements sur les fonctions cellulaires reste peu caractérisée. En utilisant la levure à fission *Schizosaccharomyces pombe* comme modèle d'étude, notre laboratoire a montré que l'utilisation d'un programme de réplication particulier durant la phase S de méiose avait des conséquences sur la formation de cassures doubles brins de l'ADN. Ces résultats montrent pour la première fois qu'un changement du programme de réplication à l'échelle du génome a des conséquences sur les fonctions cellulaires. Basés sur ces résultats, mes travaux de thèse visent à comprendre le lien existant entre la réplication du génome et la recombinaison méiotique, via deux approches.

Dans un premier temps, nous avons exploré l'impact de l'organisation chromosomique sur la réplication de l'ADN et la recombinaison méiotique. Pour cela nous avons généré des réarrangements chromosomiques qui nous ont permis d'échanger la position de domaines de réplication ayant des efficacités et des timings différents. Nos résultats ont montré que ces réarrangements induisaient des changements de l'efficacité des origines localisées spécifiquement de part et d'autre des extrémités des régions réarrangées, et ce durant les phases S mitotique et méiotique. Alors que l'analyse des cassures doubles brins de l'ADN sur l'ensemble du génome montre également des changements aux extrémités de la région réarrangée, ces changements ne reflètent pas les changements du programme de réplication. Ces résultats inattendus suggèrent que le contrôle des cassures doubles brins de l'ADN durant la méiose est régulé de manière complexe et que le contexte chromosomique pourrait jouer un rôle dans ce procédé.

En parallèle, nous nous sommes intéressés à déterminer quelles étaient les étapes de la réplication de l'ADN importantes pour la formation des cassures doubles brins. Nous nous sommes spécialement concentrés à déterminer si la machinerie de réplication doit passer par un site de cassure avant que celle-ci soit faite ou si

l'initiation de la réplication est suffisante pour induire les cassures doubles brins adjacentes. Pour cela nous avons construit et caractérisé un système dans lequel nous pouvons induire une barrière de réplication durant la phase S de méiose.

Mes travaux de thèse ouvrent ainsi de nouvelles pistes de recherche pour comprendre le lien entre l'organisation chromosomique, la réplication de l'ADN et la recombinaison méiotique.

Remerciements

Tout d'abord, je voudrais remercier ma directrice de thèse le Docteur Pei-Yun Jenny Wu pour m'avoir accueilli au sein de son équipe, de m'avoir suivi, soutenu, guidé et surtout accordé sa confiance tout au long de ma thèse. Jenny, merci encore ! Ces trois années à tes côtés m'ont grandement fait mûrir.

J'aimerais ensuite remercier le Docteur Daniel Fisher, le Docteur Pilar Perez Gonzalez, le Docteur Benoit Arcangioli et le Docteur Gilles Salbert pour avoir accepté d'évaluer mes travaux de thèse. Un grand merci au Docteur Daniel Fisher, au Docteur Pilar Perez Gonzalez ainsi qu'au Docteur Benoit Arcangioli pour avoir accepté d'être rapporteur, et un grand merci au Docteur Gilles Salbert qui me fait l'honneur de présider ce jury.

Je voudrais aussi remercier tous les membres de l'équipe, passés et présents : Anthony Perrot, Diane Schausi-Tiffoche, Blanca Gómez-Escoda, Miguel Estravis-Sastre, Balveer Singh, Nena Martin, Diego Molina-Serrano et Christopher Lee-Millington. Sans eux rien n'aurait été pareil, rien n'aurait été possible! Merci encore pour vos encouragements, votre gentillesse, votre aide, votre sourire et toutes vos qualités !

Je voudrais également remercier le « Dark Side » du labo, l'équipe Synthecell avec qui nous partageons le laboratoire, les discussions scientifiques… mais aussi les moments de bonne humeur et les nombreuses sorties ! Merci à vous tous, que ce soit les membres passés ou présents, merci, Damien Coudreuse, Céline Callens, Fériel Baidi, Julien Babic, Javier Munoz-García, Maria-Rosa Domingo-Sananes, Sarah Dixon, Laurent Griscom, Nelson Castilho Coehlo et Vasanthakrishnan Radhakrishnan Balasubramaniam.

Je remercie également les membres de mon comité de Thèse qui m'ont aidé, guidé et soutenu au cour de ces trois années. Je vous remercie, Anne-Marie Chèvre, Pascal Bernard et Marie-Dominique Galibert pour votre écoute et nos discussions scientifiques.

Bien sûr, je ne peux m'empêcher de remercier l'ensemble des membres de l'institut. Je remercie aussi particulièrement Géraldine Le Provost pour toute l'aide administrative et les « Bonjours » qui réveillent ainsi que Bénédicte, ma petite maman du labo qui me prépare des bons petits plats quand je suis dans le besoin ! Je remercie aussi mes compatriotes thésards pour tous les bons moments passés ensemble !

Mes remerciements à la Ligue contre le Cancer et à la Région Bretagne pour m'avoir soutenu durant ces trois ans !

Un grand merci aussi à tous mes amis sans qui la thèse aurait été bien dure ! Merci à ma collègue, Lucie Vaufrey, merci à Mon Juju, à mon Guigui, au jeunots Floflo et Marie, au bébé Soso et à Olive ! Je ne sais pas ce que je serais

devenu sans vous !

Merci aussi à Enzo, François, et Louis, mes trois compatriotes ! Même si on ne s'est pas vu souvent, chaque fois vous avez été là quand j'étais dans le besoin ! Merci aussi aux Rennais pour tous ces bons moments et merci aussi à mes petits monstres qui ont su me sortir et me faire changer d'air !

Merci Papa, Merci Maman, merci à vous pour votre soutien sans borne. J'espère que maintenant vous comprenez un peu plus ce que je fais ! Merci d'être venus me voir, merci pour les surprises, merci pour les bons repas, pour ce sourire maintes et maintes fois rendu, sans vous je n'e(n) serais pas là ! Merci à mes grands parents aussi qui, même sans leur présence, m'encouragent tous les jours !

Enfin, je voudrais remercier Amanda, ou 'Mandilla pour les intimes ! Depuis presque 8 ans maintenant tu me soutiens, crois en moi, m'accompagnes et me redonnes le sourire. Merci de m'avoir supporté, merci de m'avoir donné ce flyier il y a 8 ans déjà ! Merci de partager ma vie.

Merci à vous tous ! Et aussi à ceux que j'aurais oublié ! Sans vous ces trois ans n'auraient jamais été possibles

Table of contents

Chapter I

Introduction

Introduction

The control of genome duplication is critical for cell growth and proliferation as well as for development and differentiation. In eukaryotes, the mechanism of genome duplication is highly conserved and is ensured by multiple layers of regulation. DNA synthesis initiates at discrete sites known as origins, which are distributed along the genome. Cells harbor a large number of potential replication origins but only a subset of these is used in each S-phase. At the population level, the overall pattern of replication, also called the replication program, differs between distinct types of cells. The program of DNA replication is defined by 1) the timing at which each origin initiates replication and 2) the frequency of usage of each origin in a cell population, termed origin efficiency (Méchali, 2010). The replication program is modulated by different inputs such as nucleotide levels, chromatin modification, gene transcription, or cell cycle regulation (Aladjem, 2007; Anglana et al., 2003; Méchali, 2010), suggesting that origin firing is highly regulated. However, at the single-cell level, cells within the same population display plasticity in origin usage. The subset of origins activated during S-phase varies from cell to cell in a population as well as from one cell cycle to the next (Patel et al., 2006). While changes in the pattern of replication have been observed in *Xenopus* and *Drosophila* during development, in differentiating mouse and human cells, and in a number of cancers (Méchali, 2010), it remained unknown whether undergoing S-phase with particular programs of replication has actual consequences for cellular function.

To address this question, previous work in my thesis laboratory has focused on the process of meiosis, a physiological transition that involves specific events in DNA metabolism. Meiosis is a specialized cell division that generates four haploid cells after two rounds of chromosome segregation starting from a diploid progenitor. During this process, pre-meiotic DNA replication is followed by the formation of DNA double-strand breaks (DSBs), a process that is a key contributor to the exchange of genetic material during sexual reproduction. While DSBs are extremely deleterious for genome stability in proliferating cells, their formation is induced in a programmed and tightly regulated process during meiosis. Indeed, meiotic cells specifically generate DSBs that are then repaired via different mechanisms that result in distinct genetic outcomes. Although

meiotic recombination has long been associated with DNA replication (Borde, 2000), the mechanisms that couple these critical processes have remained elusive. Recently, Wu et *al.* (2014) have demonstrated that the selection of replication origins during pre-meiotic S-phase regulates the sites of double-strand break (DSB) formation during meiosis (Wu and Nurse, 2014), providing the first evidence for the functional consequences of genome-wide changes in origin usage. In addition, Murakami and Kenney (2014) proposed a model in which Cdc7, a kinase important for DNA replication, is recruited to the replication machinery and subsequently phosphorylates the critical recombination factor Mer2 (Murakami and Keeney, 2014a). However, the mechanisms linking replication and DSB formation remain unclear, and there are likely to be additional layers of regulation that couple these two processes (Miyoshi et al., 2012; Wan et al., 2008).

During my thesis, I used the fission yeast *Schizosaccharomyces pombe* to investigate the interplay between genome duplication and meiotic DSB formation. On one hand, higher levels of origin activation in a region may increase the local concentration of replication factors that interact with and modify recombination components and would not require *per se* the replication of the sites of DSB formation. Alternatively, the establishment of marks permissive for recombination may be intimately linked to the progression of the replication machinery along the DNA and would therefore rely on duplication of the region containing the DSB. To address these possibilities, I have taken two complementary approaches. First, I have generated chromosomal rearrangements that produce regional changes in origin usage and determined the local and long-range interplay between replication initiation and meiotic DSB formation. Second, I have engineered a system using inducible replication fork barriers to assess the direct relationship between the progression of the replication machinery and the establishment of recombination sites. These studies have led to interesting new observations about DNA replication during the mitotic and meiotic cycles as well as about the relationship between genome duplication and meiotic recombination.

I - *Schizosaccharomyces pombe* as a model organism

Over the past century, the fission yeast *Schizosaccharomyces pombe* has served as a powerful model for understanding the basis of cellular biology. Originally described by P. Lindner in 1893, *S. pombe* was isolated from East African beer and takes its name from the Swahili language, in which *pombe* is the word for beer (Hayles and Nurse, 1992). This non-pathological unicellular eukaryote is part of the *Schizosaccharomyces* genus, which includes *S. japonicas* (Niki, 2014), *S. octosporus* (Coker and Wilson, 1911) and *S. cryophilus* (Helston et al., 2010). *S. pombe* cells have a cylindrical shape and vary between 7 to 14 µm in length and 3 to 4 µm in diameter(Hayles and Nurse, 1992). Fission yeast cells grow from their extremities and divide at their centers, generating two cells of identical size (Figure 1).

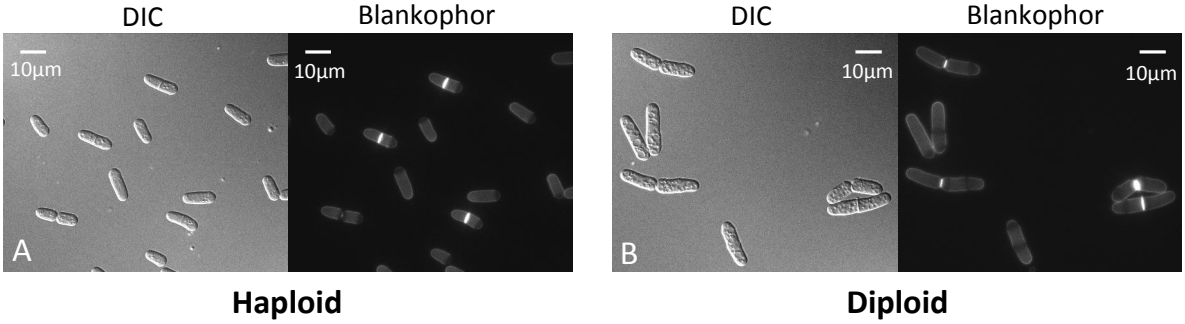

Figure 1: ***Schizosaccharomyces pombe*.**
Microscopic images of A) haploid and B) diploid *S. pombe* cells in DIC and blankophor. Blankophor stains the cell wall and show septum. Diploid cells are longer and wider than haploid cells .

One of the major advantages of *S. pombe* as model organism is its short cell cycle duration, which varies depending on temperature and nutritional conditions. The length of the cell cycle ranges from 2h at 32°C to 4h at 25°C in nutrient rich liquid medium (Forsburg, 2003; Petersen and Russell, 2016). Moreover, the fission yeast serves as a genetic tool: from the wild type homothallic strain (called h^{90}), which is able to switch between its two mating types (h+ and h-), two heterothallic strains of opposite mating type have been generated (Gutz et al., 1974), and both strains can be maintained as either haploids or diploids (Leupold, 1987). These two strains of opposite mating type can mate and undergo meiosis, a process highly conserved in eukaryotes.

The genome of *S. pombe* is approximately 14 Mb in size, distributed in three linear chromosomes (5.7, 4.7 and 3.5 Mb in size) (Wood et al., 2002b). Genome sequence and annotation revealed 5118 genes, of which ~73% are essential (McDowall et al., 2015; Wood et al., 2012). Moreover, recent RNA sequencing data identified ~1850 noncoding RNAs; among these, a large number (694) appear to be antisense transcripts (Hoffman et al., 2015; McDowall et al., 2015). Although biological processes in *S. pombe* cells are in general less complex than in mammalian cells, many of the underlying mechanisms are conserved, and around 68% of *S. pombe* genes have orthologues in metazoa (McDowall et al., 2015).

Importantly, fission yeast has been an excellent model for studying fundamental cellular pathways such as cell cycle control, genome duplication and maintenance, chromatin, epigenetic and gene expression (Hoffman et al., 2015). As a result, a number of resources are available for researchers using this organism: the entire genome is sequenced and annotated (McDowall et al., 2015; Wood et al., 2002a), and a variety of molecular and genetic tools have been generated. This includes a library of deletions of all fission yeast genes (Kim et al., 2010; Spirek et al., 2010), temperature sensitive mutant collections (Hirano et al., 1986; Matsumura et al., 2003), and various plasmids and expression systems (Forsburg and Rhind, 2006). Thus, the large number of genetic and genomic tools available, the detailed characterization of its cell cycle, and the conservation of fundamental biological processes make *S. pombe* as an excellent system for addressing the questions presented in my thesis.

II - The eukaryotic cell cycle

The cell cycle is a complex and highly regulated biological process that produces two daughter cells from one mother. The fundamental mechanisms of the cell cycle are shared among eukaryotic organisms and play important roles in cell growth and proliferation as well as in development. Their deregulation is associated with a number of pathologies, in particular with cancers (Malumbres and Barbacid, 2009). The cell cycle is divided into 4 different phases, G1, S (synthesis), G2 and M (mitosis), which are tightly controlled to ensure proper cell proliferation (Morgan, 2007) (Figure 2). DNA synthesis occurs during S phase, and in M phase, the duplicated genome is distributed

into the two daughter cells that will be produced after cytokinesis (Morgan, 2007). G1 and G2 represent the phases of the cell cycle during which cell growth occurs; moreover, they provide time for the cell to monitor the internal and external environment to ensure that conditions are suitable and that preparations are complete before the cell commits itself to the next phase (Morgan, 2007). If conditions are unfavorable, such as when cells encounter a shortage of nutrients or suffer damage to their genomes, they can delay progress through G1 or G2 until conditions are suitable (Barnum and O'Connell, 2014). Some cells may even enter a specialized resting state known as G0 or quiescence from G1, in which they can remain for days to years before re-entering into a proliferative state. For instance, in *S. pombe*, a lack of nitrogen induces the cell to enter a G0 state until a nitrogen source becomes available (Su et al., 1996). Thus, cell cycle regulation is fundamental to the development and functioning of all life forms.

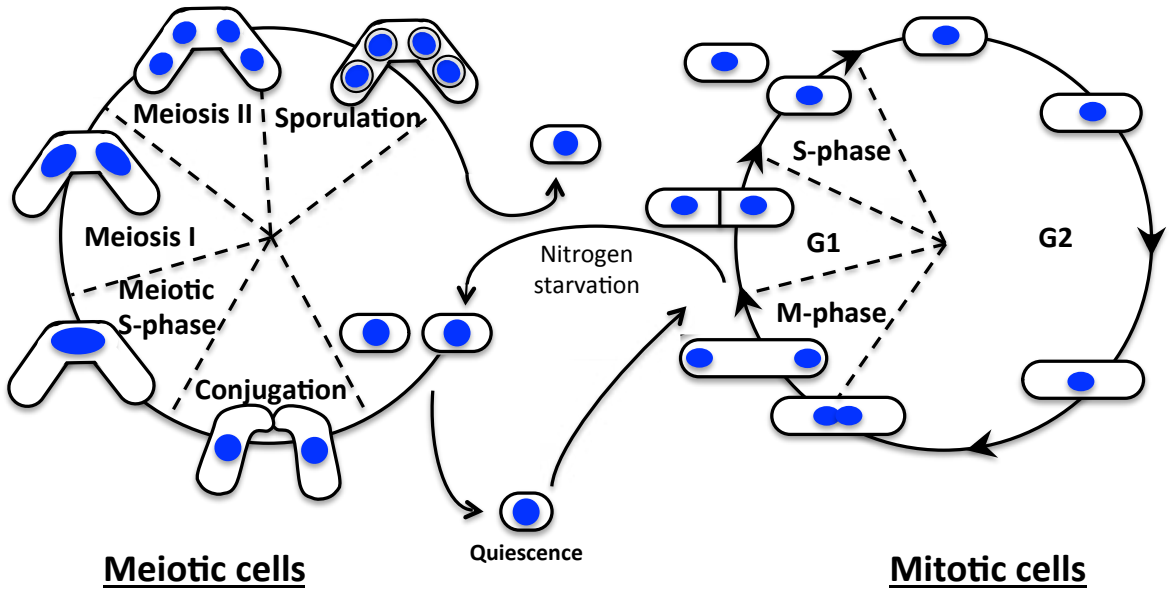

Figure 2: The *S. pombe* meiotic and mitotic cell cycles.
The mitotic cell cycle of fission yeast is represented in the right portion of the diagram. In conditions that favor cell proliferation, G1 cells elongate and replicate their DNA before cytokinesis. Cytokinesis gives rise to two daughter cells in early G2. At the end of G2, mitosis occurs and cells enter G1 as transient binucleated cells. Upon nutrient depletion, such as nitrogen starvation, cells exit the cell cycle and enter a quiescent state in which they can stay until nutrients become available. Alternatively, a cell can conjugate with another cell of opposite mating type and undergo meiosis. The meiotic cycle is represented in the left part of the schematic. After mating, the diploid cell that is formed undergoes pre-meiotic S-phase, followed by two rounds of nuclear division (meiosis I and meiosis II). This results in the formation of a tetrad containing four haploid spores. These spores can then re-enter the mitotic cell cycle in the presence of favorable growth conditions. Figure adapted from http://www-bcf.usc.edu/~forsburg/main4.html.

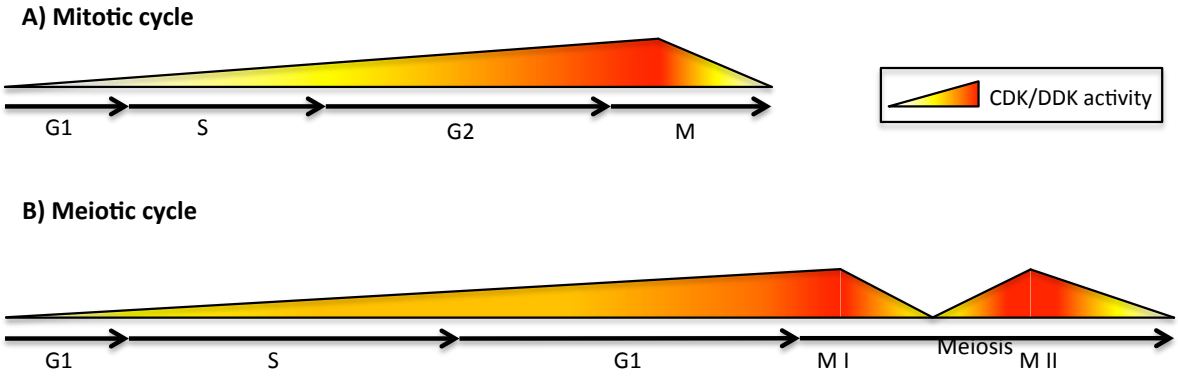

Figure 3: Schematic representation of CDK and DDK activity during mitotic and meiotic cell cycle.
Schematic representation of CDK /DDK activity during A) mitosis and B) meiosis. CDK/DDK activity is represented by the color gradient (white, low activity and red, high activity) Lengths of the cell cycle phases are not shown to scale. Adapted from Gómez-Escoda and Wu, 2010

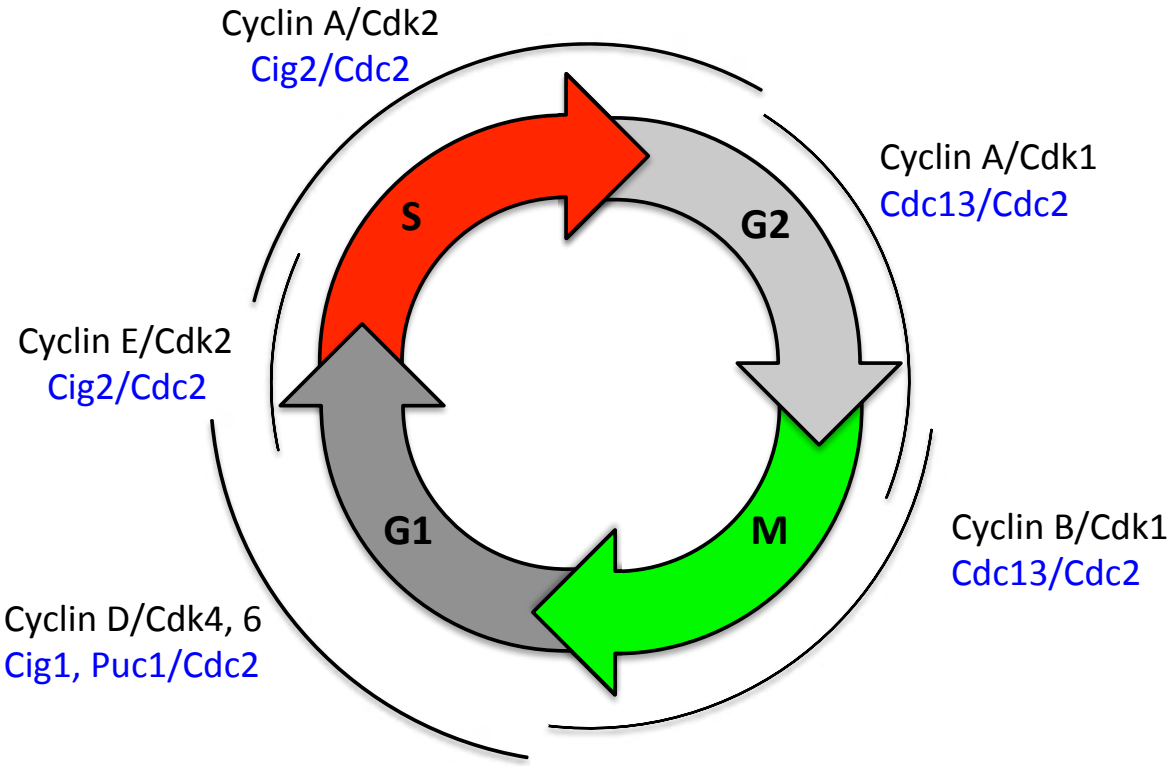

Figure 4: Cell cycle regulation by different cyclin/CDK complexes in mammalian and fission yeast cells.
Schematic representation of the different cyclin/CDK pairs governing the different phases of the cell cycle in mammalian (black) and fission yeast (blue) cells. Cyclin/CDK activity varies during the cell cycle and shapes the succession of the different phases. Adapted from Suryadinata et *al*. 2010

The order of the different phases of the cell cycle is crucial for the faithful transmission of the genetic material and for proper cell division (Morgan, 2007). For example, the genome is duplicated once and only once per cell cycle, and mitosis occurs only when S-phase is completed so that the genetic material is equally transmitted to the two daughter cells. Similarly, during meiosis, which is a specialized cell division that allows sexual reproduction, the proper chronology of the events is crucial to generate viable gametes (Figure 2). Coordination of both these processes requires a large number of regulatory pathways, and many of the major regulators are shared between mitosis and meiosis. These mechanisms will be described in the following sections.

II.1 - Regulation of the cell cycle by cyclin-dependent kinases (CDK)

In eukaryotes, cell cycle progression is driven by a family of serine/threonine protein kinases known as the cyclin-dependent kinases (CDKs). CDK activity requires the association of the enzyme with a partner cyclin, and cyclin/CDK complexes phosphorylate key substrates that promote different cell cycle events (Morgan, 1997; Schafer, 1998; Suryadinata et al., 2010). The level of CDK activity dictates the orderly succession of cell cycle phases (Coudreuse and Nurse, 2010; Fisher and Nurse, 1996; Morgan, 1997): it is low during G1, attains a threshold that allows for S-phase entry, further increases during G2 to attain a high threshold that is required for the G2/M transition, and then is reduced to allow mitotic exit (Figure 3). This precise control of the dynamics of CDK activity is essential for proper execution and completion of the different phases of the cell cycle.

The interactions between different CDKs and their cyclin partners play a key role in modulating CDK function during cell cycle regulation. In mammalian cells, there are four CDKs (CDK1-2-4-6) that associate with distinct cyclins expressed during different phases of the cell cycle (Figure 4). First, progression through G1 is mediated by the association of CDK4 and CDK6 with D-type cyclins (Matsushime et al., 1992; Meyerson and Harlow, 1994), while association of CDK2 with cyclin E is important for the G1/S transition (Dulić et al., 1992; Koff et al., 1992). Next, the cyclin A/CDK2 and cyclin A/CDK1 complexes are important for S-phase and progression through G2, respectively

(Pagano et al., 1992). Finally, cyclin B/CDK1 acts at the G2/M transition (Hagan et al., 1988; Moreno et al., 1989) Although different cyclin/CDK complexes are believed to provide substrate specificities that are required for particular cell cycle transitions, similar but less complex associations have been found in simpler eukaryotes. For instance, in the budding yeast *Saccharomyces cerevisiae*, several different cyclins (Clb1 to 6 and Cln1 to 3) bind to only one cell cycle CDK (Cdc28) (Nasmyth, 1993). Similarly, fission yeast cells possess a single cell cycle CDK (Cdc2) that associates with four cyclins (Cig1, Cig2, Puc1, Cdc13) (Connolly and Beach, 1994; Coudreuse and Nurse, 2010; Fisher and Nurse, 1996; Moreno et al., 1989; Stern and Nurse, 1996) (Figure 4). Intriguingly, it has been demonstrated that distinct combinations of cyclin/CDK are not required for cell proliferation and that it is the level of CDK activity that drives cell cycle progression. In this quantitative model, S-phase and mitosis rely on low and high CDK thresholds, respectively, independently of the cyclin/CDK complex (Fisher and Nurse, 1996; Stern and Nurse, 1996). In support of this model, a number of studies from yeast to murine systems have shown a high degree of redundancy in the functions of different cyclins and CDKs (Donaldson et al., 1998; Fisher and Nurse, 1996; Kozar et al., 2004; Moore et al., 2003; Santamaría et al., 2007). Importantly, work in the fission yeast has demonstrated that a single fusion protein consisting of one cyclin (Cdc13) and CDK (Cdc2) drives the cell cycle through oscillation of its activity even in the absence of all other cyclins (Coudreuse and Nurse, 2010). Subsequent studies have found that CDK activity levels have a direct impact not only on substrate phosphorylation but also on the periodic transcription of cell cycle genes (Swaffer et al., 2016). Therefore, the level of CDK activity, rather than the substrate specificities of distinct cyclin/CDK complexes, is the master regulator of cell cycle progression.

The control of CDK activity is achieved by a variety of mechanisms that include alterations in cyclin abundance, associations with CDK inhibitors, and inhibitory phosphorylation of the CDK itself (Félix et al., 1990; Morgan, 1995). In early G1, S and M-cyclins are targeted for degradation by the anaphase promoting complex (APC/cyclosome), and associated CDKs are inactivated by an increase in the concentration of CDK inhibitor (Gérard and Goldbeter, 2009). Then, at the end of G1, G1/S cyclins are expressed and bind to G1/S CDKs, which results in an increase in CDK activity that triggers destruction of the CDK inhibitor and inactivates APC (Mittnacht,

1998; Ramanujan and Tiwari, 2016). Consequently, S-cyclin level rises and leads to an increase in S-CDK activity, bringing about the phosphorylation of proteins involved in DNA replication and triggering S-phase entry. In addition, S-CDK activity promotes degradation of G1/S-cyclins, preventing cells from re-entering G1 and starting another round of DNA replication. At the end of S-phase, M-cyclin level increases, leading to the accumulation of M-cyclin/M-CDK complex during G2. At this point, M-CDK activity is regulated by a mechanism that involves the inhibitory Wee1 protein kinase (Gould and Nurse, 1989; Lundgren et al., 1991) and the activating Cdc25 phosphatase (Russell and Nurse, 1986). During interphase, Wee1 phosphorylation of M-CDK keeps its activity low. As M-CDK concentration increases during G2, M-CDK-dependent inactivation of Wee1 and activation of Cdc25 generate a double negative and positive feedback loop in which M-CDK/cyclin activates its activator and inhibits its inhibitor (Pomerening et al., 2005). This leads to an increase in M-CDK activity that reaches a high threshold to drive mitotic entry(Solomon et al., 1990). This high CDK activity then phosphorylates and activates APC, decreasing CDK activity for mitotic exit. Thus, the regulation of cyclin/CDK activity ensures proper cell cycle progression.

To counter the activity of CDKs during the cell cycle, protein phosphatases have also been reported to have important roles in cell cycle regulation. Indeed, two serine/threonine phosphatases, PP2A-B55 and PP1, target CDK substrates during different cell cycle phases (Domingo-Sananes et al., 2011) This regulation is not detailed here but can be found in the following review: Domingo-Sananes et al., 2011. These enzymes are modulated by complex feedback mechanisms involving CDK activity and its regulators (Domingo-Sananes et al., 2011), and they work together with CDKs to mediate progression through the different phases of the cell cycle.

II.2 – Cell cycle regulation in *Schizosaccharomyces pombe*

The fission yeast *S. pombe* has only one cell cycle CDK, Cdc2 (CDK1), that can associate with four different cyclins: Cig1, Cig2, Puc1 and Cdc13 (Fisher and Nurse, 1995) (Figure 4). G1 progression in fission yeast is regulated by the Cig1/Cdc2 and Puc1/Cdc2 complexes (Benito et al., 1998; Martín-Castellanos et al., 2000). During this period, CDK activity is low as a result of the regulation of Cdc13 by APC-auxiliary

protein Ste9 (Blanco et al., 2000). This level is maintained low during G1 by the CDK inhibitor Rum1, whose binding to the Cdc13/Cdc2 complex targets Cdc13 for degradation (Correa-Bordes et al., 1997). Similarly, Rum1 binds to the Cig2/Cdc2 complex that is involved in the G1 to S transition (Mondesert et al., 1996), inhibiting S-phase entry. At G1/S, Rum1 is targeted for degradation by Cig1/Cdc2 (Correa-Bordes et al., 1997), and Cig2/Cdc2 activity triggers the start of S-phase. The abundance of Cdc13 increases during G2; during this time, CDK activity is controlled by the Wee1/Cdc25 feedback loop. Commitment to mitosis then occurs upon Cdc13/Cdc2 reaching the high threshold of activity required for this event (Millar et al., 1991). This network, with only one CDK and four cyclins, makes fission yeast a simple system for studying cell cycle regulation compared to metazoa. Moreover, the four cyclins are not all required to drive the cell cycle in fission yeast: as described above, a single cyclin/CDK complex (Cdc2/Cdc13) is sufficient to drive orderly progression through the four phases of the cell cycle (Coudreuse and Nurse, 2010; Fisher and Nurse, 1996).

III - DNA replication

In order to ensure the transmission of the genetic material from one generation to the next, a cell generates a copy of its genome that is then equally distributed into the two daughter cells. Duplication of the DNA takes place during S-phase, and this process is tightly regulated so that it occurs only once during the cell cycle. Misregulation of this process can lead to severe consequences such as aneuploidy, a hallmark of cancer cells.

The mechanism of DNA replication is highly conserved throughout eukaryotes. DNA synthesis starts at sites referred to as replication origins and requires the coordinated assembly of a large number of conserved proteins at these sites (Boye and Grallert, 2009). First, the Origin Recognition Complex (ORC) binds to origin sequences in the genome, followed by the formation of the pre-Replication Complex (pre-RC) that contains the MCM helicase complex. The phosphorylation of pre-RC components by CDK and the Dbf4-dependent kinase (DDK) then promotes the formation of the pre-Initiation Complex (pre-IC), in which the enzymes essential for DNA synthesis are loaded at

origins. The regulation of the ordered assembly of the replication machinery is critical for origin activation and for ensuring the fidelity of genome duplication.

III.1 – Initiation of DNA replication in eukaryotes

III.1.a - Characteristics of eukaryotic replication origins

While the factors that are required for DNA replication are conserved among eukaryotic species, the sequences that serve as initiation sites are widely varied. In the budding yeast, a 11 base pairs AT-rich consensus sequence called the ACS (ARS Consensus Sequence) is required for origin function (Theis and Newlon, 1997). However, in most other eukaryotes, there appears to be no consensus DNA sequence that defines replication origins. For instance, origins in the fission yeast *S. pombe* are AT-rich tracts that are located in intergenic regions (Mojardín et al., 2013). Furthermore, genome-wide analyses of the human, *Drosophila* and mouse genomes reveals that origins tend to localize in GC-rich regions (Cadoret et al., 2008; Cayrou et al., 2011) and are associated with G-quadruplex motifs (Valton et al., 2014). These observations suggest that replication origins may not be defined by specific DNA sequence, but rather that a structural motif may be involved in their specification.

III.1.b - Formation of the pre-Replicative Complex (pre-RC)

Initiation of DNA replication is a multi-step process that begins with the binding of ORC to replication origins (Figure 5). The ORC complex is composed of 6 subunits (Orc1 to Orc6) and is conserved throughout eukaryotes. ORC regulation relies on the phosphorylation of Orc2 by CyclinB/Cdk1 (Lee et al., 2012), which occurs from the start of S-phase and continues until the end of mitosis. This phosphorylation plays an important role in preventing re-replication. As CDK activity is low in early G1, hypophosphorylation of ORC favors the recruitment of the other factors that form the pre-RC (Vas et al., 2001). Thus, ORC serves as a platform for pre-RC assembly, as it is the first component of the replication machinery to bind to DNA (Figure 5).

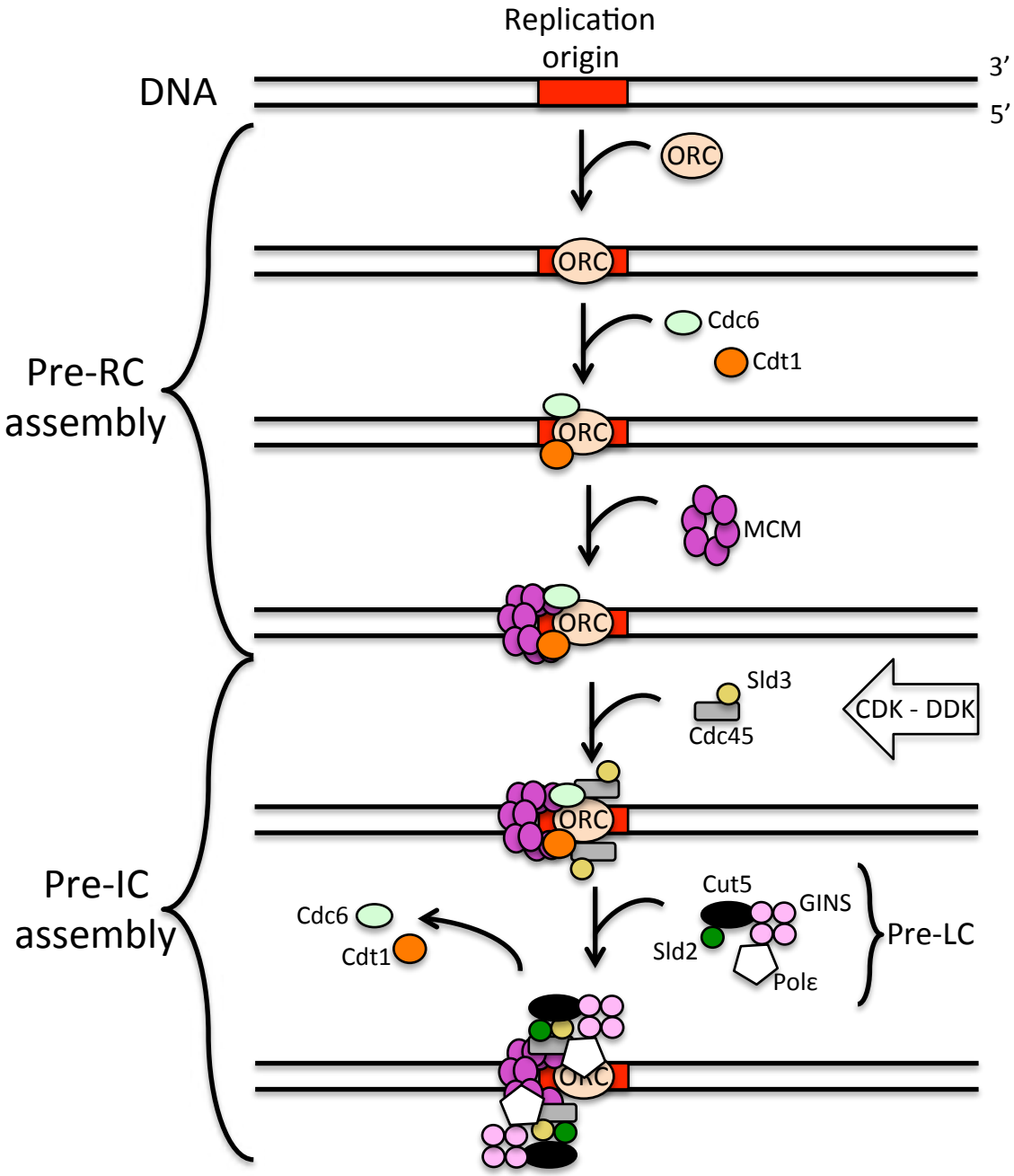

Figure 5: Initiation of DNA replication in eukaryotes.
Replication initiation is divided into two majors steps. First, the pre-RC forms at replication origins. This begins with the recruitment of ORC proteins to origins, followed by the binding Cdc6 and Cdt1 to ORC, and ends with the loading of MCM proteins. Pre-RC formation licenses the origin and prepares it for the assembly of the pre-IC, which requires the recruitment of Cdc45, Sld3 and the pre-LC in a DDK and CDK phosphorylation-dependent manner. Once the pre-IC is assembled, replication initiates bidirectionally. Origin firing then releases Cdc6 and Cdt1, which are targeted for proteolysis to prevent re-replication. Adapted from Fragkos et *al*. 2015

Following ORC binding to origins, the Cdc6 (Cdc18 in *S. pombe*) and Cdt1 replication factors are recruited. The ATP-dependent association of Cdc6/Cdc18 (Speck et al., 2005) is crucial for the subsequent loading of Cdt1 to this complex (Nishitani et al., 2000). Regulation of Cdc6/Cdc18 and Cdt1 follow the same dynamics during the cell cycle (Nishitani et al., 2000): both proteins are subject to phosphorylation by CDK, which results in their degradation; their levels are also modulated by cell cycle-dependent transcriptional regulation (Hateboer et al., 1998; Yoshida and Inoue, 2004). Thus, CDK activity and coordinated transcription regulate the formation of the pre-RC through the production and the degradation of Cdc6/Cdc18 and Cdt1 (Coverley et al., 2000; Kelly et al., 1993; Nishitani et al., 2000).

The assembly of Cdc6/Cdc18 and Cdt1 then promotes the binding of the MCM (Mini-Chromosome Maintenance) complex at the origin. MCM is composed of 6 proteins (Mcm2 to Mcm7) and possesses the helicase activity required to unwind double-stranded DNA for replication. Loading of a double hexamer of MCM helicase onto DNA is the final step of DNA replication licensing. This configuration allows the bi-directional progression replication fork on DNA (Evrin et al., 2009). Thus, pre-RC formation requires the assembly of ORC, Cdc6, Cdt1 and MCM at origins (Figure 5).

III.1.c - Formation of the pre-Initiation Complex (pre-IC)

During G1, the recruitment of the double MCM hexamer to origins completes the formation of the pre-RC. In this state, MCM hexamers are inactive for DNA unwinding and DNA synthesis, and the pre-RC is inactive for DNA replication. The formation of an active complex that is capable of initiating DNA synthesis requires the assembly of the pre-IC, which involves the binding of additional replication factors. This transition from pre-RC to pre-IC is dependent on phosphorylation of pre-RC components by two kinases, the CDK and the Dbf4-dependent kinase (DDK) (Heller et al., 2011). DDK phosphorylates the Mcm4 and Mcm6 subunits, and this modification is a key step that allows the recruitment of critical factors to the pre-RC, including Cdc45 and the tetrameric GINS complex (go-ichi-ni-san; consists of Sld5-Psf1-Psf2-Psf3). The Cdc45-MCM-GINS complex, also called CMG, is formed through two main steps. First, the phosphorylated form of Sld3/Treslin associates with Cdc45 and binds MCM at the origin

(Kamimura et al., 2001; Zegerman and Diffley, 2007). Next, the pre-LC (pre-Loading Complex) is formed when phosphorylated Sld2/RecQL4 associates with Cut5/TOPBP1 (Kamimura et al., 1998) and allows the recruitment of DNA polymerase and GINS (Muramatsu et al., 2010). Interaction of Cut5 with Sld3 then results in the loading of the pre-LC to the pre-RC (Kumagai et al., 2010), which completes the formation of the pre-IC (Figure 5). At this point, the CMG helicase is activated and the origin is ready to begin DNA synthesis.

III.2 – The roles of CDK and Dbf4-dependent kinases in replication

The CDK and DDK are both involved in origin activation. Their levels remain constant throughout the cell cycle (Arellano and Moreno, 1997; Jackson et al., 1993; Sclafani et al., 1988; Yoon et al., 1993) while their activities vary. As discussed in section II, CDK activity depends on association with cyclins, whose levels oscillate during the cell cycle, and is modulated by additional regulatory factors and networks. Similarly, the activity of DDK (Cdc7 in most organisms, Hsk1 in *S. pombe*) relies on association with its partner Dbf4/Dfp1 protein (Jackson et al., 1993). Regulation of DDK activity also occurs through oscillation of Dbf4 protein level, which is low in G1, increases from G1/S to be maintained at it highest level during S-phase, and finally decreased at G2/M (Brown and Kelly, 1999; Nougarède et al., 2000; Oshiro et al., 1999).

Origin licensing and activation are thus controlled by different levels of CDK and DDK activities. Low CDK and DDK activities permit pre-RC formation at the origin, and increases in these activities promote the association of Cdc45 and other pre-IC factors with the pre-RC (Fisher, 2011; Masumoto et al., 2002; Tanaka et al., 2007; Zegerman and Diffley, 2007). As CDK activity increases, pre-RC reassembly is inhibited, thus preventing origins from re-licensing and re-firing. This occurs via phosphorylation of pre-RC components such as ORC, Cdc6, Cdt1 and MCM (Labib et al., 1999; Larasati and Duncker, 2017; Liku et al., 2005; Mimura et al., 2004; Moll et al., 1991; Nguyen et al., 2001; 2000; Vas et al., 2001; Wuarin et al., 2002). Therefore, the activities of CDK and DDK are critical for replication initiation as well as for restricting origins from firing

more than once per cell cycle.

III.3 - Replication origin usage in eukaryotes

During each cell cycle, replication initiates at multiple sites across the genome. The number of origins identified per genome varies greatly, from 400 in the budding yeast to 30000-50000 in human cells (Huberman and Riggs, 1966; Wyrick et al., 2001). Interestingly, not all the origins in a genome are used the same way, and they show different characteristics of activation. First, there are differences in the timing of origin firing. At the population level, each origin fires at a characteristic time during S-phase. Second, not all origins are used during each S-phase. Only a subset of all potential origins is activated during each cell cycle, and this subset is not the same from one cell cycle to the next or between two genetically identical cells. This probability of usage is termed origin efficiency, which is assessed as the frequency of usage of an origin in a population of cells. The timing and efficiency of origin usage for all the origins in a given genome gives rise to the program of DNA replication along the chromosomes. This pattern of replication initiation is linked to the spatio-temporal organization of DNA replication in the nucleus (Kaykov and Nurse, 2015; Rhind and Gilbert, 2013). Indeed, in mammalian cells, large segments of the genome are replicated at the same time through the synchronous firing of origins in particular regions (Pope and Gilbert, 2013; Rhind and Gilbert, 2013). The temporal order in which these replication domains is duplicated is closely associated with their nuclear localization (Foti et al., 2016). Interestingly, the factors that coordinate the spatio-temporal organization of replication within the nucleus appear to be conserved throughout eukaryotes (Cornacchia et al., 2012; Hayano et al., 2012; Knott et al., 2012; Yamazaki et al., 2012), highlighting the importance of this architecture.

One key mechanism that regulates the timing and efficiency of origin usage is through the modulation of pre-RC and pre-IC assembly. In the fission yeast, the timing of origin firing has been linked to the timing of ORC and pre-RC recruitment to origins; competition for limiting pre-IC factors (such as Cdc45, Hsk1 and Dfp1) among origins then establishes origin efficiencies (Patel et al., 2008; Wu and Nurse, 2009). Similarly, in

the budding yeast, overexpression of limiting CDK substrates such as Sld2, Sld3, and Dpb11 allow late origins to fire earlier during S-phase, suggesting a competition for these factors at origins (Mantiero et al., 2011). In addition, other factors have been shown to regulate the timing and the efficiency of origin firing. For instance, when an origin fires in S-phase has been linked with the number of loaded MCMs (Das et al., 2015), and the density of ORC binding along the chromosomes reflects the timing of origin firing in *Drosophila* (MacAlpine et al., 2010). These observations therefore identify pre-RC and pre-IC formation as crucial steps in determining the timing and the efficiency of origin activation.

Intriguingly, despite the tight control of replication initiation described above, the replication program is flexible and changes in response to developmental stimuli and nutritional conditions. For example, in mouse embryonic stem cells, alterations in the replication program occur as cell differentiate (Hiratani et al., 2008). In addition, in *X. laevis* or *D. melanogaster* early embryonic development, many more origins are activated during each cell cycle than later in development (Hyrien and Mechali, 1993; Hyrien et al., 1995; Méchali, 2010). Origin selection can also be modulated in environmentally challenging conditions. Indeed, exposure of cells to hydroxyurea, which depletes cells of dNTPs, results in the activation of dormant origins that are initiated to promote the completion of genome duplication (Woodward et al., 2006). In the fission yeast, cell re-entering S-phase after nitrogen starvation also show changes in their replication program (Wu and Nurse, 2014). All together, these data demonstrate that origin selection and activation are modulated by environmental and developmental requirements. This has important implications for the interplay between DNA replication and other cellular processes, a subject which will be explored in the following sections.

IV – Meiosis

Meiosis is a specialized cell division that allows sexual reproduction. This process, which is highly conserved among eukaryotes, produces haploid cells starting from a diploid progenitor. During this process, DNA is first replicated and then

undergoes two rounds of segregation referred to meiosis I and meiosis II, resulting in the formation of haploid gametes. Meiosis also generates genome diversity through homologous recombination, which produces different combinations of genes from those in the parental genomes.

IV.1 – Chronology of meiotic events

Meiosis is comprised of a succession of events that generate four haploid cells from a diploid cell. The chronology of events is shared among eukaryotic cells, and the precise order and control of the steps is crucial for generate viable gametes. Once cells enter meiosis, they replicate their DNA and undergo a reductional division (meiosis I) and an equational division (meiosis II) (Figure 6). These divisions have specificities that distinguish them from mitosis, which will be discussed in the following sections.

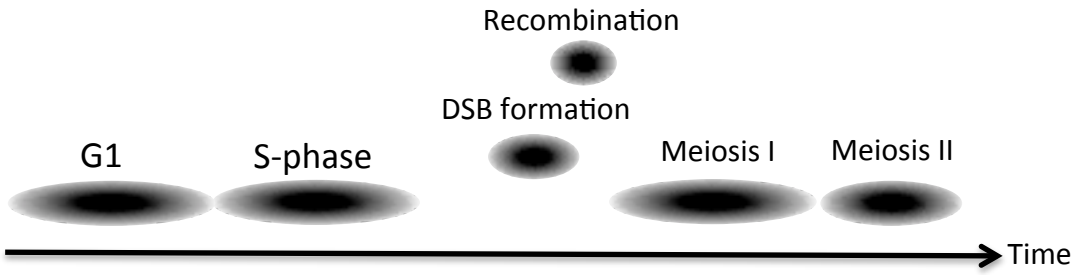

Figure 6: Sequence of meiotic events.
After G1, DNA replication is followed by DSB formation and recombination. After recombination, cells undergo two rounds of division (meiosis I and meiosis II).

The signals that lead to commitment to undergoing meiosis differ depending on the organism. In mammals, retinoic acid activates the expression of the STRA8 gene that governs meiotic entry (Kimble, 2011). In yeasts, meiotic entry is driven by nutritional cues: for instance, in the budding yeast *S. cerevisiae*, nutritional cues are essential for regulating the IME1 transcription factor that acts in late G1 to activate meiotic genes (Mitchell 1994; Vershon and Pierce 2000; Kassir et al. 2003). In *S. pombe*, the decision to initiate meiosis relies on nutritional conditions and pheromone signaling (Harigaya and Yamamoto, 2007). Indeed, pheromone signaling leads to induction of *mei3* gene, which encodes a pseudo-substrate that bind and inactivates the Pat1 Ser/Thr protein kinase

(McLeod and Beach, 1988; Yamamoto, 1996). In parallel, pheromone signaling activates the transcription of the transcription factor Ste11, which induces the Mei2 RNA-binding protein expression. Mei2 and Ste11 activate each other through a positive feedback loop (Sukegawa et al., 2011), which results in the expression of meiotic related genes (van Werven and Amon, 2011) (Figure 7). In non-inducing conditions, Pat1 phosphorylation of the Mei2 RNA-binding protein on its Ser438 and Thr527 residues inhibits its function as a positive regulator of meiosis and targets Mei2 for degradation (Harigaya and Yamamoto, 2007) (Figure 7). Moreover, Pat1 inhibits the transcription factor Ste11 (Kitamura et al., 2001). Thus, meiosis can be ectopically induced in fission yeast by inactivation of the *pat1* gene. For instance, the *pat1-114* thermosensitive mutation or the *pat1-as2* allele that renders the kinase sensitive to inhibition by nonhydrolyzable ATP analogs have been used to induce meiosis and sporulation, regardless or the nutritional conditions or the ploidy of the cell (Bähler et al., 1991; Cipak et al., 2012; Guerra-Moreno et al., 2012; Iino and Yamamoto, 1985).

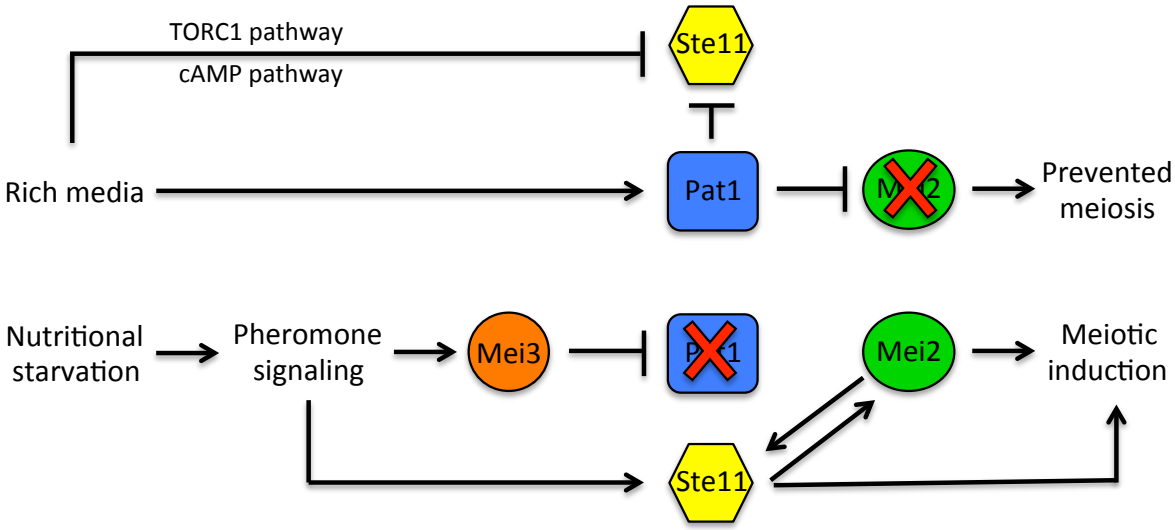

Figure 7: Signaling pathway for meiosis in *S. pombe*
In vegetative cells, Mei2 is modified by the protein kinase Pat1, resulting in its ubiquitin-dependent degradation. In parallel, presence of nitrogen and carbon source in the media induces inhibition of Ste11 transcription factor. Under nutritional starvation conditions, cells of opposite mating types can mate, leading to induction of *mei3* and *Ste11* expression. Mei3 binds and inactivates the Pat1 kinase, which alleviates its inhibition of Mei2. In turn, Ste11 activates *mei2* and allows it to positively regulate meiotic entry and enhances expression of ste11 through a positive feedback loop. Thus Mei2 and Ste11 positively regulate expression of meiotic genes.

After meiotic commitment, the genome is duplicated via mechanisms that use the same machinery as in a mitotic cycle (Forsburg and Hodson, 2000; Lindner et al., 2002; Murakami et al., 2003; Ofir et al., 2004). While meiotic S-phase in all organisms studied is longer than that in proliferating cells (Zickler and Kleckner, 1998), the significance of this difference remains elusive. Importantly, the steps following meiotic DNA replication show clear distinctions from their mitotic counterparts (Figure 8). First, chromosomes are condensed during prophase I, which is the longest phase and is subdivided into 5 phases called leptotene, zygotene, pachytene, diplotene and diakinesis. In leptotene, sister chromatids associate and condense to form visible chromosomes. This compaction is achieved due to the formation of chromatin loops along the axial elements (linear elements in *S. pombe*). Next, in zygotene, chromosomes are further condensed (Zickler and Kleckner, 1998), and chromatids develop a shared kinetochore while their telomeres are anchored at the nuclear envelope. In budding and fission yeasts, telomeres are clustered near the Spindle Pole Body (SPB; the equivalent of the centrosome in higher eukaryotes) (Chikashige et al., 1994; 1997), producing a "bouquet" configuration that facilitates the efficiency of homologous chromosome pairing (Harper et al., 2004; Niwa et al., 2000). Bouquet formation is followed by the onset of nuclear movements. The nucleus oscillates back and forth in the cytoplasm, creating an elongated nuclear shape called a "horsetail" (Chikashige et al., 1994; Hiraoka et al., 2000). Those movements are led by the SPB through the action of the cytoplasmic microtubules (Ding et al., 1998; Miki et al., 2002; Yamamoto et al., 1999) during pachytene and are important for homologous chromosome pairing (Yamamoto et al., 1999). This pairing is stabilized by the formation of the synaptonemal complex (SC) (Harper et al., 2004), a multi-protein structure composed of two lateral elements (theaxial element of each homolog) joined by transverse filaments (Zickler and Kleckner, 1999). Thus, at pachytene, one sister chromatid is synapsed with a chromatid of the homologous chromosome along it entire length. It is at this moment that programmed double strand breaks are produced by the transesterase Spo11 (Rec12 in *S. pombe*). These breaks not only promote accurate chromosome segregation (Murakami and Keeney, 2008), but their subsequent repair prior to metaphase I gives rise to the possibility of generating crossover recombinants with an exchange of parental genetic material. This reshuffling of maternal and paternal alleles increases

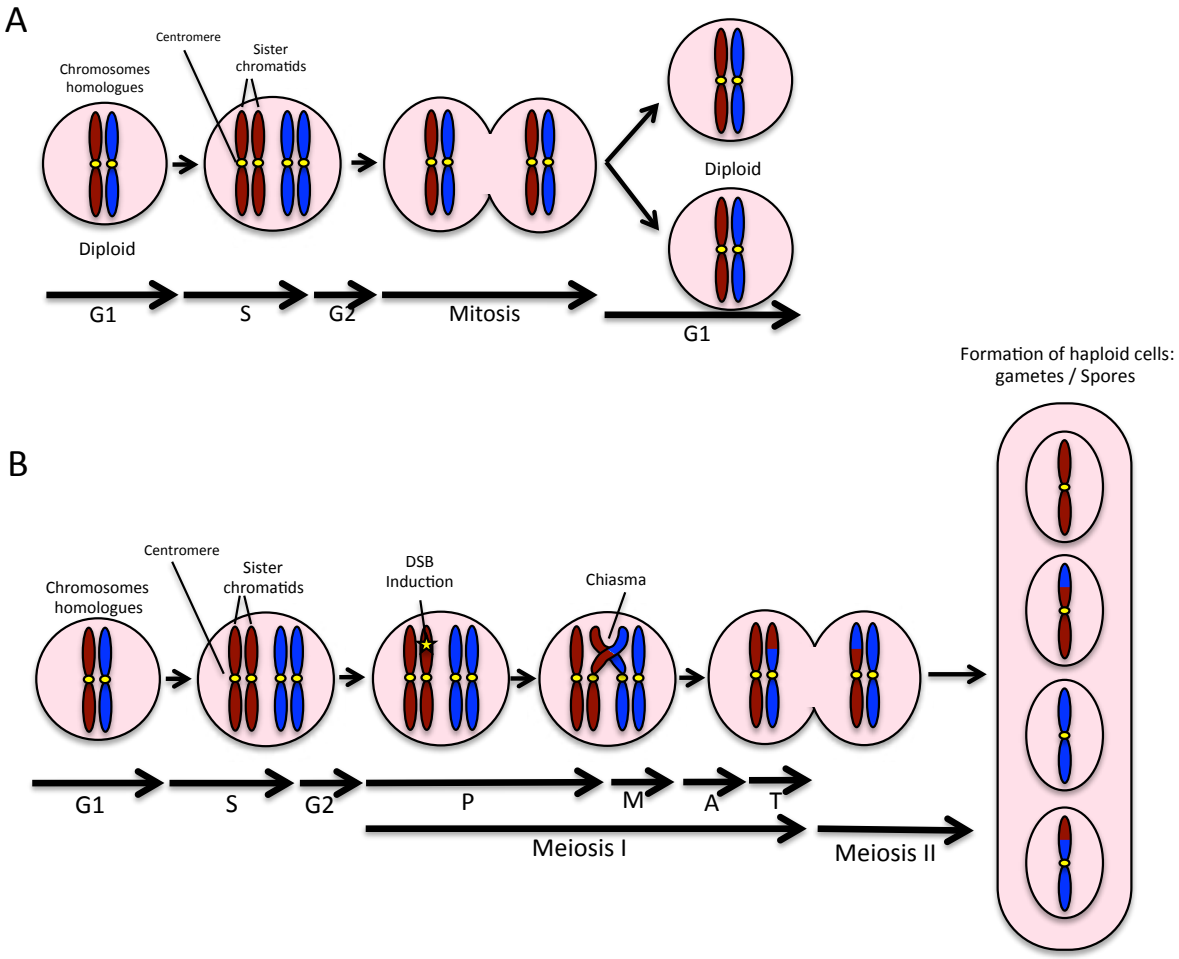

Figure 8: The mitosis and meiotic progression.
A) Mitosis in a diploid cell. Following G1, cells replicate their DNA during S-phase. Sister chromatids are then segregated during M phase to generate two diploid cells. Haploid cells follow the same succession of events. B) Meiosis in a diploid. Pre-meiotic S-phase is followed by two round of chromosome segregation. During meiosis I, programmed double strand breaks (DSBs) are formed, which are subsequently repaired by homologous recombination. Then, homologous chromosomes are segregated to the opposite poles. This is followed by sister chromatids segregation during meiosis II. This results in the formation of haploid gametes/spores. P, M, A and T refer to prophase, metaphase, anaphase and telophase, respectively.

genetic diversity in the progeny (Handel and Schimenti, 2010; Székvölgyi and Nicolas, 2010). If the repair of the breaks is not accomplished, checkpoint mechanism blocks the entry to metaphase I until breaks are repaired (Longhese et al., 2009; 2008). Then, at diplotene, the synaptonemal complex disintegrates between the two chromosomal arms, while sister chromatid cohesion is maintained by chiasma(ta) (Zickler and Kleckner, 1998). The final compaction of the chromosomes then continues until diakinesis (Zickler and Kleckner, 1998). Following the intricate steps described above, in metaphase I, microtubules are nucleated from centrosomes/SPBs and attach to homologous chromosome pairs, which move together along the metaphase plate. At this point, sister chromatids are still held together by at least one chiasma as well as cohesion proteins (Page and Hawley, 2003). Chiasmata are then resolved and cohesion is lost on the chromosome arms at the onset of anaphase I (Buonomo et al., 2000). Kinetochores from sister chromatid pairs are orientated toward the same cellular pole (Marston and Amon, 2004), and microtubule traction separates the homologs, which migrate to the opposite poles of the cell (Nicklas, 1988). Finally, in telophase I, two nuclei containing sister chromatids are produced as result of the reductional segregation. A second round of nuclear division occurs during meiosis II, which is more similar to mitosis even if the genetic outcomes are fundamentally different. There, the sister chromatids are separated, generating four haploid cells are at the end of telophase II.

Thus, meiosis is a succession of events that differs from mitosis in two main aspects. First, two round of chromosome segregation result in the formation of four haploid cells. Second, the generation of induced double-strand breaks, a form of DNA damage that is extremely deleterious when left unrepaired, allows parental genetic exchange and increases genome diversity.

IV.2 – Regulation of meiotic events by CDK and DDK.

As in mitosis, CDK and DDK activities are key regulators of the meiotic cycle. Interestingly, there are additional elements that modulate their function in meiosis: in *S. pombe,* for example, two meiotic-specific cyclins (Rem1 and Crs1), as well as one DDK-like protein (Spo4) and its regulator (Spo6), have been shown to drive

meiotic events (Averbeck et al., 2005; Malapeira et al., 2005; Nakamura et al., 2002). Although their roles are not fully understood, they contribute to the increase in CDK and DDK activity that is required for late meiotic events such as meiotic recombination (Wan et al., 2008) and monoorientation of sister kinetochores (Matos et al., 2008). This is consistent with a model in which changes in in CDK and DDK activity promote the temporal order of meiotic progression (Gómez-Escoda and Wu, 2017). First, CDK activity is required for pre-meiotic S-phase (Figure 3); again, rather than the diversity in cyclin/CDK pairs, it appears that changes in CDK activity are the critical regulator (Gutiérrez-Escribano and Nurse, 2015). Similarly, DDK activity is also essential for meiotic DNA replication: deletion of the DDK partner Dbf4 prevents DNA replication (Valentin et al., 2006), while reducing its activity via an analog-sensitive mutation delays S-phase (Wan et al., 2006). Furthermore, CDK and DDK activities are critical for later meiotic events, from DSB formation through meiosis II (Figure 3). Elevated levels of CDK and DDK promote meiotic progression, and both activities play an important role in the formation of DSBs through phosphorylation of recombination factors. Indeed, CDK and DDK phosphorylation of Mer2 in budding yeast (homolog of Rec15 in *S. pombe*) is required for normal DSB formation (Henderson et al., 2006; Murakami and Keeney, 2014b). The increase in CDK and DDK activities after meiotic S-phase (Sclafani et al., 1988; Stuart and Wittenberg, 1998; Wan et al., 2008) is crucial for DSB formation as well as for commitment to meiosis I and meiosis II (Gutiérrez-Escribano and Nurse, 2015; Matos et al., 2008). Thus, regulation of CDK and DDK activities during meiosis is precisely regulated in order to ensure proper meiotic progression (Carlile and Amon, 2008).

IV.3 - Meiotic recombination

A prominent feature of meiosis is programmed recombination, which involves the formation of DNA double-strand breaks (DSB) that cells inflict on their own genomes (de Massy, 2013; Keeney, 2008). Generation of DSBs has potentially negative consequences, but in meiosis, this process is induced and highly regulated to promote both proper chromosome segregation during meiosis I (Page and Hawley, 2003) and the genetic shuffling that is a critical part of sexual reproduction (Handel and Schimenti, 2010; Székvölgyi and Nicolas, 2010). Programmed DSBs during meiosis are produced by

the conserved Spo11 protein (Rec12 in fission yeast) (Bergerat et al., 1997; Keeney et al., 1997; Steiner et al., 2002) in prophase I and requires its association with a number of regulatory partners (Keeney, 2008). Moreover, the formation of these DSBs is tightly controlled, as they have to occur at the right time during prophase I. Their deregulation provoke genome instability and can lead to pathologies such as cancer.

IV.3.a Meiotic DNA double-strand break formation by Spo11/Rec12

Meiotic DSBs are catalyzed by the evolutionarily conserved Spo11/Rec12 protein (De Veaux et al., 1992; Keeney, 2001) that is expressed only during meiosis (Lin and Smith, 1994). Spo11 shows homology with the archaeal Topoisomerase VIA (Keeney et al., 1997) and cleaves DNA via a type II topoisomerase-like mechanism (Keeney, 2008). It dimerizes and cleaves DNA in a transesterification reaction, which results in phosphodiester links between Spo11 and the DNA (Liu et al., 1995). The cleavage results in the formation of a two-nucleotide 5' overhang, leaving Spo11 covalently attached to the DNA (Liu et al., 1995).

Interestingly, Spo11 alone is not sufficient to generate DSBs. Its nuclease activity relies on its association with other proteins, which have so far been best characterized in the budding and fission yeasts (Figure 9A). These proteins interacts directly or indirectly with Spo11/Rec12 (Keeney, 2001; 2008; Miyoshi et al., 2012), forming complexes that interact with axial/linear element proteins and trigger the catalytic activity of Spo11/Rec12. In *S. pombe*, Rec7, Rec15 and Rec24 form the SFT (Seven-Fifteen-Twenty-four) subcomplex (Miyoshi et al., 2012), which interacts with the linear protein Rec10 through Rec15 (Miyoshi et al., 2012). In addition, Rec6, Rec14, and Rec12 form another subcomplex called the DSBC (DSB catalytic core) (Miyoshi et al., 2012). These subcomplexes then interact with Mde2 through Rec14 in the DSBC and Rec15 in the SFT (Miyoshi et al., 2012). Thus, the Rec12-associated proteins in fission yeast are organized in three different groups: SFT binds to DNA, while Mde2 structures the DNA to prepare for the binding of the DSBC, which then generates the DSBs (Figure 9B). Although the proteins involved in the generation of DSBs differs slightly in other organisms, the core components remain conserved among eukaryotes (Figure 9A) (Lam and Keeney, 2014).

A

	S. pombe	*S. cerevisiae*	Mammal
Function in *S. pombe*			
SFT	Rec7 [a]	Rec114 [a]	REC114 [a]
	Rec15 [a]	Mer2 [a]	-
	Rec24 [a]	Mei4 [a]	MEI4 [a]
Linear element	Rec10 [a]	Red1 [b]	
DSBC	Rec6 [a]	-	-
	Rec14 [a]	Ski8 [a]	WDR61 [c]
	Rec12 [a]	Spo11 [a]	SPO11 [a]
Link SFT and DSBC	Mde2 [a]	-	-
Other meiotic DSB		Rec102 [a]	
		Rec104 [a]	
	Rad32 [b]	Mre11 [a]	MRE11 [c]
	Rad50 [b]	Rad50 [a]	RAD50 [c]
	Nds1 [b]	Xrs2 [a]	NBS1 [c]
			MEI1 [c]

[a] Essential for DSB formation. [b] Not essential for DSB formation. [c] Unknown role in DSB formation.

B

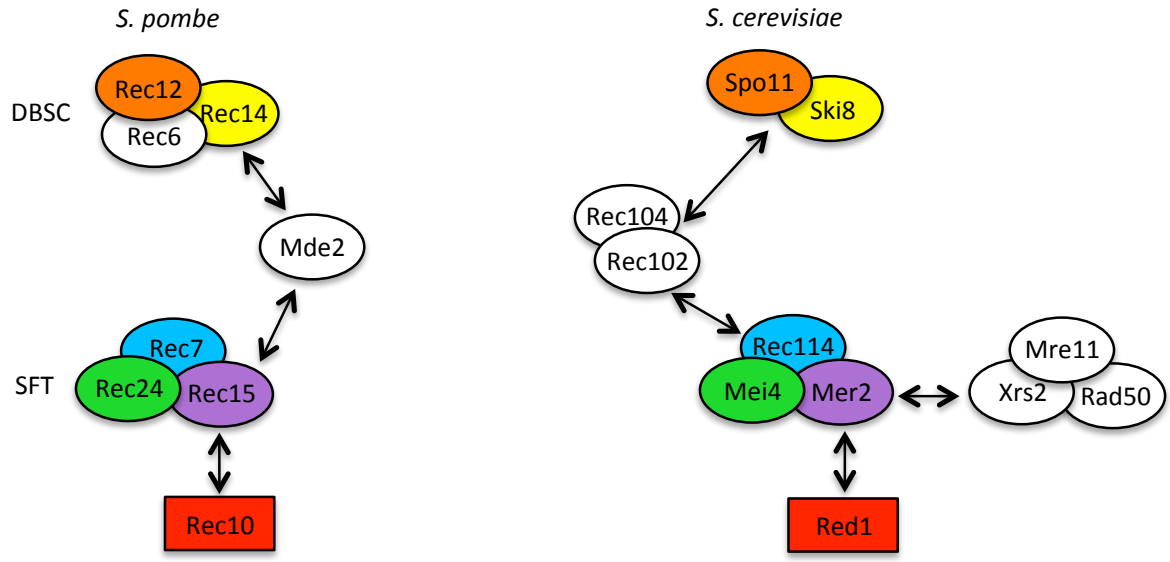

<u>Figure 9:</u> Proteins required for meiotic DSB in different organisms.
A) List of proteins required for meiotic DSB formation in *S. pombe, S. cerevisiae* and mammal (*Mus musculus*). B) Representation of the interactions between essential DSB proteins in *S. pombe* and *S. cerevisiae*. In fission yeast (left panel), seven proteins are known to be essential for the generation of of DSBs and are grouped in two subcomplexes (SFT and DSBC) that interact with on another through Mde2. In budding yeast (right panel), 10 proteins have been identified to be required for the generation of DSBs, subdivided in four complexes. The color code highlights homologous proteins between the two yeasts. Adapted from Lam et al. 2014.

IV.3.b From meiotic DNA double-strand break formation to repair

Once the Spo11/Rec12 dimer exerts its nuclease activity, it remains covalently linked to the 5' terminus of each broken DNA strand (Keeney et al., 1997). Removal of Spo11/Rec12 is achieved through the endonucleolytic activity of Mre11 (part of the Mre11-Rad50-Xrs2, or MRX, complex) and/or Sae2, which releases it along with a short oligonucleotide (12 to 14 nts) (Neale et al., 2005). The DNA is then resected by the endonuclease Exo1, which generates a longer 3' single-stranded tail on each DNA strand; in budding yeast, DSBs are resected by a mean length of 800 nts (Zakharyevich et al., 2010). The 3'-ssDNA tails are then bound by Replication Protein A (RPA), which helps to promote 5-3' DNA processing (Yan et al., 2011). RPA is then replaced by the Rad51 and Dmc1 recombinases (Fukushima et al., 2000; San Filippo et al., 2008), which catalyze strand invasion into the homologous duplex DNA, thus initiating repair synthesis. At this point, repair can be achieved by either the synthesis-dependent strand-annealing (SDSA) pathway or through the formation of a double holiday junction (dHJ). In SDSA, an important mechanism of non-crossover recombination, the homologous chromosome is used as a template by the invading DNA. The free 3' end invades the duplex DNA and forms a D-loop that then translocates as the invading strand is extended. The extended strand is then displaced from the template strand during branch migration of the single Holliday junction, which then base pairs with the opposite end of the original double-strand break. Following this, break repair is completed by DNA synthesis and ligation (Allers and Lichten, 2001; Lam and Keeney, 2014). In the dHJ pathway, the 5' end of the DSB is captured by the homologous chromosome, and a double Holliday junction is formed through DNA synthesis and ligation. Resolution of the dHJ then occurs through cutting the outside or crossed strands of each junction (Matos and West, 2014). Depending on the method of resolution, dHJs can result in either crossover or non-crossover events (Matos and West, 2014; Oke et al., 2014). Thus, the outcome of recombination initiated by a Spo11/Rec12-induced DSB relies on the repair strategy undertaken by the cell (Figure 10).

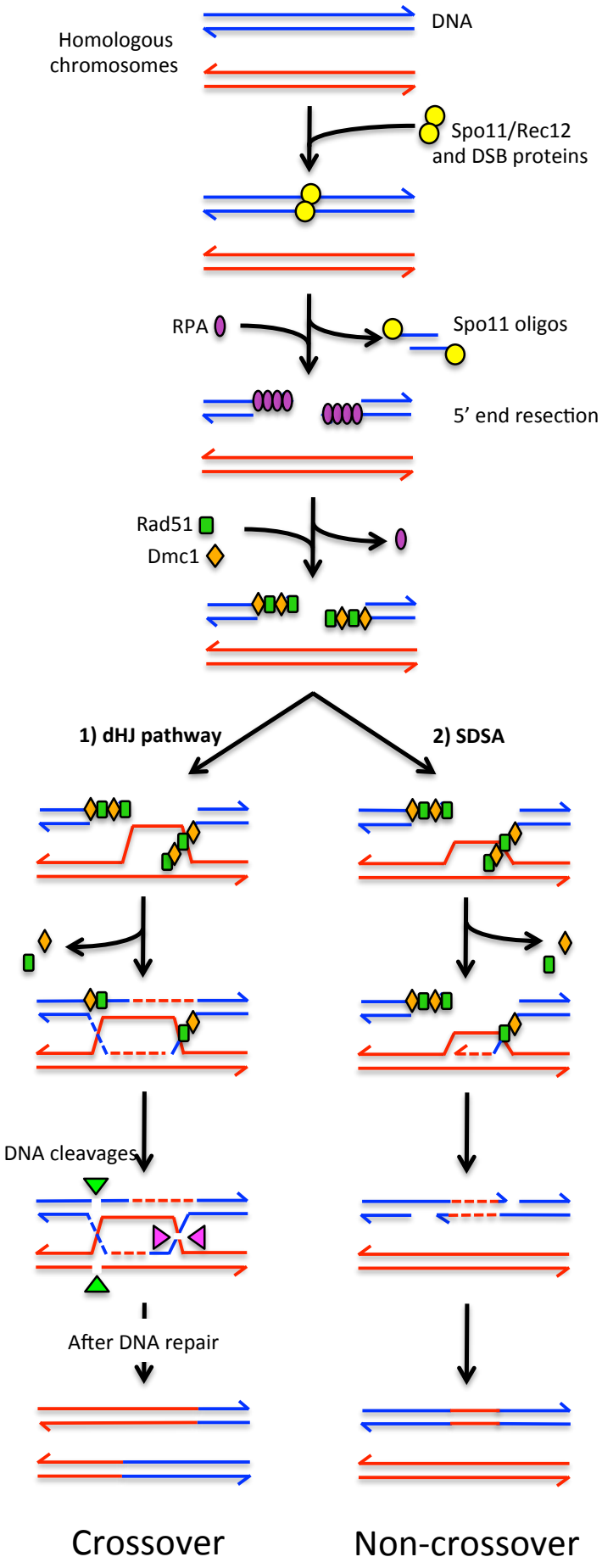
Homologous chromosomes
DNA
Spo11/Rec12 and DSB proteins
RPA
Spo11 oligos
5' end resection
Rad51
Dmc1
1) dHJ pathway
2) SDSA
DNA cleavages
After DNA repair
Crossover
Non-crossover

Figure 10: Overview of the meiotic recombination pathway.
Blue and red segments represent one sister chromatid of each of the homologous chromosomes. DSBs are catalyzed by Spo11/Rec12 in association with other DSB proteins. After cleavage, Spo11/Rec12 remains covalently linked to the 5' terminus of the broken DNA. Endonuclease activity to the 5' of Spo11/Rec12 releases oligos attached to Spo11. After cleavage, DNA ends are resected and capped by RPA protein. RPA is replaced by Rad51 and Dmc1 proteins, which promote DSB invasion into the homologous duplex DNA. Repair can proceed by two pathways. In the dHJ pathway, a double Holliday junction is formed whose resolution relies on DNA cleavages. One cleavage pattern which gives rise to a crossover (green and purple arrows) is represented here. The dHJ pathway does not always result in crossover products: non-crossover products can be generated as the result of specific cleavage patterns and/or repair mechanisms (Oke et al. 2014). In the SDSA pathway, the invading 3' strand is displaced after DNA synthesis and re-anneals to the other 3' end of the DSB. DNA synthesis and ligation give rise to non-crossover recombinant products. Adapted from Keeney, 2008.

IV.3.c Characteristics of the sites of double-strand break formation

The sites of Spo11/Rec12-dependent DSB formation do not occur randomly in the genome. There are "hot" and "cold" domains that cover large portion of the genome (Petes, 2001), and within "hot" regions, DSBs are clustered (70-250bp (de Massy, 2003)), surrounded by areas in which breaks forms rarely or at all (Keeney, 2008; Petes, 2001). Localized hotspots appear to be a common feature of meiotic recombination in eukaryotes (Cromie et al., 2007; Gerton et al., 2000; Keeney, 2008), but how they are determined remains unclear. Interestingly, while a number of studies have found no consensus sequences after analyzing the landscape of meiotic DSBs in eukaryotes (de Castro et al., 2012; Ohta et al., 1994; Wu and Lichten, 1994; Yamada et al., 2017a), DSB sites have been linked to specific chromatin contexts. First, in humans and mice, H3K4 trimethylation (H3K4me4) by the PRDM9 methyltransferase has been implicated in the specification of recombination hotspots (Baudat et al., 2010; Smagulova et al., 2011). Similarly, this modification has been associated with DSB sites in budding yeast (Kniewel and Keeney, 2009), although recent studies have indicated that this relationship may be indirect, as many DSB hotspots are not enriched for H3K4me3 (Tischfield and Keeney, 2012). The situation is unresolved in fission yeast as well: DSB hotspots have increased acetylation of histone H3 lysine 9 (H3K9), while H3K4me3 is not significantly enriched (Yamada et al., 2013; 2004). Nevertheless, deletion of the gene encoding the H3K4 methyltransferase *set1* was shown to alter DSB formation (Yamada

et al., 2013), confirming a potential role for this modification in DSB regulation. In addition to histone modifications, work in the fission yeast has identified a co-localization between DSBs and nucleosome-depleted regions (NDR), which have been proposed promote accessibility to the complexes that generate DSBs (de Castro et al., 2012). This study also highlighted a potential link between DSB formation and transcription. Indeed, modifications in the transcriptional pattern during meiosis affect the profile of DSB formation (de Castro et al., 2012): overexpression of the *caf5* gene generates an NDR in its promoter that coincides with a new site of DSB formation (de Castro et al., 2012). Moreover, comparison of meiotic transcriptome and recombination maps indicate that DSB hotpots are frequently located next to meiotically transcribed regions (Yamada et al., 2017b). Taken together, these observations highlight the multi-layered regulation of the sites of DSB formation during meiosis.

V – A link between meiotic DNA replication and double-strand break formation

During meiosis, the proper succession of genome duplication followed by the formation and repair of DNA breaks and chromosome segregation is tightly regulated in order to ensure the generation of viable haploid gametes. As we discussed previously, this succession of events is controlled by changes in CDK and DDK activity. Intriguingly, several studies have suggested a link between the crucial processes of DNA replication and meiotic recombination (Borde and Lichten, 2014; Miyoshi et al., 2012; Murakami and Nurse, 2001; Murakami and Keeney, 2014a; Wu and Nurse, 2014). However, the mechanisms that connect replication with subsequent meiotic events remain largely unexplored.

V.1 – Coordination between replication and meiotic recombination

Temporal regulation of meiotic DSB formation is essential: unrepaired DSBs are extremely deleterious for genome integrity, so it is crucial that they occur after DNA

replication and chromosome axis establishment in order to direct proper repair. The temporal coordination between pre-meiotic DNA replication and meiotic DSB formation has been demonstrated in several studies. Initial evidence for this relationship was provided by work in the budding yeast, which showed that a delay in meiotic replication resulted in a delay in meiotic DSB formation (Borde et al., 2000). In this study, the removal of specific ARS sequences on the left arm of chromosome III delayed replication of this region by about 60 min; this arm was passively replicated by replication forks that initiated in the right arm of the chromosome III. Interestingly, DSB generation was similarly delayed by 60 min compared to the right arm of the chromosome III. These and other findings therefore suggest that the timing of replication of a region determines the timing of DSB formation and that this regulation occurs in *cis* (Borde et al., 2000; Murakami et al., 2003). However, it is interesting to note that DSBs can form even when the genome is not completely duplicated in both budding and fission yeasts (Blitzblau et al., 2012) (Murakami and Nurse, 2001; Tonami et al., 2005). For instance, in fission yeast, the lack of functional component of the replication machinery blocked the completion of DNA replication but not the formation of DSB, which remains made at the same timing (Murakami and Nurse, 2001).

More recently, evidence was provided for a direct link between origin usage and meiotic DSB formation in the fission yeast (Wu and Nurse, 2014). By inducing meiosis in different nutritional conditions, which resulted in a genome-wide alteration of the pre-meiotic replication program, this study revealed corresponding changes in the frequency and the genome-wide distribution of DSB formation. Specifically, the authors showed that local changes in origin activity were linked to local changes in the frequency of DSB formation (Figure 11). Moreover, directly decreasing origin efficiencies through changes in Cdc45 levels led to a reduction in DSB formation. Thus, the authors hypothesized that the local recruitment of CDK or DDK, which phosphorylates both replication initiation (Labib et al., 1999; Larasati and Duncker, 2017; Liku et al., 2005; Mimura et al., 2004; Moll et al., 1991; Nguyen et al., 2000; 2001; Vas et al., 2001; Wuarin et al., 2002) and meiotic recombination proteins (Sasanuma et al., 2008; Wan et al., 2008), could locally regulate both processes. Taken together, these studies demonstrated a link between the two temporally separated events of pre-meiotic DNA replication and DSB formation.

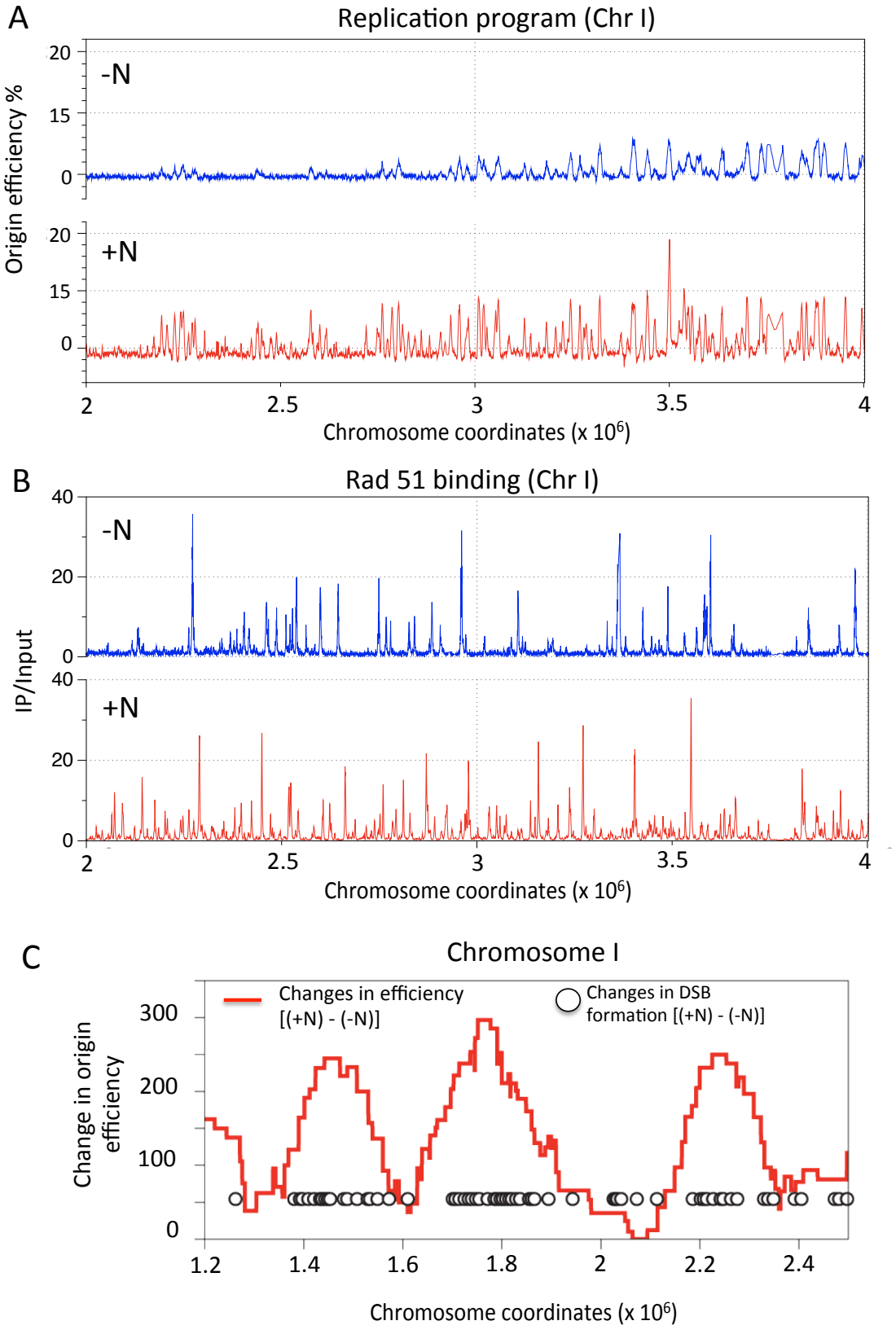
A
Replication program (Chr I)
Origin efficiency %
-N
+N
20
15
0
2
2.5
3
3.5
4
Chromosome coordinates (x 10⁶)
B
Rad 51 binding (Chr I)
IP/Input
-N
+N
40
20
0
2
2.5
3
3.5
4
Chromosome coordinates (x 10⁶)
C
Chromosome I
Changes in efficiency [(+N) - (-N)]
Changes in DSB formation [(+N) - (-N)]
Change in origin efficiency
300
200
100
0
1.2
1.4
1.6
1.8
2
2.2
2.4
Chromosome coordinates (x 10⁶)

Figure 11: Origin efficiency and meiotic recombination.
A) Replication profile of a region of chromosome 1 in diploid *pat1-114* fission yeast cells undergoing pre-meiotic S-phase after nitrogen deprivation (Top, blue) or in continuous nitrogen-rich conditions (Bottom, red). B) Profile of Rad51 binding, reflecting meiotic DSB formation, in cells undergoing meiosis after nitrogen deprivation (Top, blue) or in nitrogen-rich conditions (Bottom, red). C) Local changes in efficiency and DSB formation between nitrogen-deprived and nitrogen-rich conditions. Red line: sum of the differences in origin efficiencies [(+N)-(-N)] over 200 kb windows. Black circles: sites of greater than 2-fold changes in Rad51 binding ([(+N)/(-N)] ≥ 2). Adapted from Wu and Nurse, 2014.

V.2 – A role for DDK activity in linking replication and recombination in meiosis.

What then might be the links that associate pre-meiotic DNA replication and meiotic DSB formation? One mechanism is suggested by work in the budding yeast that implicates DDK as a key coordinator of these events (Murakami and Keeney, 2014a). As described in the previous sections, completion of pre-meiotic DNA replication and meiotic recombination requires phosphorylation of Mer2/Rec15 by both CDK and DDK. This led the authors to hypothesize that DDK recruited to the replisome may phosphorylate Mer2 after passage of the replication machinery, thus establishing the spatio-temporal coordination of replication and DSB formation. For this model to work, DDK levels must be limiting, and its kinase activity should be targeted to the replicated chromosome. To test this model, they first took advantage of budding yeast cells lacking ARSs on the left arm of the chromosome III (Borde et al., 2000), which delays both replication and DSB formation in this region. Overexpression of DDK restored the delay in DSB formation observed in the left arm of the chromosome III, suggesting that DDK activity is limiting for the establishment of DSBs. Next, as the DDK partner Dbf4 had been previously shown to interact with the fork protection complex (FPC), which travels with the replication machinery (Katou et al., 2003), the authors asked if the DDK may be recruited via this mechanism. Mutation in FPC components results a global delay in DSB formation in meiosis compared to wild type cells, and this delay is rescued by the fusion of Dbf4 to Cdc45. Finally, they showed that Mer2 phosphorylation by DDK is coordinated with local replication timing. These results thus indicate that the DDK

efficient recruitment to the replication fork may represent a key link between pre-meiotic DNA replication and meiotic DSB formation.

Despite these important findings, the mechanisms by which replication and DSB formation are coupled remain an open question. First, while DDK may be recruited to DNA through the interaction between Dbf4 and the replication machinery, the association between Dbf4 and the FPC appears to be transient or unstable (Murakami and Keeney, 2014b). Consequently, it remains unclear whether DDK travels with the replication fork during DNA synthesis. Alternatively, DDK may be recruited specifically to origins to modify nearby recombination factors. Next, evidence suggests that there may be mechanisms other than DDK phosphorylation of Mer2 that couple replication with recombination. For instance, a phosphomimetic form of Mer2 is not sufficient to produce DSBs (Wan et al., 2008), indicating that Mer2 may not be the only substrate of DDK that is required for recombination. Moreover, as Mer2/Rec15 function is essential for DSB formation, one prediction may be that its genome-wide binding profile reflects the pattern of DSB formation. However, comparison of the pattern of Rec15 binding in fission yeast (Miyoshi et al., 2012) with that of DSB formation as determined by localization of the Rad51 recombination factor (Wu et al., 2014) reveals a lack of overall co-localization (Figure 12). Finally, although DSB formation requires high levels of CDK and DDK activity (Sclafani et al., 1988; Stuart and Wittenberg, 1998; Wan et al., 2008), the current model suggests that the phosphorylation of Mer2 by DDK would occur during S-phase, when DDK activity is low. One intriguing possibility is that the increasing level of DDK and CDK may coordinate additional mechanisms that regulate DSB formation that may be established during the time interval between replication and DSB formation. All together, these findings indicate that there are potentially multiple layers of regulation that link pre-meiotic DNA replication with DSB formation and recombination.

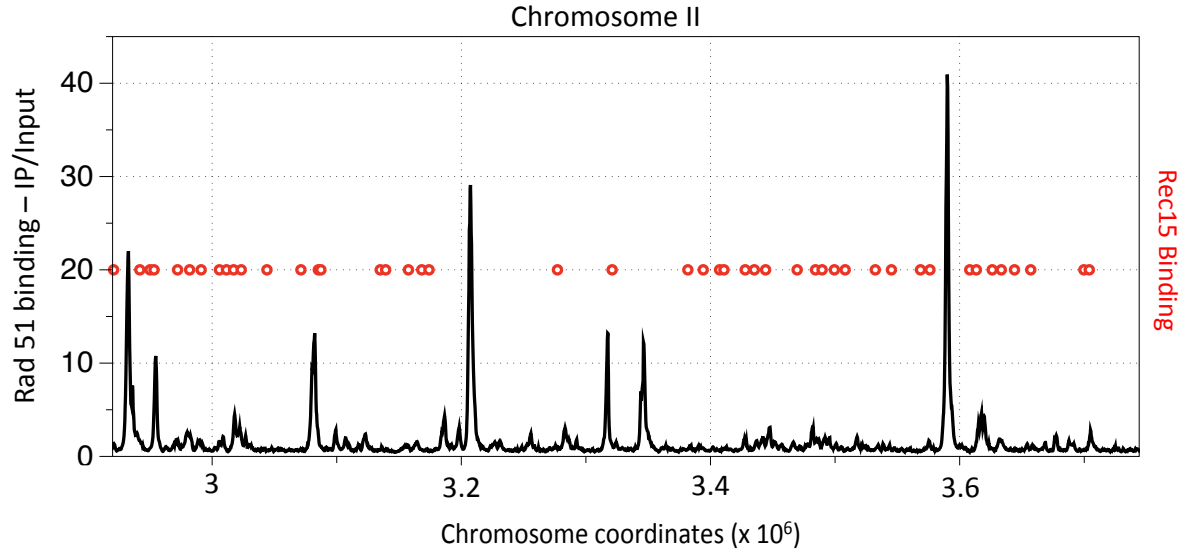

Figure 12: Pattern of Rad51 and Rec15 binding to DNA in during meiosis.
Recruitment of Rad51 (black) (Wu and Nurse. 2014) and Rec15/Mer2 (red circle) (Miyoshi et al 2012) in a representative region of the genome during meiosis in a *pat1-114* diploid after nitrogen depletion. Rad51 is bound at sites of meiotic DSB formation.

VI – Objectives

Over the last decades, a number of studies have suggested a link between DNA replication and meiotic DSB formation (Borde et al., 2000; Murakami and Nurse, 2001; Murakami and Keeney, 2014a; Wu and Nurse, 2014). However, the mechanisms linking these two critical processes are not fully understood. My thesis takes two approaches to investigate the crosstalk between genome duplication and meiotic recombination.

VI.1 – Evaluating the impact of regional changes in origin selection on DSB formation

Previous work has shown that increases in origin usage in a region are associated with increases in meiotic DSB formation (Wu and Nurse, 2014). One potential model would be that higher levels of replication initiation increase the concentration of replication factors that interact with recombination components, thus favouring DSB formation. Interestingly, DNA replication is organized in timing and efficiency domains along the chromosomes, (Heichinger et al., 2006; Wu and Nurse,

2009) and regions that are duplicated at the same time tend to be located next one another in the nucleus (Berezney et al., 2000; Pichugina et al., 2016). Thus, regional alterations of replication initiation may have local or even long-range effects on DSB formation. To study this possibility, I have used chromosomal arrangements that alter the replication program and assessed the impact of these changes on meiotic recombination.

VI.2 – Assessing the local requirement for DNA replication in DSB formation.

While replication initiation itself may promote meiotic recombination, it is also possible that the interaction between replication and recombination factors requires passage of the replication machinery through DSB sites. To address this hypothesis, I have constructed a system that integrates inducible replication fork barriers to determine whether the replication machinery must progress through a DSB site before breaks are formed or whether origin activation is sufficient to induce the formation of a nearby DSB.

References

Aladjem, M.I. (2007). Replication in context: dynamic regulation of DNA replication patterns in metazoans. Nat Rev Genet *8*, 588–600.

Allers, T., and Lichten, M. (2001). Differential timing and control of noncrossover and crossover recombination during meiosis. Cell *106*, 47–57.

Anglana, M., Apiou, F., Bensimon, A., and Debatisse, M. (2003). Dynamics of DNA replication in mammalian somatic cells: nucleotide pool modulates origin choice and interorigin spacing. Cell *114*, 385–394.

Arellano, M., and Moreno, S. (1997). Regulation of CDK/cyclin complexes during the cell cycle. Int. J. Biochem. Cell Biol. *29*, 559–573.

Averbeck, N., Sunder, S., Sample, N., Wise, J.A., and Leatherwood, J. (2005). Negative control contributes to an extensive program of meiotic splicing in fission yeast. Molecular Cell *18*, 491–498.

Barnum, K.J., and O'Connell, M.J. (2014). Cell cycle regulation by checkpoints. Methods Mol. Biol. *1170*, 29–40.

Baudat, F., Buard, J., Grey, C., Fledel-Alon, A., Ober, C., Przeworski, M., Coop, G., and de Massy, B. (2010). PRDM9 is a major determinant of meiotic recombination hotspots in humans and mice. Science *327*, 836–840.

Bähler, J., Schuchert, P., Grimm, C., and Kohli, J. (1991). Synchronized meiosis and recombination in fission yeast: observations with pat1-114 diploid cells. Curr Genet.

Benito, J., Martín-Castellanos, C., and Moreno, S. (1998). Regulation of the G1 phase of the cell cycle by periodic stabilization and degradation of the p25rum1 CDK inhibitor. Embo J. *17*, 482–497.

Berezney, R., Dubey, D.D., and Huberman, J.A. (2000). Heterogeneity of eukaryotic replicons, replicon clusters, and replication foci. Chromosoma *108*, 471–484.

Bergerat, A., de Massy, B., Gadelle, D., Varoutas, P.C., Nicolas, A., and Forterre, P. (1997). An atypical topoisomerase II from Archaea with implications for meiotic recombination. Nature *386*, 414–417.

Blanco, M.A., Sánchez-Díaz, A., de Prada, J.M., and Moreno, S. (2000). APC(ste9/srw1) promotes degradation of mitotic cyclins in G(1) and is inhibited by cdc2 phosphorylation. Embo J. *19*, 3945–3955.

Blitzblau, H.G., Chan, C.S., Hochwagen, A., and Bell, S.P. (2012). Separation of DNA replication from the assembly of break-competent meiotic chromosomes. PLoS Genet *8*, e1002643.

Borde, V. (2000). Direct Coupling Between Meiotic DNA Replication and Recombination Initiation. Science *290*, 806–809.

Borde, V., Goldman, A.S., and Lichten, M. (2000). Direct coupling between meiotic DNA replication and recombination initiation. Science *290*, 806–809.

Borde, V., and Lichten, M. (2014). A Timeless but Timely Connection between Replication and Recombination. Cell *158*, 697–698.

Boye, E., and Grallert, B. (2009). In DNA Replication, the Early Bird Catches the Worm. Cell *136*, 812–814.

Brown, G.W., and Kelly, T.J. (1999). Cell cycle regulation of Dfp1, an activator of the Hsk1 protein kinase. Proc. Natl. Acad. Sci. U.S.a. *96*, 8443–8448.

Buonomo, S.B., Clyne, R.K., Fuchs, J., Loidl, J., Uhlmann, F., and Nasmyth, K. (2000). Disjunction of homologous chromosomes in meiosis I depends on proteolytic cleavage of the meiotic cohesin Rec8 by separin. Cell *103*, 387–398.

Cadoret, J.-C., Meisch, F., Hassan-Zadeh, V., Luyten, I., Guillet, C., Duret, L., Quesneville, H., and Prioleau, M.-N. (2008). Genome-wide studies highlight indirect links between human replication origins and gene regulation. Proc. Natl. Acad. Sci. U.S.a. *105*, 15837–15842.

Carlile, T.M., and Amon, A. (2008). Meiosis I is established through division-specific translational control of a cyclin. Cell *133*, 280–291.

Cayrou, C., Coulombe, P., Vigneron, A., Stanojcic, S., Ganier, O., Peiffer, I., Rivals, E., Puy, A., Laurent-Chabalier, S., Desprat, R., et al. (2011). Genome-scale analysis of metazoan replication origins reveals their organization in specific but flexible sites defined by conserved features. Genome Res. *21*, 1438–1449.

Chikashige, Y., Ding, D.Q., Funabiki, H., Haraguchi, T., Mashiko, S., Yanagida, M., and Hiraoka, Y. (1994). Telomere-led premeiotic chromosome movement in fission yeast. Science *264*, 270–273.

Chikashige, Y., Ding, D.Q., Imai, Y., Yamamoto, M., Haraguchi, T., and Hiraoka, Y. (1997). Meiotic nuclear reorganization: switching the position of centromeres and telomeres in the fission yeast Schizosaccharomyces pombe. Embo J. *16*, 193–202.

Cipak, L., Hyppa, R.W., Smith, G.R., and Gregan, J. (2012). ATP analog-sensitive Pat1 protein kinase for synchronous fission yeast meiosis at physiological temperature. Cell Cycle *11*, 1626–1633.

Coker, W.C., and Wilson, L. (1911). Schizosaccharomyces octosporus. Mycologia.

Connolly, T., and Beach, D. (1994). Interaction between the Cig1 and Cig2 B-type cyclins in the fission yeast cell cycle. Molecular and Cellular Biology *14*, 768–776.

Cornacchia, D., Dileep, V., Quivy, J.-P., Foti, R., Tili, F., Santarella-Mellwig, R., Antony, C., Almouzni, G., Gilbert, D.M., and Buonomo, S.B.C. (2012). Mouse Rif1 is a key regulator of the replication-timing programme in mammalian cells. Embo J. *31*, 3678–3690.

Correa-Bordes, J., Gulli, M.P., and Nurse, P. (1997). p25rum1 promotes proteolysis of the

mitotic B-cyclin p56cdc13 during G1 of the fission yeast cell cycle. Embo J. *16*, 4657–4664.

Coudreuse, D., and Nurse, P. (2010). Driving the cell cycle with a minimal CDK control network. Nature *468*, 1074–1079.

Coverley, D., Pelizon, C., Trewick, S., and Laskey, R.A. (2000). Chromatin-bound Cdc6 persists in S and G2 phases in human cells, while soluble Cdc6 is destroyed in a cyclin A-cdk2 dependent process. J. Cell. Sci. *113 (Pt 11)*, 1929–1938.

Cromie, G.A., Hyppa, R.W., Cam, H.P., Farah, J.A., Grewal, S.I.S., and Smith, G.R. (2007). A discrete class of intergenic DNA dictates meiotic DNA break hotspots in fission yeast. PLoS Genet *3*, e141.

Das, S.P., Borrman, T., Liu, V.W.T., Yang, S.C.H., Bechhoefer, J., and Rhind, N. (2015). Replication timing is regulated by the number of MCMs loaded at origins. Genome Res. *25*, 1886–1892.

de Castro, E., Soriano, I., Marín, L., Serrano, R., Quintales, L., and Antequera, F. (2012). Nucleosomal organization of replication origins and meiotic recombination hotspots in fission yeast. Embo J. *31*, 124–137.

de Massy, B. (2003). Distribution of meiotic recombination sites. Trends in Genetics *19*, 514–522.

de Massy, B. (2013). Initiation of Meiotic Recombination: How and Where? Conservation and Specificities Among Eukaryotes. Annu. Rev. Genet. *47*, 563–599.

De Veaux, L.C., Hoagland, N.A., and Smith, G.R. (1992). Seventeen complementation groups of mutations decreasing meiotic recombination in Schizosaccharomyces pombe. Genetics *130*, 251–262.

Ding, D.Q., Chikashige, Y., Haraguchi, T., and Hiraoka, Y. (1998). Oscillatory nuclear movement in fission yeast meiotic prophase is driven by astral microtubules, as revealed by continuous observation of chromosomes and microtubules in living cells. J. Cell. Sci. *111 (Pt 6)*, 701–712.

Domingo-Sananes, M.R., Kapuy, O., Hunt, T., and Novák, B. (2011). Switches and latches: a biochemical tug-of-war between the kinases and phosphatases that control mitosis. Philos. Trans. R. Soc. Lond., B, Biol. Sci. *366*, 3584–3594.

Donaldson, A.D., Raghuraman, M.K., Friedman, K.L., Cross, F.R., Brewer, B.J., and Fangman, W.L. (1998). CLB5-dependent activation of late replication origins in S. cerevisiae. Molecular Cell *2*, 173–182.

Dulić, V., Lees, E., and Reed, S.I. (1992). Association of human cyclin E with a periodic G1-S phase protein kinase. Science *257*, 1958–1961.

Evrin, C., Clarke, P., Zech, J., Lurz, R., Sun, J., Uhle, S., Li, H., Stillman, B., and Speck, C. (2009). A double-hexameric MCM2-7 complex is loaded onto origin DNA during licensing of eukaryotic DNA replication. Proc. Natl. Acad. Sci. U.S.a. *106*, 20240–20245.

Félix, M.A., Labbé, J.C., Dorée, M., Hunt, T., and Karsenti, E. (1990). Triggering of cyclin degradation in interphase extracts of amphibian eggs by cdc2 kinase. Nature *346*, 379–382.

Fisher, D., and Nurse, P. (1995). Cyclins of the fission yeast Schizosaccharomyces pombe. Semin. Cell Biol. *6*, 73–78.

Fisher, D.L., and Nurse, P. (1996). A single fission yeast mitotic cyclin B p34cdc2 kinase promotes both S-phase and mitosis in the absence of G1 cyclins. Embo J. *15*, 850–860.

Fisher, D. (2011). Control of DNA replication by cyclin-dependent kinases in development. Results Probl Cell Differ *53*, 201–217.

Forsburg, S.L., and Hodson, J.A. (2000). Mitotic replication initiation proteins are not required for pre-meiotic S phase. Nat. Genet. *25*, 263–268.

Forsburg, S.L. (2003). S. pombe strain maintenance and media. Curr Protoc Mol Biol *Chapter 13*, Unit13.15.

Forsburg, S.L., and Rhind, N. (2006). Basic methods for fission yeast. Yeast *23*, 173–183.

Foti, R., Gnan, S., Cornacchia, D., Dileep, V., Bulut-Karslioglu, A., Diehl, S., Buness, A., Klein, F.A., Huber, W., Johnstone, E., et al. (2016). Nuclear Architecture Organized by Rif1 Underpins the Replication-Timing Program. Molecular Cell *61*, 260–273.

Fukushima, K., Tanaka, Y., Nabeshima, K., Yoneki, T., Tougan, T., Tanaka, S., and Nojima, H. (2000). Dmc1 of Schizosaccharomyces pombe plays a role in meiotic recombination. Nucleic Acids Research *28*, 2709–2716.

Gerton, J.L., DeRisi, J., Shroff, R., Lichten, M., Brown, P.O., and Petes, T.D. (2000). Global mapping of meiotic recombination hotspots and coldspots in the yeast Saccharomyces cerevisiae. Proc. Natl. Acad. Sci. U.S.a. *97*, 11383–11390.

Gérard, C., and Goldbeter, A. (2009). Temporal self-organization of the cyclin/Cdk network driving the mammalian cell cycle. Proc. Natl. Acad. Sci. U.S.a. *106*, 21643–21648.

Gould, K.L., and Nurse, P. (1989). Tyrosine phosphorylation of the fission yeast cdc2+ protein kinase regulates entry into mitosis. Nature *342*, 39–45.

Gómez-Escoda, B., and Wu, P.-Y.J. (2017). Roles of CDK and DDK in Genome Duplication and Maintenance: Meiotic Singularities. Genes *8*.

Guerra-Moreno, A., Alves-Rodrigues, I., Hidalgo, E., and Ayté, J. (2012). Chemical genetic induction of meiosis in Schizosaccharomyces pombe. Cell Cycle *11*, 1621–1625.

Gutiérrez-Escribano, P., and Nurse, P. (2015). A single cyclin-CDK complex is sufficient for both mitotic and meiotic progression in fission yeast. Nature Communications *6*, 6871.

Gutz, H., Heslot, H., Leupold, U., and Loprieno, N. (1974). Schizosaccharomyces pombe.

Handbook of Genetics; Vol1 Bacteria, Bacteriophages and Fungi, 395-446.

Hagan, I., Hayles, J., and Nurse, P. (1988). Cloning and sequencing of the cyclin-related cdc13+ gene and a cytological study of its role in fission yeast mitosis. J. Cell. Sci. *91 (Pt 4)*, 587–595.

Handel, M.A., and Schimenti, J.C. (2010). Genetics of mammalian meiosis: regulation, dynamics and impact on fertility. Nat Rev Genet *11*, 124–136.

Harigaya, Y., and Yamamoto, M. (2007). Molecular mechanisms underlying the mitosis-meiosis decision. Chromosome Res. *15*, 523–537.

Harper, L., Golubovskaya, I., and Cande, W.Z. (2004). A bouquet of chromosomes. J. Cell. Sci. *117*, 4025–4032.

Hateboer, G., Wobst, A., Petersen, B.O., Le Cam, L., Vigo, E., Sardet, C., and Helin, K. (1998). Cell cycle-regulated expression of mammalian CDC6 is dependent on E2F. Molecular and Cellular Biology *18*, 6679–6697.

Hayano, M., Kanoh, Y., Matsumoto, S., Renard-Guillet, C., Shirahige, K., and Masai, H. (2012). Rif1 is a global regulator of timing of replication origin firing in fission yeast. Genes & Development *26*, 137–150.

Hayles, J., and Nurse, P. (1992). Genetics of the fission yeast Schizosaccharomyces pombe. Annu. Rev. Genet. *26*, 373–402.

Heichinger, C., Penkett, C.J., Bähler, J., and Nurse, P. (2006). Genome-wide characterization of fission yeast DNA replication origins. Embo J. *25*, 5171–5179.

Heller, R.C., Kang, S., Lam, W.M., Chen, S., Chan, C.S., and Bell, S.P. (2011). Eukaryotic origin-dependent DNA replication in vitro reveals sequential action of DDK and S-CDK kinases. Cell *146*, 80–91.

Helston, R.M., Box, J.A., Tang, W., and Baumann, P. (2010). Schizosaccharomyces cryophilus sp. nov., a new species of fission yeast. FEMS Yeast Res. *10*, 779–786.

Henderson, K.A., Kee, K., Maleki, S., Santini, P.A., and Keeney, S. (2006). Cyclin-dependent kinase directly regulates initiation of meiotic recombination. Cell.

Hirano, T., Funahashi, S., Uemura, T., and Yanagida, M. (1986). Isolation and characterization of Schizosaccharomyces pombe cutmutants that block nuclear division but not cytokinesis. Embo J. *5*, 2973–2979.

Hiraoka, Y., Ding, D.Q., Yamamoto, A., Tsutsumi, C., and Chikashige, Y. (2000). Characterization of fission yeast meiotic mutants based on live observation of meiotic prophase nuclear movement. Chromosoma *109*, 103–109.

Hiratani, I., Ryba, T., Itoh, M., Yokochi, T., Schwaiger, M., Chang, C.-W., Lyou, Y., Townes, T.M., Schübeler, D., and Gilbert, D.M. (2008). Global reorganization of replication domains during embryonic stem cell differentiation. PLoS Biol *6*, e245.

Hoffman, C.S., Wood, V., and Fantes, P.A. (2015). An Ancient Yeast for Young Geneticists: A Primer on the Schizosaccharomyces pombe Model System. Genetics *201*, 403–423.

Huberman, J.A., and Riggs, A.D. (1966). Autoradiography of chromosomal DNA fibers from Chinese hamster cells. Proc. Natl. Acad. Sci. U.S.a. *55*, 599–606.

Hyrien, O., and Mechali, M. (1993). Chromosomal replication initiates and terminates at random sequences but at regular intervals in the ribosomal DNA of Xenopus early embryos. Embo J. *12*, 4511–4520.

Hyrien, O., Maric, C., and Mechali, M. (1995). Transition in specification of embryonic metazoan DNA replication origins. Science *270*, 994–997.

Iino, Y., and Yamamoto, M. (1985). Negative control for the initiation of meiosis in Schizosaccharomyces pombe. Proc. Natl. Acad. Sci. U.S.a. *82*, 2447–2451.

Jackson, A.L., Pahl, P.M., Harrison, K., Rosamond, J., and Sclafani, R.A. (1993). Cell cycle regulation of the yeast Cdc7 protein kinase by association with the Dbf4 protein. Molecular and Cellular Biology *13*, 2899–2908.

Kamimura, Y., Masumoto, H., Sugino, A., and Araki, H. (1998). Sld2, which interacts with Dpb11 in Saccharomyces cerevisiae, is required for chromosomal DNA replication. Molecular and Cellular Biology *18*, 6102–6109.

Kamimura, Y., Tak, Y.S., Sugino, A., and Araki, H. (2001). Sld3, which interacts with Cdc45 (Sld4), functions for chromosomal DNA replication in Saccharomyces cerevisiae. Embo J. *20*, 2097–2107.

Katou, Y., Kanoh, Y., Bando, M., Noguchi, H., Tanaka, H., Ashikari, T., Sugimoto, K., and Shirahige, K. (2003). S-phase checkpoint proteins Tof1 and Mrc1 form a stable replication-pausing complex. Nature *424*, 1078–1083.

Kaykov, A., and Nurse, P. (2015). The spatial and temporal organization of origin firing during the S-phase of fission yeast. Genome Res. *25*, 391–401.

Keeney, S. (2001). Mechanism and control of meiotic recombination initiation. Curr. Top. Dev. Biol. *52*, 1–53.

Keeney, S., Giroux, C.N., and Kleckner, N. (1997). Meiosis-specific DNA double-strand breaks are catalyzed by Spo11, a member of a widely conserved protein family. Cell *88*, 375–384.

Keeney, S. (2008). Spo11 and the Formation of DNA Double-Strand Breaks in Meiosis. Genome Dyn Stab *2*, 81–123.

Kelly, T.J., Martin, G.S., Forsburg, S.L., Stephen, R.J., Russo, A., and Nurse, P. (1993). The fission yeast cdc18+ gene product couples S phase to START and mitosis. Cell *74*, 371–382.

Kim, D.-U., Hayles, J., Kim, D., Wood, V., Park, H.-O., Won, M., Yoo, H.-S., Duhig, T., Nam, M., Palmer, G., et al. (2010). Analysis of a genome-wide set of gene deletions in the fission

yeast Schizosaccharomyces pombe. Nat. Biotechnol. *28*, 617–623.

Kimble, J. (2011). Molecular Regulation of the Mitosis/Meiosis Decision in Multicellular Organisms. Cold Spring Harb Perspect Biol *3*, a002683–a002683.

Kitamura, K., Katayama, S., Dhut, S., Sato, M., Watanabe, Y., Yamamoto, M., and Toda, T. (2001). Phosphorylation of Mei2 and Ste11 by Pat1 kinase inhibits sexual differentiation via ubiquitin proteolysis and 14-3-3 protein in fission yeast. Developmental Cell *1*, 389–399.

Kniewel, R., and Keeney, S. (2009). Histone methylation sets the stage for meiotic DNA breaks. Embo J. *28*, 81–83.

Knott, S.R.V., Peace, J.M., Ostrow, A.Z., Gan, Y., Rex, A.E., Viggiani, C.J., Tavaré, S., and Aparicio, O.M. (2012). Forkhead transcription factors establish origin timing and long-range clustering in S. cerevisiae. Cell *148*, 99–111.

Koff, A., Giordano, A., Desai, D., Yamashita, K., Harper, J.W., Elledge, S., Nishimoto, T., Morgan, D.O., Franza, B.R., and Roberts, J.M. (1992). Formation and activation of a cyclin E-cdk2 complex during the G1 phase of the human cell cycle. Science *257*, 1689–1694.

Kozar, K., Ciemerych, M.A., Rebel, V.I., Shigematsu, H., Zagozdzon, A., Sicinska, E., Geng, Y., Yu, Q., Bhattacharya, S., Bronson, R.T., et al. (2004). Mouse development and cell proliferation in the absence of D-cyclins. Cell *118*, 477–491.

Kumagai, A., Shevchenko, A., Shevchenko, A., and Dunphy, W.G. (2010). Treslin collaborates with TopBP1 in triggering the initiation of DNA replication. Cell *140*, 349–359.

Labib, K., Diffley, J.F., and Kearsey, S.E. (1999). G1-phase and B-type cyclins exclude the DNA-replication factor Mcm4 from the nucleus. Nat. Cell Biol. *1*, 415–422.

Lam, I., and Keeney, S. (2014). Mechanism and regulation of meiotic recombination initiation. Cold Spring Harb Perspect Biol *7*, a016634.

Larasati, and Duncker, B. (2017). Mechanisms Governing DDK Regulation of the Initiation of DNA Replication. Genes *8*, 3.

Lee, K.Y., Bang, S.W., Yoon, S.W., Lee, S.-H., Yoon, J.-B., and Hwang, D.S. (2012). Phosphorylation of ORC2 protein dissociates origin recognition complex from chromatin and replication origins. Journal of Biological Chemistry *287*, 11891–11898.

Leupold, U. (1987). Sex appeal in fission yeast. Curr Genet.

Liku, M.E., Nguyen, V.Q., and Rosales, A.W. (2005). CDK phosphorylation of a novel NLS-NES module distributed between two subunits of the Mcm2-7 complex prevents chromosomal rereplication. Molecular Biology of the ….

Lin, Y., and Smith, G.R. (1994). Transient, meiosis-induced expression of the rec6 and rec12 genes of Schizosaccharomyces pombe. Genetics *136*, 769–779.

Lindner, K., Gregan, J., Montgomery, S., and Kearsey, S.E. (2002). Essential role of MCM proteins in premeiotic DNA replication. Mol. Biol. Cell *13*, 435–444.

Liu, J., Wu, T.C., and Lichten, M. (1995). The location and structure of double-strand DNA breaks induced during yeast meiosis: evidence for a covalently linked DNA-protein intermediate. Embo J. *14*, 4599–4608.

Longhese, M.P., Bonetti, D., Guerini, I., Manfrini, N., and Clerici, M. (2009). DNA double-strand breaks in meiosis: checking their formation, processing and repair. DNA Repair *8*, 1127–1138.

Longhese, M.P., Guerini, I., Baldo, V., and Clerici, M. (2008). Surveillance mechanisms monitoring chromosome breaks during mitosis and meiosis. DNA Repair *7*, 545–557.

Lundgren, K., Walworth, N., Booher, R., Dembski, M., Kirschner, M., and Beach, D. (1991). mik1 and wee1 cooperate in the inhibitory tyrosine phosphorylation of cdc2. Cell *64*, 1111–1122.

MacAlpine, H.K., Gordân, R., Powell, S.K., Hartemink, A.J., and MacAlpine, D.M. (2010). Drosophila ORC localizes to open chromatin and marks sites of cohesin complex loading. Genome Res. *20*, 201–211.

Malapeira, J., Moldón, A., Hidalgo, E., Smith, G.R., Nurse, P., and Ayté, J. (2005). A meiosis-specific cyclin regulated by splicing is required for proper progression through meiosis. Molecular and Cellular Biology *25*, 6330–6337.

Malumbres, M., and Barbacid, M. (2009). Cell cycle, CDKs and cancer: a changing paradigm. Nat Rev Cancer *9*, 153–166.

Mantiero, D., Mackenzie, A., Donaldson, A., and Zegerman, P. (2011). Limiting replication initiation factors execute the temporal programme of origin firing in budding yeast. Embo J. *30*, 4805–4814.

Marston, A.L., and Amon, A. (2004). Meiosis: cell-cycle controls shuffle and deal. Nat. Rev. Mol. Cell Biol. *5*, 983–997.

Martín-Castellanos, C., Blanco, M.A., de Prada, J.M., and Moreno, S. (2000). The puc1 cyclin regulates the G1 phase of the fission yeast cell cycle in response to cell size. Mol. Biol. Cell *11*, 543–554.

Masumoto, H., Muramatsu, S., Kamimura, Y., and Araki, H. (2002). S-Cdk-dependent phosphorylation of Sld2 essential for chromosomal DNA replication in budding yeast. Nature *415*, 651–655.

Matos, J., and West, S.C. (2014). ARTICLE IN PRESS. DNA Repair 1–6.

Matos, J., Lipp, J.J., Bogdanova, A., Guillot, S., Okaz, E., Junqueira, M., Shevchenko, A., and Zachariae, W. (2008). Dbf4-dependent CDC7 kinase links DNA replication to the segregation of homologous chromosomes in meiosis I. Cell *135*, 662–678.

Matsumura, T., Yuasa, T., Hayashi, T., Obara, T., Kimata, Y., and Yanagida, M. (2003). A

brute force postgenome approach to identify temperature-sensitive mutations that negatively interact with separase and securin plasmids. Genes Cells *8*, 341–355.

Matsushime, H., Ewen, M.E., Strom, D.K., Kato, J.Y., Hanks, S.K., Roussel, M.F., and Sherr, C.J. (1992). Identification and properties of an atypical catalytic subunit (p34PSK-J3/cdk4) for mammalian D type G1 cyclins. Cell *71*, 323–334.

McDowall, M.D., Harris, M.A., Lock, A., Rutherford, K., Staines, D.M., Bähler, J., Kersey, P.J., Oliver, S.G., and Wood, V. (2015). PomBase 2015: updates to the fission yeast database. Nucleic Acids Research *43*, D656–D661.

McLeod, M., and Beach, D. (1988). A specific inhibitor of the ran1+ protein kinase regulates entry into meiosis in Schizosaccharomyces pombe. Nature *332*, 509–514.

Meyerson, M., and Harlow, E. (1994). Identification of G1 kinase activity for cdk6, a novel cyclin D partner. Molecular and Cellular Biology *14*, 2077–2086.

Méchali, M. (2010). Eukaryotic DNA replication origins:many choices for appropriate answers. Nature Publishing Group *11*, 728–738.

Miki, F., Okazaki, K., Shimanuki, M., Yamamoto, A., Hiraoka, Y., and Niwa, O. (2002). The 14-kDa dynein light chain-family protein Dlc1 is required for regular oscillatory nuclear movement and efficient recombination during meiotic prophase in fission yeast. Mol. Biol. Cell *13*, 930–946.

Millar, J.B., McGowan, C.H., Lenaers, G., Jones, R., and Russell, P. (1991). p80cdc25 mitotic inducer is the tyrosine phosphatase that activates p34cdc2 kinase in fission yeast. Embo J. *10*, 4301–4309.

Mimura, S., Seki, T., Tanaka, S., and Diffley, J. (2004). Phosphorylation-dependent binding of mitotic cyclins to Cdc6 contributes to DNA replication control. Nature.

Mittnacht, S. (1998). Control of pRB phosphorylation. Current Opinion in Genetics & Development *8*, 21–27.

Miyoshi, T., Ito, M., Kugou, K., Yamada, S., Furuichi, M., Oda, A., Yamada, T., Hirota, K., Masai, H., and Ohta, K. (2012). A central coupler for recombination initiation linking chromosome architecture to S phase checkpoint. Molecular Cell *47*, 722–733.

Mojardín, L., Vázquez, E., and Antequera, F. (2013). Specification of DNA replication origins and genomic base composition in fission yeasts. J. Mol. Biol. *425*, 4706–4713.

Moll, T., Tebb, G., Surana, U., Robitsch, H., and Nasmyth, K. (1991). The role of phosphorylation and the CDC28 protein kinase in cell cycle-regulated nuclear import of the S. cerevisiae transcription factor SW15. Cell.

Mondesert, O., Mondesert, O., McGowan, C.H., McGowan, C.H., Russell, P., and Russell, P. (1996). Cig2, a B-type cyclin, promotes the onset of S in Schizosaccharomyces pombe. Molecular and Cellular Biology *16*, 1527–1533.

Moore, J.D., Kirk, J.A., and Hunt, T. (2003). Unmasking the S-phase-promoting potential

of cyclin B1. Science *300*, 987–990.

Moreno, S., Hayles, J., and Nurse, P. (1989). Regulation of p34cdc2 protein kinase during mitosis. Cell *58*, 361–372.

Morgan, D.O. (1995). Principles of CDK regulation. Nature *374*, 131–134.

Morgan, D.O. (1997). Cyclin-dependent kinases: engines, clocks, and microprocessors. Annual Review of Cell and Developmental Biology *13*, 261–291.

Morgan, D.O. (2007). The Cell Cycle: Principles of Control.

Murakami, H., and Nurse, P. (2001). Regulation of premeiotic S phase and recombination-related double-strand DNA breaks during meiosis in fission yeast. Nat. Genet.

Murakami, H., and Keeney, S. (2008). Regulating the formation of DNA double-strand breaks in meiosis. Genes & Development *22*, 286–292.

Murakami, H., and Keeney, S. (2014a). Temporospatial Coordination of Meiotic DNA Replication and Recombination via DDK Recruitment to Replisomes. Cell *158*, 861–873.

Murakami, H., and Keeney, S. (2014b). DDK links replication and recombination in meiosis. Cell Cycle *13*, 3621–3622.

Murakami, H., Borde, V., Shibata, T., Lichten, M., and Ohta, K. (2003). Correlation between premeiotic DNA replication and chromatin transition at yeast recombination initiation sites. Nucleic Acids Research *31*, 4085–4090.

Muramatsu, S., Hirai, K., Tak, Y.-S., Kamimura, Y., and Araki, H. (2010). CDK-dependent complex formation between replication proteins Dpb11, Sld2, Pol (epsilon}, and GINS in budding yeast. Genes & Development *24*, 602–612.

Nakamura, T., Nakamura-Kubo, M., Nakamura, T., and Shimoda, C. (2002). Novel fission yeast Cdc7-Dbf4-like kinase complex required for the initiation and progression of meiotic second division. Molecular and Cellular Biology *22*, 309–320.

Nasmyth, K. (1993). Control of the yeast cell cycle by the Cdc28 protein kinase. Current Opinion in Cell Biology *5*, 166–179.

Neale, M.J., Pan, J., and Keeney, S. (2005). Endonucleolytic processing of covalent protein-linked DNA double-strand breaks. Nature *436*, 1053–1057.

Nguyen, V.Q., Co, C., and Li, J.J. (2001). Cyclin-dependent kinases prevent DNA re-replication through multiple mechanisms. Nature *411*, 1068–1073.

Nguyen, V.Q., Co, C., Irie, K., and Li, J.J. (2000). Clb/Cdc28 kinases promote nuclear export of the replication initiator proteins Mcm2-7. Current Biology *10*, 195–205.

Nicklas, R.B. (1988). The forces that move chromosomes in mitosis. Annu Rev Biophys Biophys Chem *17*, 431–449.

Niki, H. (2014). Schizosaccharomyces japonicus: the fission yeast is a fusion of yeast and hyphae. Yeast *31*, 83–90.

Nishitani, H., Lygerou, Z., Nishimoto, T., and Nurse, P. (2000). The Cdt1 protein is required to license DNA for replication in fission yeast. Nature *404*, 625–628.

Niwa, O., Shimanuki, M., and Miki, F. (2000). Telomere-led bouquet formation facilitates homologous chromosome pairing and restricts ectopic interaction in fission yeast meiosis. Embo J. *19*, 3831–3840.

Nougarède, R., Seta, Della, F., Zarzov, P., and Schwob, E. (2000). Hierarchy of S-phase-promoting factors: yeast Dbf4-Cdc7 kinase requires prior S-phase cyclin-dependent kinase activation. Molecular and Cellular Biology *20*, 3795–3806.

Ofir, Y., Sagee, S., Guttmann-Raviv, N., Pnueli, L., and Kassir, Y. (2004). The role and regulation of the preRC component Cdc6 in the initiation of premeiotic DNA replication. Mol. Biol. Cell *15*, 2230–2242.

Ohta, K., Shibata, T., and Nicolas, A. (1994). Changes in chromatin structure at recombination initiation sites during yeast meiosis. Embo J. *13*, 5754–5763.

Oke, A., Anderson, C.M., Yam, P., and Fung, J.C. (2014). Controlling meiotic recombinational repair - specifying the roles of ZMMs, Sgs1 and Mus81/Mms4 in crossover formation. PLoS Genet *10*, e1004690.

Oshiro, G., Owens, J.C., Shellman, Y., Sclafani, R.A., and Li, J.J. (1999). Cell cycle control of Cdc7p kinase activity through regulation of Dbf4p stability. Molecular and Cellular Biology *19*, 4888–4896.

Pagano, M., Pepperkok, R., Verde, F., Ansorge, W., and Draetta, G. (1992). Cyclin A is required at two points in the human cell cycle. Embo J. *11*, 961–971.

Page, S.L., and Hawley, R.S. (2003). Chromosome choreography: the meiotic ballet. Science *301*, 785–789.

Patel, P.K., Arcangioli, B., Baker, S.P., Bensimon, A., and Rhind, N. (2006). DNA replication origins fire stochastically in fission yeast. Mol. Biol. Cell *17*, 308–316.

Patel, P.K., Kommajosyula, N., Rosebrock, A., Bensimon, A., Leatherwood, J., Bechhoefer, J., and Rhind, N. (2008). The Hsk1(Cdc7) replication kinase regulates origin efficiency. Mol. Biol. Cell *19*, 5550–5558.

Petersen, J., and Russell, P. (2016). Growth and the Environment of Schizosaccharomyces pombe. Cold Spring Harb Protoc *2016*, pdb.top079764.

Petes, T.D. (2001). Meiotic recombination hot spots and cold spots. Nat Rev Genet *2*, 360–369.

Pichugina, T., Sugawara, T., Kaykov, A., Schierding, W., Masuda, K., Uewaki, J., Grand, R.S., Allison, J.R., Martienssen, R.A., Nurse, P., et al. (2016). A diffusion model for the coordination of DNA replication in Schizosaccharomyces pombe. Sci. Rep. *6*, 18757.

Pomerening, J.R., Kim, S.Y., and Ferrell, J.E. (2005). Systems-level dissection of the cell-cycle oscillator: bypassing positive feedback produces damped oscillations. Cell *122*, 565–578.

Pope, B.D., and Gilbert, D.M. (2013). The Replication Domain Model: Regulating Replicon Firing in the Context of Large-Scale Chromosome Architecture. J. Mol. Biol. *425*, 4690–4695.

Ramanujan, A., and Tiwari, S. (2016). APC/C and retinoblastoma interaction: cross-talk of retinoblastoma protein with the ubiquitin proteasome pathway. Biosci. Rep. *36*.

Rhind, N., and Gilbert, D.M. (2013). DNA Replication Timing. Cold Spring Harb Perspect Biol *5*, a010132–a010132.

Russell, P., and Nurse, P. (1986). cdc25+ functions as an inducer in the mitotic control of fission yeast. Cell *45*, 145–153.

San Filippo, J., Sung, P., and Klein, H. (2008). Mechanism of eukaryotic homologous recombination. Annu. Rev. Biochem. *77*, 229–257.

Santamaría, D., Barrière, C., Cerqueira, A., Hunt, S., Tardy, C., Newton, K., Cáceres, J.F., Dubus, P., Malumbres, M., and Barbacid, M. (2007). Cdk1 is sufficient to drive the mammalian cell cycle. Nature *448*, 811–815.

Sasanuma, H., Hirota, K., Fukuda, T., Kakusho, N., Kugou, K., Kawasaki, Y., Shibata, T., Masai, H., and Ohta, K. (2008). Cdc7-dependent phosphorylation of Mer2 facilitates initiation of yeast meiotic recombination. Genes & Development *22*, 398–410.

Schafer, K.A. (1998). The cell cycle: a review. Veterinary Pathology.

Sclafani, R.A., Patterson, M., Rosamond, J., and Fangman, W.L. (1988). Differential regulation of the yeast CDC7 gene during mitosis and meiosis. Molecular and Cellular Biology *8*, 293–300.

Smagulova, F., Gregoretti, I.V., Brick, K., Khil, P., Camerini-Otero, R.D., and Petukhova, G.V. (2011). Genome-wide analysis reveals novel molecular features of mouse recombination hotspots. Nature *472*, 375–378.

Solomon, M.J., Glotzer, M., Lee, T.H., Philippe, M., and Kirschner, M.W. (1990). Cyclin activation of p34cdc2. Cell *63*, 1013–1024.

Speck, C., Chen, Z., Li, H., and Stillman, B. (2005). ATPase-dependent cooperative binding of ORC and Cdc6 to origin DNA. Nat. Struct. Mol. Biol. *12*, 965–971.

Spirek, M., Benko, Z., Carnecka, M., Rumpf, C., Cipak, L., Batova, M., Marova, I., Nam, M., Kim, D.-U., Park, H.-O., et al. (2010). S. pombe genome deletion project: an update. Cell Cycle *9*, 2399–2402.

Steiner, W.W., Schreckhise, R.W., and Smith, G.R. (2002). Meiotic DNA breaks at the S. pombe recombination hot spot M26. Molecular Cell *9*, 847–855.

Stern, B., and Nurse, P. (1996). A quantitative model for the cdc2 control of S phase and mitosis in fission yeast. Trends in Genetics : TIG *12*, 345–350.

Stuart, D., and Wittenberg, C. (1998). CLB5 and CLB6 are required for premeiotic DNA replication and activation of the meiotic S/M checkpoint. Genes & Development *12*, 2698–2710.

Su, S.S., Tanaka, Y., Samejima, I., Tanaka, K., and Yanagida, M. (1996). A nitrogen starvation-induced dormant G0 state in fission yeast: the establishment from uncommitted G1 state and its delay for return to proliferation. J. Cell. Sci. *109 (Pt 6)*, 1347–1357.

Sukegawa, Y., Yamashita, A., and Yamamoto, M. (2011). The fission yeast stress-responsive MAPK pathway promotes meiosis via the phosphorylation of Pol II CTD in response to environmental and feedback cues. PLoS Genet *7*, e1002387.

Suryadinata, R., Sadowski, M., and Sarcevic, B. (2010). Control of cell cycle progression by phosphorylation of cyclin-dependent kinase (CDK) substrates. Biosci. Rep. *30*, 243–255.

Swaffer, M.P., Jones, A.W., Flynn, H.R., Snijders, A.P., and Nurse, P. (2016). CDK Substrate Phosphorylation and Ordering the Cell Cycle. Cell *167*, 1750–1761.e16.

Székvölgyi, L., and Nicolas, A. (2010). From meiosis to postmeiotic events: homologous recombination is obligatory but flexible. FEBS Journal *277*, 571–589.

Tanaka, S., Umemori, T., Hirai, K., Muramatsu, S., Kamimura, Y., and Araki, H. (2007). CDK-dependent phosphorylation of Sld2 and Sld3 initiates DNA replication in budding yeast. Nature *445*, 328–332.

Theis, J.F., and Newlon, C.S. (1997). The ARS309 chromosomal replicator of Saccharomyces cerevisiae depends on an exceptional ARS consensus sequence. Proc. Natl. Acad. Sci. U.S.a. *94*, 10786–10791.

Tischfield, S.E., and Keeney, S. (2012). Scale matters: the spatial correlation of yeast meiotic DNA breaks with histone H3 trimethylation is driven largely by independent colocalization at promoters. Cell Cycle *11*, 1496–1503.

Tonami, Y., Murakami, H., Shirahige, K., and Nakanishi, M. (2005). A checkpoint control linking meiotic S phase and recombination initiation in fission yeast. Proc. Natl. Acad. Sci. U.S.a. *102*, 5797–5801.

Valentin, G., Schwob, E., and Seta, Della, F. (2006). Dual role of the Cdc7-regulatory protein Dbf4 during yeast meiosis. J. Biol. Chem. *281*, 2828–2834.

Valton, A.-L., Hassan-Zadeh, V., Lema, I., Boggetto, N., Alberti, P., Saintomé, C., Riou, J.-F., and Prioleau, M.-N. (2014). G4 motifs affect origin positioning and efficiency in two vertebrate replicators. Embo J. *33*, 732–746.

van Werven, F.J., and Amon, A. (2011). Regulation of entry into gametogenesis. Philos. Trans. R. Soc. Lond., B, Biol. Sci. *366*, 3521–3531.

Vas, A., Mok, W., and Leatherwood, J. (2001). Control of DNA rereplication via Cdc2 phosphorylation sites in the origin recognition complex. Molecular and Cellular Biology *21*, 5767–5777.

Wan, L., Niu, H., Futcher, B., Zhang, C., Shokat, K.M., Boulton, S.J., and Hollingsworth, N.M. (2008). Cdc28-Clb5 (CDK-S) and Cdc7-Dbf4 (DDK) collaborate to initiate meiotic recombination in yeast. Genes & Development *22*, 386–397.

Wan, L., Zhang, C., Shokat, K.M., and Hollingsworth, N.M. (2006). Chemical inactivation of cdc7 kinase in budding yeast results in a reversible arrest that allows efficient cell synchronization prior to meiotic recombination. Genetics *174*, 1767–1774.

Wood, V., Gwilliam, R., Rajandream, M.A., Lyne, M., and Lyne, R. (2002a). The genome sequence of Schizosaccharomyces pombe. Nature.

Wood, V., Gwilliam, R., Rajandream, M.A., Lyne, M., Lyne, R., Stewart, A., Sgouros, J., Peat, N., Hayles, J., Baker, S., et al. (2002b). The genome sequence of Schizosaccharomyces pombe. Nature *415*, 871–880.

Wood, V., Harris, M.A., McDowall, M.D., Rutherford, K., Vaughan, B.W., Staines, D.M., Aslett, M., Lock, A., Bähler, J., Kersey, P.J., et al. (2012). PomBase: a comprehensive online resource for fission yeast. Nucleic Acids Research *40*, D695–D699.

Woodward, A.M., Göhler, T., Luciani, M.G., Oehlmann, M., Ge, X., Gartner, A., Jackson, D.A., and Blow, J.J. (2006). Excess Mcm2-7 license dormant origins of replication that can be used under conditions of replicative stress. J. Cell Biol. *173*, 673–683.

Wu, L., Liu, Y., and Kong, D. (2014). Mechanism of chromosomal DNA replication initiation and replication fork stabilization in eukaryotes. Sci China Life Sci *57*, 482–487.

Wu, P.-Y.J., and Nurse, P. (2009). Establishing the Program of Origin Firing during S Phase in Fission Yeast. Cell *136*, 852–864.

Wu, P.-Y.J., and Nurse, P. (2014). Replication origin selection regulates the distribution of meiotic recombination. Molecular Cell *53*, 655–662.

Wu, T.C., and Lichten, M. (1994). Meiosis-induced double-strand break sites determined by yeast chromatin structure. Science *263*, 515–518.

Wuarin, J., Buck, V., Nurse, P., and Millar, J.B.A. (2002). Stable association of mitotic cyclin B/Cdc2 to replication origins prevents endoreduplication. Cell *111*, 419–431.

Wyrick, J.J., Aparicio, J.G., Chen, T., Barnett, J.D., Jennings, E.G., Young, R.A., Bell, S.P., and Aparicio, O.M. (2001). Genome-wide distribution of ORC and MCM proteins in S. cerevisiae: high-resolution mapping of replication origins. Science *294*, 2357–2360.

Yamada, S., Ohta, K., and Yamada, T. (2013). Acetylated Histone H3K9 is associated with meiotic recombination hotspots, and plays a role in recombination redundantly with other factors including the H3K4 methylase Set1 in fission yeast. Nucleic Acids Research *41*, 3504–3517.

Yamada, S., Kim, S., Tischfield, S.E., Jasin, M., Lange, J., and Keeney, S. (2017a). Genomic and chromatin features shaping meiotic double-strand break formation and repair in mice. 1–16.

Yamada, S., Okamura, M., Oda, A., Murakami, H., Ohta, K., and Yamada, T. (2017b). Correlation of Meiotic DSB Formation and Transcription Initiation Around Fission Yeast Recombination Hotspots. Genetics *206*, 801–809.

Yamada, T., Mizuno, K.-I., Hirota, K., Kon, N., Wahls, W.P., Hartsuiker, E., Murofushi, H., Shibata, T., and Ohta, K. (2004). Roles of histone acetylation and chromatin remodeling factor in a meiotic recombination hotspot. Embo J. *23*, 1792–1803.

Yamamoto, A., West, R.R., McIntosh, J.R., and Hiraoka, Y. (1999). A cytoplasmic dynein heavy chain is required for oscillatory nuclear movement of meiotic prophase and efficient meiotic recombination in fission yeast. J. Cell Biol. *145*, 1233–1249.

Yamamoto, M. (1996). Regulation of meiosis in fission yeast. Cell Struct. Funct. *21*, 431–436.

Yamazaki, S., Ishii, A., Kanoh, Y., Oda, M., Nishito, Y., and Masai, H. (2012). Rif1 regulates the replication timing domains on the human genome. Embo J. *31*, 3667–3677.

Yan, H., Toczylowski, T., McCane, J., Chen, C., and Liao, S. (2011). Replication protein A promotes 5→3 end processing during homology-dependent DNA double-strand break repair. J. Cell Biol. *192*, 251–261.

Yoon, H.J., Loo, S., and Campbell, J.L. (1993). Regulation of Saccharomyces cerevisiae CDC7 function during the cell cycle. Mol. Biol. Cell *4*, 195–208.

Yoshida, K., and Inoue, I. (2004). Regulation of Geminin and Cdt1 expression by E2F transcription factors. Oncogene *23*, 3802–3812.

Zakharyevich, K., Ma, Y., Tang, S., Hwang, P.Y.-H., Boiteux, S., and Hunter, N. (2010). Temporally and biochemically distinct activities of Exo1 during meiosis: double-strand break resection and resolution of double Holliday junctions. Molecular Cell *40*, 1001–1015.

Zegerman, P., and Diffley, J.F.X. (2007). Phosphorylation of Sld2 and Sld3 by cyclin-dependent kinases promotes DNA replication in budding yeast. Nature *445*, 281–285.

Zickler, D., and Kleckner, N. (1998). The leptotene-zygotene transition of meiosis. Annu. Rev. Genet. *32*, 619–697.

Zickler, D., and Kleckner, N. (1999). Meiotic chromosomes: integrating structure and function. Annu. Rev. Genet. *33*, 603–754.

Chapter II

Impact of chromosomal organization on replication origin selection and meiotic recombination

Impact of chromosomal organization on replication origin selection and meiotic recombination

Lilian Lanteri, Diane Schausi-Tiffoche, Anthony Perrot, Pei-Yun Jenny Wu*

Genome Duplication and Maintenance team, Institute of Genetics and Development, CNRS UMR 6290, 2 avenue du Pr. Léon Bernard, 35043 Rennes, France

*Corresponding author: pei-yun.wu@univ-rennes1.fr

The results in this chapter are part of a manuscript that is currently being prepared for submission.

Introduction

The control of genome duplication is critical for cell growth and proliferation as well as for development and differentiation. The duplication of the genetic material is precisely regulated and controlled by various mechanisms, which are conserved among eukaryotes (Gómez-Escoda and Wu, 2017; Méchali, 2010). One aspect of this control is the specification of a pattern, or program, of DNA replication. In a cell, DNA synthesis initiates from a large number of sites known as replication origins. Only a subset of origins are used in each S-phase, and this subset differs in each cell and from one cell cycle to the next. At the cell population level, the program of replication is defined by 1) the timing at which each origin is activated and 2) the frequency of usage of each origin in a cell population, termed origin efficiency (Méchali, 2010). These properties are modulated by different inputs such as nucleotide levels, chromatin modification, gene transcription, or cell cycle regulation (Aladjem, 2007; Anglana et al., 2003; Méchali, 2010), suggesting that origin firing is highly regulated. While alterations of the replication program have been observed in differentiating mouse embryonic stem cells (Hiratani et al., 2008a), in *Xenopus* and *Drosophila* during development (Hyrien and Mechali, 1993; Hyrien et al., 1995; Méchali, 2010) and in cancer cells (Dotan et al., 2004), it remains unclear whether undergoing a particular replication program has actual consequences for cellular function.

To investigate this question, previous work has addressed whether the replication has important functions during meiosis in the fission yeast *Schizosaccharomyces pombe* (Wu and Nurse, 2014). Meiosis is a specialized cell division that generates four gametes for sexual reproduction, and the mechanisms underlying this process are conserved in eukaryotes. During meiosis, pre-meiotic DNA replication is followed by the formation of DNA double-strand breaks (DSBs). The subsequent repair of these breaks results in the exchange of genetic material for sexual reproduction and promotes genome diversity. Interestingly, meiosis *per se* does not require a particular replication program in fission yeast (Wu and Nurse, 2014): for instance, mitotic and meiotic cells undergoing DNA replication in nitrogen-rich medium (+N) possess very similar replication programs. However, origin selection is dependent on nutritional conditions, as the pattern of origin usage in +N medium is significantly

different from that in cells entering the meiotic cycle after temporary nitrogen starvation (-N) (Wu and Nurse, 2014). Taking advantage of these differences, the authors then demonstrated that alterations of the pre-meiotic replication program between the -N and +N conditions lead to corresponding changes in the pattern of DSB formation (Wu and Nurse, 2014). More precisely, regions with significantly increased origin usage showed higher levels of DSB formation. Thus, the program of DNA replication has a crucial impact on subsequent events in DNA metabolism during this specialized cell cycle.

Although meiotic recombination has long been associated with DNA replication (Borde et al., 2000), the mechanisms that couple these two processes have remained elusive. Following the link between origin usage and DSB formation described above, Murakami and Kenney (2014) proposed a model in which the DDK Cdc7, a kinase important for DNA replication (Valentin et al., 2006; Wan et al., 2008), is recruited to the replication machinery and subsequently phosphorylates the critical recombination factor Mer2 (Murakami and Keeney, 2014). Their work suggested that DDK is recruited to the replisome via interactions with a component of the replication fork protection complex (FPC), which travels with the replication machinery (Katou et al., 2003). Moreover, they showed that Mer2 phosphorylation by DDK is coordinated with local replication timing. Thus, these results indicate that DDK recruitment to the replication fork may be a key step for coordinating pre-meiotic DNA replication with meiotic DSB formation. However, the molecular mechanisms underlying this model are not known, and there are likely to be additional layers of regulation that couple these two processes (Miyoshi et al., 2012; Wan et al., 2008). First, due to the transient or unstable interaction between DDK and the FPC (Murakami and Keeney, 2014), it remains unclear whether DDK travels with the replication fork during DNA replication. Indeed, DDK may be recruited to the replisome at origins during initiation or during the process of elongation. Moreover, a phosphomimetic form of Mer2 is not sufficient to produce DSBs (Wan et al., 2008), suggesting that the DDK may have other targets or that additional pathways are required. Altogether, these findings indicate that Mer2/Rec15 phosphorylation by DDK may not be the only link between meiotic DNA replication and recombination, and there are likely multiple layers of regulation connecting these two processes.

As mentioned above, recent work in the fission yeast has linked changes in the pattern of replication initiation to the profile of DSB formation along the chromosomes. Specifically, domains with significantly increased origin usage between two replication programs showed new and increased DSB formation (Wu and Nurse, 2014). Thus, one can speculate that chromatin environment and chromosomal context may be key players in the origin selection and the distribution of DSBs. Interestingly, one interesting aspect of genome architecture that has emerged in recent years is its arrangement in regulatory domains (Pope et al., 2010). Relevant to our studies, a conserved feature of the replication program in eukaryotes is the existence of regions that duplicate at particular times during S-phase. For example, mammalian cells partition their genome into around 5000 units of synchronously firing replicon clusters (Rivera-Mulia and Gilbert, 2016) that are activated throughout S-phase (Jackson and Pombo, 1998). Moreover, DNA replication is spatiotemporally organized in the nucleus, and regions that duplicate at the same time are believed to be located next to each other (Berezney et al., 2000; Pichugina et al., 2016). Thus, the context of a chromosomal region may play an important role in the establishment of the profile of replication timing and efficiency. For example, early studies showed that the timing of replication and efficiency of the SV40 (simian virus 40) origin is dependent of its insertion in the genome in Chinese hamster cells (Gilbert and Cohen, 1990). In addition, in fission yeast, insertion of an efficient origin into a low efficiency region decreases its activity (Kiang et al., 2010). Thus, these data suggest that chromatin environment and chromosomal context may play a role on origin selection during S-phase.

Since chromatin environment and chromosomal context are important regulators of DNA replication, these features may also be involved in the control of meiotic DSB formation, in particular given the known coupling between replication and recombination (Borde et al., 2000; Murakami and Keeney, 2014; Murakami et al., 2003; Wu and Nurse, 2014). In the present work, we have explored the impact of chromosomal organization on the program of DNA replication and meiotic recombination using the fission yeast *Schizosaccharomyces pombe.* For our studies, we have taken an approach in which we engineer chromosomal rearrangements that exchange the positions of replication domains with different efficiency and timing characteristics. This approach allows us to move large regions containing replication

domains rather than individual origin sequences, thus conserving the sequence characteristics of origins as well as the surrounding regulatory sequences that might be important for proper origin firing. Our results show that the 1-2 Mb chromosomal inversions that we generated did not have an effect on cell proliferation and meiotic progression. Interestingly, we found that these rearrangements induced local changes in origin efficiencies proximal to the endpoints of the inversions and that these changes are common to both mitotic and meiotic S-phase. Finally, genome-wide analyses of the DSB profile using the Rad51 recombination as a marker revealed alterations in Rad51 binding near the rearranged ends. Surprisingly, these changes do not directly follow what would be predicted from the differences in origin usage in these regions, suggesting a complex regulation of DSB formation during meiosis.

Results

Generation of chromosomal rearrangements

To test whether chromosomal context has an effect on DNA replication and meiotic recombination, we generated *S. pombe* strains containing distinct rearrangements of chromosomes I and II. To this end, we took advantage of the Cre-LoxP site-specific recombinase technology (Sternberg and Hamilton, 1981; Werler et al., 2003), with transient induction of Cre leading to recombination between LoxP sites that are integrated at selected genomic sites (Watson et al., 2008).

For our study, we chose to produce chromosomal rearrangements that re-organize the origin efficiency domains that have been identified in the fission yeast (Wu and Nurse, 2014). In particular, previous work from our laboratory has demonstrated that in cells that re-enter the cell cycle after having been arrested in G0/G1 following nitrogen depletion, both the mitotic and pre-meiotic replication program show distinct domains of origin efficiencies, with large regions (1-2 Mb) that contain few active origins (Figure 1A and 1B). These differences provide us with an excellent model for determining the impact of chromosomal context on origin usage and associated processes. To this end, we chose to insert LoxP sites in order to generate chromosomal

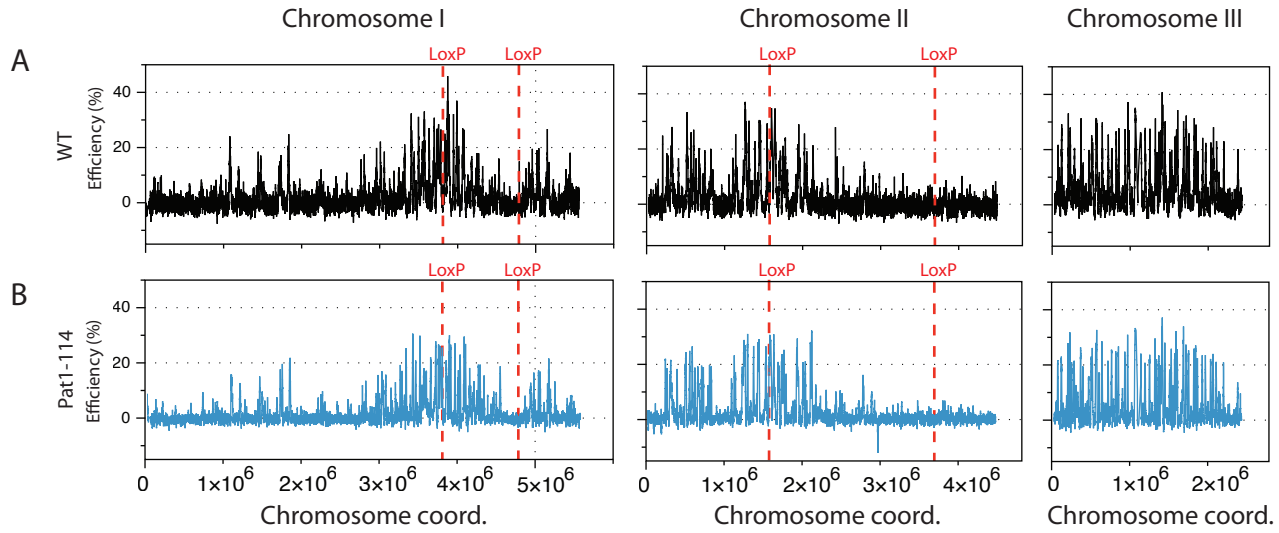
A
B
Chromosome I
Chromosome II
Chromosome III
LoxP
WT
Efficiency (%)
Pat1-114
Chromosome coord.

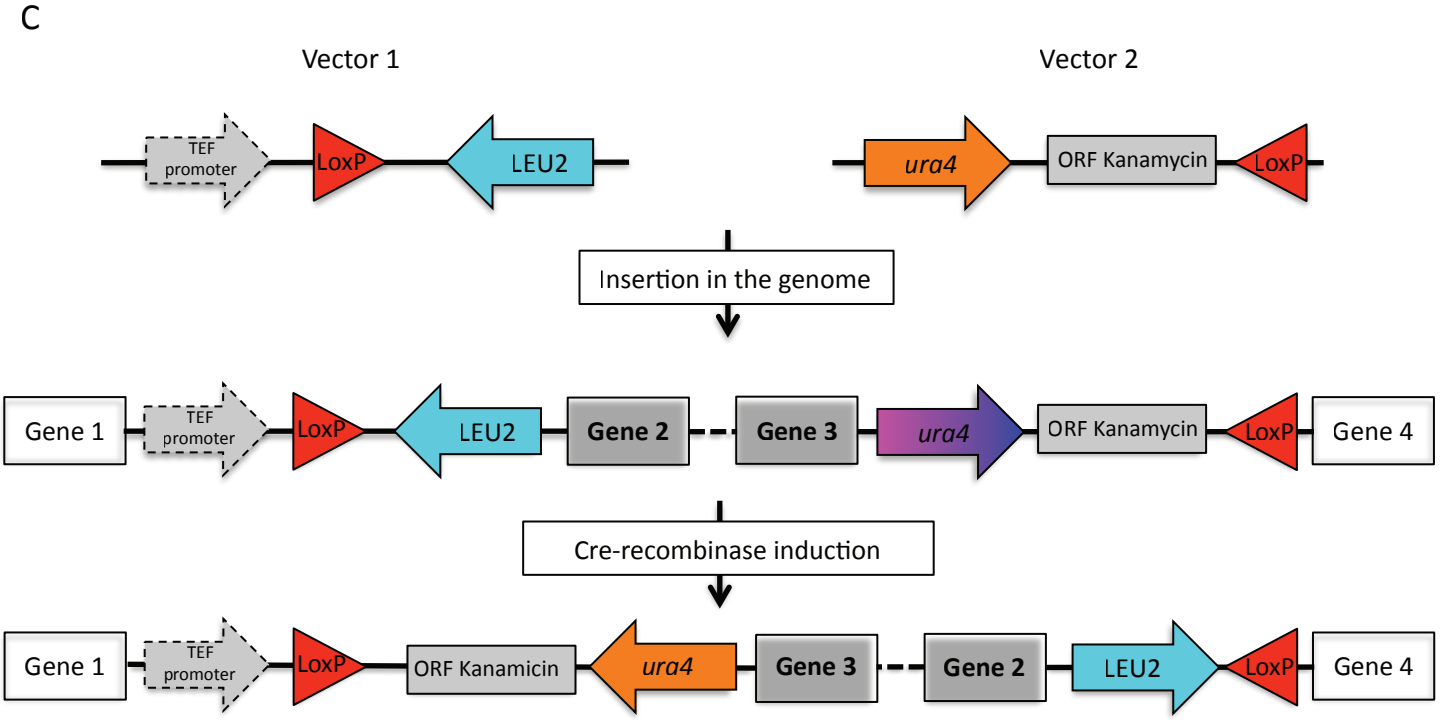
C
Vector 1
Vector 2
TEF promoter
LoxP
LEU2
ura4
ORF Kanamycin
Insertion in the genome
Gene 1
Gene 2
Gene 3
Gene 4
Cre-recombinase induction
ORF Kanamicin

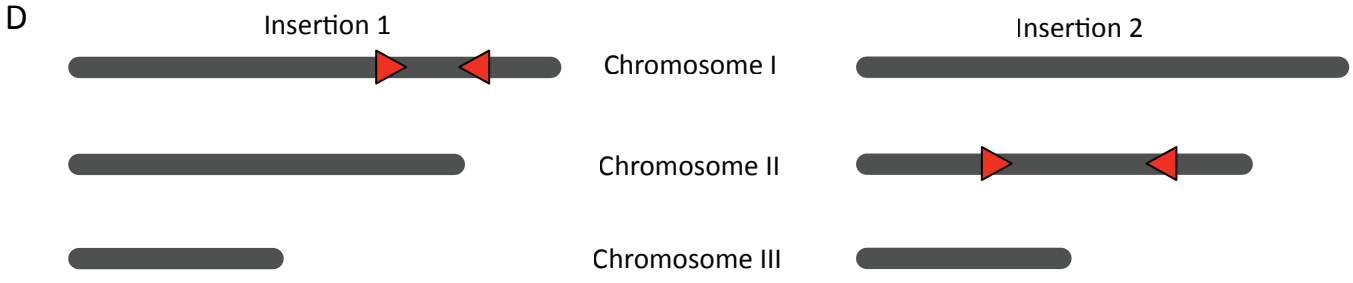
D
Insertion 1
Insertion 2
Chromosome I
Chromosome II
Chromosome III

Figure 1: Scheme of chromosomal rearrangement strategy.
A-B) Origin usage profile of a WT strain undergoing mitosis after nitrogen starvation (A, black) and a *pat1-114* diploid undergoing meiosis after nitrogen starvation (B, blue). X-axis: chromosome coordinates. Y-axis: origin efficiencies. Red dashed lines represent the location of the loxP sites: ChrI: 3810766 and ChrI 4785016, ChrII: 1577150 and ChrII: 3694900 described in C). (Data from Wu and Nurse; 2014). C) Two vectors were constructed to generate the chromosomal rearrangements: one contains the *LEU2* gene from *S. cerevisiae* and the *TEF1* promoter surrounding one LoxP site; the second contains the *ura4* gene from *S. pombe*, the ORF sequence that encodes the kanamycin resistance gene and a LoxP site. These two cassettes were amplified and inserted in different genetic backgrounds. The *LEU2* and *ura4* markers were used to select transformants. LoxP sites were oriented such that they generate an inversion after recombination. After integration of the cassettes at sites of interest, a plasmid containing an inducible Cre recombinase controlled by the thiamine repressible *nmt1* promoter was transformed into the strains. Cre was induced by growing cells in medium without thiamine and promotes recombination at the LoxP sites to generate the chromosomal rearrangement. Rearranged strains were selected on plates containing kanamycin, since the kanamycin resistance gene becomes constitutively expressed by the *TEF1* promoter after inversion. The region between the LoxP sites becomes inverted after rearrangement. D) Schematic representation of the inserted LoxP sites in the genome. LoxP sites are represented as red triangles. It is important to note the orientation of the LoxP sites. Cassettes 1 and 2 were integrated in Chromosome I and Chromosome II at the following positions: Chr I: 3810766 and Chr I: 4785016; Chr II: 1577150 and Chr II: 3694900) (see red dashed lines in A).

inversions that transpose the positions of inefficient and efficient regions in both chromosomes I (Figure 1A) and II (Figure 1B).

For generating the inversions described above, we constructed two vectors that contain the cassettes shown in Figure 1C. Each cassette contains LoxP sites and a marker (either the *S. cerevisiae LEU2* gene or the *ura4* gene from *S. pombe*) to select for its integration in the genome (Figure 1C). Importantly, each cassette also contains part of the KanR marker (Bähler et al., 1998), whose expression leads to G418 resistance. One vector contains the TEF promoter and *ura4,* while the other includes the ORF of KanR together with *LEU2.* The promoter and ORF are oriented such that the TEF promoter drives KanR expression after recombination. The two cassettes were integrated in the genome of *S. pombe* using homologous recombination after amplification by PCR using long primers that contain 80 bp of homology to each side of the integration site. For our experiments, we used both a wild-type background (referred to as Haploid) as well as one that contains a *pat1-114* temperature sensitive

A

	Haploid				
	Chromosome I		Chromosome II		Control
	Control I	Rearrangement I	Control II	Rearrangement II	WT
Generation time (min) (25°C)	144	146 ±1.54	144	146 ±3.14	141

B

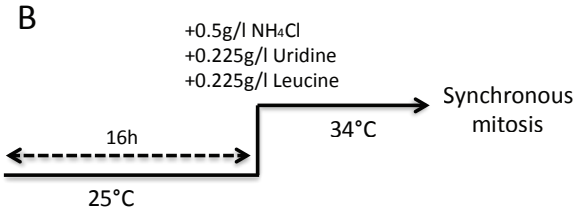

C

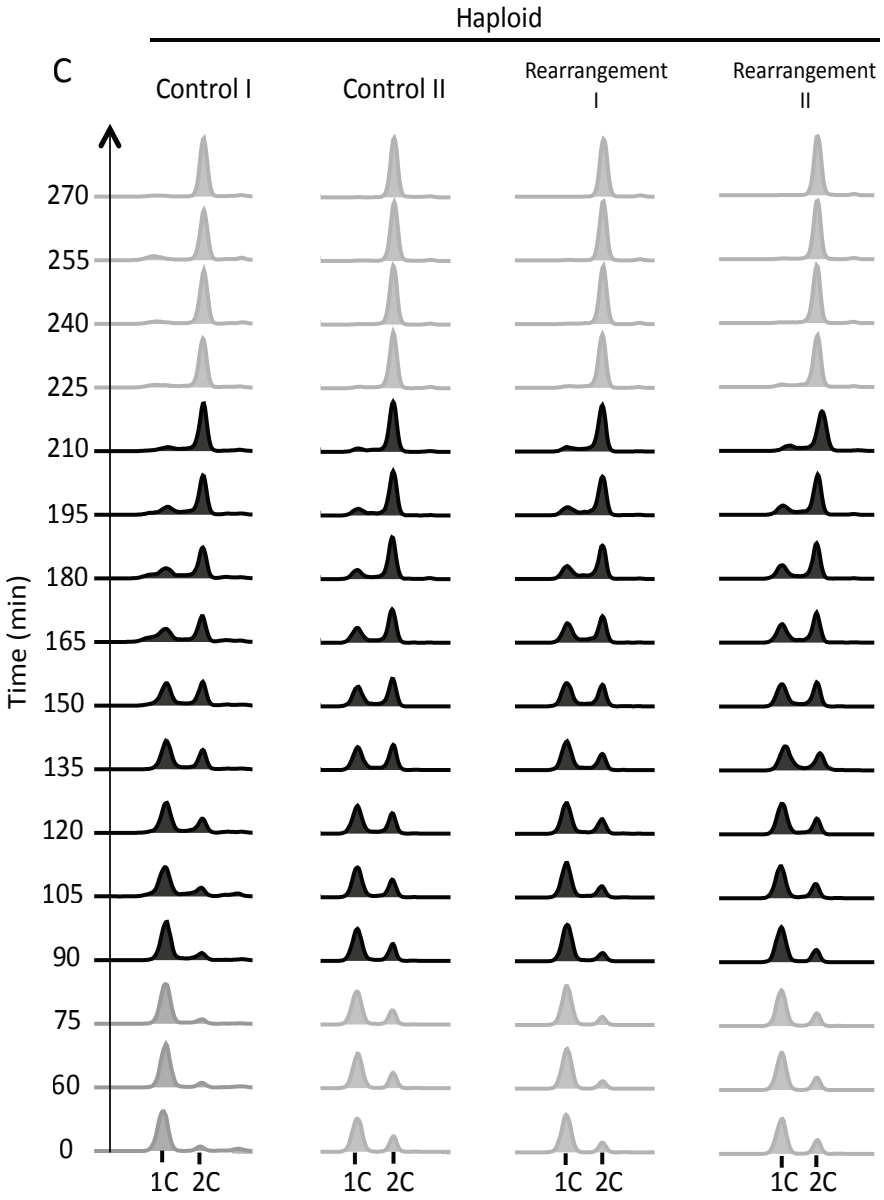

<u>Figure 2:</u> Mitotic cell cycle characterization.

A) Generation times of Haploid Rearranged strains I and II as well as their controls (Haploid Control I and II, respectively) in EMM6S at 25°C. As a reference, a wild-type prototrophic strain (JW501) was used. The averages and standard errors of three independent experiments are shown. B) Experimental design for nitrogen depletion followed by synchronous entry into a mitotic cycle. C) Flow cytometry analysis of the first S phase after the exit from the G0/G1 state induced by nitrogen starvation . t = 0 corresponds to the time at which nitrogen was added to the medium. S-phase is indicated in black and is identical between the four assayed strains.

allele that allows meiotic induction after temperature shift (referred to as Pat1) (Bähler et al., 1991).

After integration of the two cassettes containing LoxP sites, we transformed a plasmid containing the Cre-recombinase under the control of the *nmt1* thiamine inducible promoter (Watson et al., 2008). Transient Cre induction resulted in recombination at the LoxP sites that could then be selected through G418 resistance (Figure 1A), and inversions were verified by PCR. We will refer to strains with integrated LoxP sites on chromosomes I and II prior to rearrangement as Control I and Control II, respectively, and the inversions will be called Rearrangement I and Rearrangement II. These chromosomal inversions will allow us to assess the impact of chromosome organization on origin selection and meiotic recombination.

Chromosomal rearrangements do not interfere with the mitotic cell cycle

To evaluate whether the inversions that we have generated have an effect cell proliferation and genome duplication, we first characterized the generation times of the Haploid strains. The pre-arrangement strains Haploid Control I and II were used as controls. We determined the doubling times of the control rearranged strains at 32ºC in minimal medium containing supplements and found that they were virtually identical (Figure 2A); this was also very similar to the doubling time of a haploid strain without any integrated LoxP sites. This indicated that neither the integration of LoxP sites nor the induced inversions affected cell growth. We then assessed cell cycle progression in these strains. We used previously described nitrogen depletion conditions that produced the replication programs shown in Figure 1; these are also the most widely-used conditions for meiotic induction using *pat1-114*. Cells were grown to exponential phase at 25°C, depleted of nitrogen during 16 h for G0/G1 arrest, released into the cell cycle upon addition of the nitrogen source NH_4Cl, and shifted to 34°C (Figure 2B). Flow cytometry analysis showed that cell cycle progression is identical between the Control and Rearranged strains, with the duration of S-phase being ~120 min for all tested strains (Figure 2C). Thus, the chromosomal inversions showed no detectable phenotypes for cell cycle progression.

A

	Diploid				
	Chromosome I		Chromosome II		Control
	Control I	Rearrangement I	Control II	Rearrangement II	WT
Generation time (min) (25°C)	253 ± 3.06	254 ± 11.59	262 ± 6.85	257 ± 5.5	236 ± 5.5

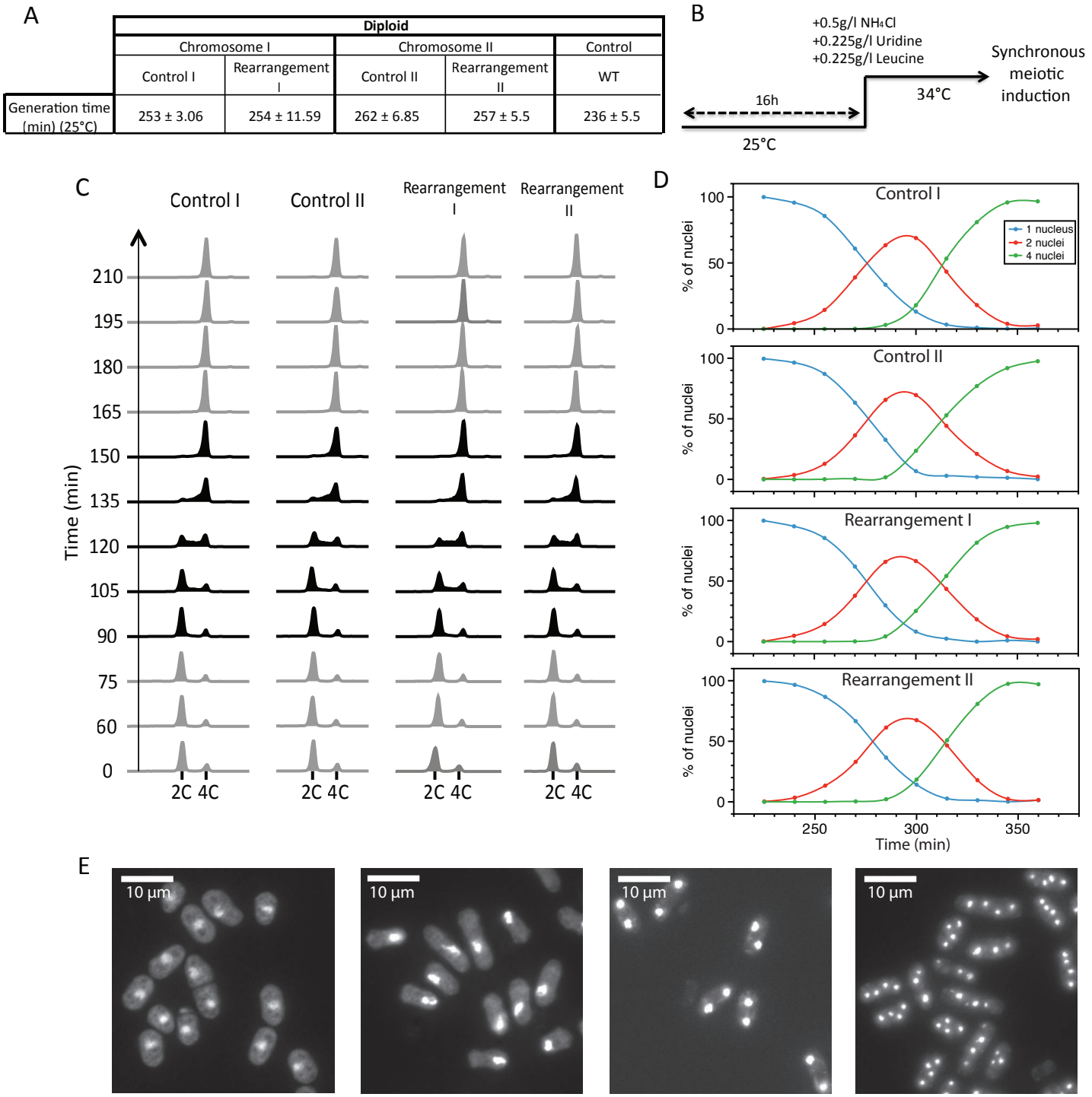

Figure 3: Meiotic cell cycle characterization and meiotic progression.
A) Generation times of Diploid Rearranged strains I and II and their controls (Diploid control I and II, respectively) in EMM6S at 25°C. As a reference, a diploid wild-type strain was used (JW1073). The averages and standard errors of three independent experiments are shown. B) Experimental design for initiating synchronous meiotic entry after temporary nitrogen depletion. C) Flow cytometry analysis of pre-meiotic S-phase. t = 0 corresponds to the time at which nitrogen was added to the medium and cells were shifted to restrictive temperature (34°C). Pre-meiotic S-phase is indicated in black and does not vary between the different conditions. D) Time course of meiotic progression of non-rearranged (control I and control II) and rearranged (rearrangement I and rearrangement II) strains induced to undergo meiosis. Ethanol-fixed cells were stained with DAPI to detect nuclei. The number of nuclei per cell was counted every 15 min to determine the kinetics of meiosis I and II. Graphs represent the average of two independent experiments (n > 300 for each time point). Cells proceed through meiosis I and meiosis II around 5h and 6h respectively after meiotic induction. E) Ethanol-fixed cells were stained with DAPI to visualize nuclei. Images show cells with one, two, or four nuclei during meiosis.

Chromosomal rearrangements do not interfere with pre-meiotic DNA replication and meiotic progression

Next, we ascertained whether the chromosomal rearrangements affect cell proliferation and meiotic progression in the Pat1 background. For these assays, we began by generating diploids of the Pat1 Control and Rearrangement strains to allow for a productive meiosis. We then determined the generation time of the diploid Pat1 strains at 25°C, the permissive temperature for the *pat1-114* allele. Our results showed similar doubling times for the Pat1 Control and Rearrangement strains, ranging from 253 min to 263 min (Figure 3A). However, we observed a 20 min delay when compared with a diploid WT control strain; this may be due to the presence of the *pat1-114* allele in our experimental strains. Nevertheless, our data indicate that the chromosomal inversions do not affect the vegetative growth of the Pat1 diploids.

We then analyzed whether the chromosomal rearrangements have consequences for pre-meiotic S-phase and meiotic progression. To this end, we induced synchronous meiosis in the diploid Pat1 strains; this is performed in the same growth conditions as used for the Haploid strains above. Briefly, cells growing in exponential phase at 25°C were depleted of nitrogen during 16 h for G0/G1 arrest. Addition of NH_4Cl and shift to 34°C resulted in synchronous entry into meiosis (Figure 3B). Flow cytometry analysis showed that the duration of pre-meiotic S-phase is around 90 min for the Control and Rearrangement Strains (Figure 3C). We noted that this is 30 min shorter than mitotic S-phase in the same conditions (Figure 2C); this may be due to a difference between haploid vs. diploid cells or between mitotic and meiotic S-phase.

Finally, we analyzed the timing and execution of meiosis I and II following the completion of DNA replication (Figure 3D-E). For this, we counted the number of nuclei during meiotic progression: cells harboring two nuclei indicate completion of meiosis I, and four nuclei are observed upon completion of meiosis II. Our results showed that there are no changes in meiotic progression due to the chromosomal rearrangements. Consistent with previous data (Wu and Nurse, 2014), the majority of the cells had completed meiosis I and II around 2h and 3h after completion of S-phase, respectively.

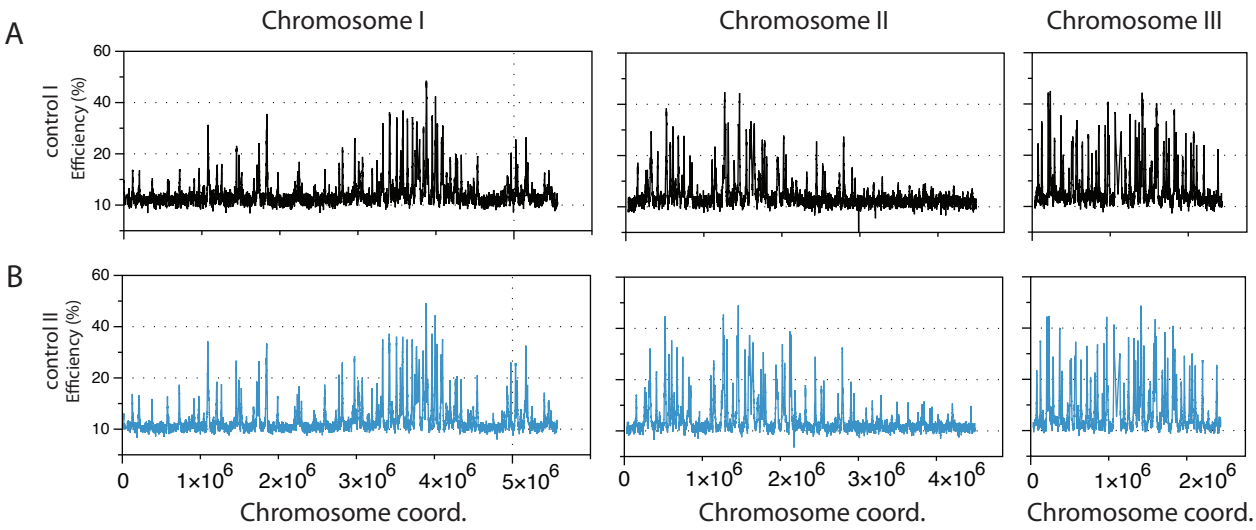

C

	Control I	Control II
Total number of origins	177	186
Average origin efficiency (%)	22.56	24.42
Number of origins in common	172	
% in common	97.18	92.47
Number of unique to each condition	5	14
% unique origin	2.09	10.47
Average efficiency of unique origins (%)	11	13
Standard deviation of efficiencies of unique origins	0.009	0.075

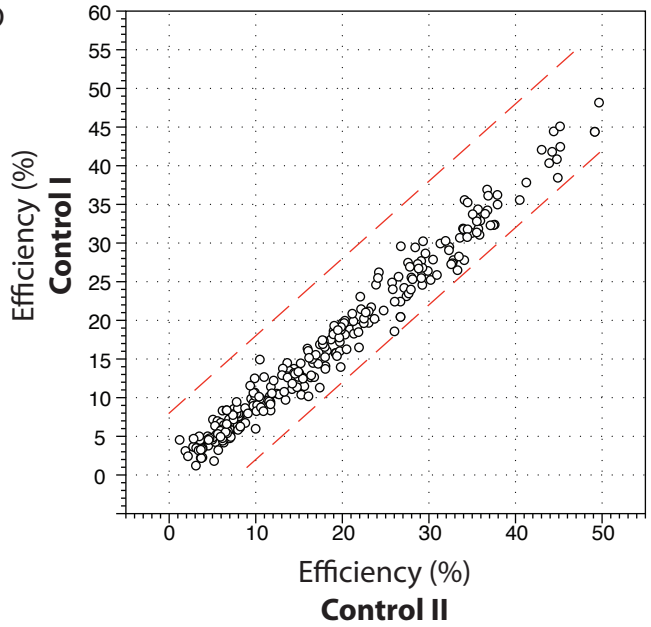

<u>Figure 4:</u> LoxP insertions do not change the replication program during mitotic S-phase.
A-B) Origin usage profiles of Haploid Control I (A, black) and Control II (B, blue). X-axis: chromosome coordinates. Y-axis: origin efficiencies. C) Analysis of origin usage in the Haploid Control I and Control II replication program. D) Comparison of origin efficiencies in Haploid Control I vs. Control II cells. The efficiencies of the origins present in the compiled list of all origins (See materials and methods) are shown. X-axis: efficiency in Control II, y-axis: efficiency in the Control I. Red dashed lines represent a 8% difference in efficiency between the two strains.

Thus, we conclude that overall meiotic progression was not affected by the chromosomal inversions in Chromosome I and Chromosome II.

Chromosomal rearrangements locally alter origin activity during mitotic and meiotic S-phase

Given that both mitotic and pre-meiotic S-phase as well as meiotic progression were not altered by the chromosome inversions, we set out to assess the effect of chromosomal inversions on the replication programs. We began by determining the profile of origin efficiencies in the Haploid Control and Rearranged strains. To this end, we synchronized cells in G0/G1 using the nitrogen depletion procedure described above and released cells for either haploid mitotic S-phase (Figure 3B) or diploid pre-meiotic S-phase (Figure 4B). To determine origin efficiencies in these experiments, cells were treated with 12mM of hydroxyurea (HU) prior to replication. HU limits the extent of replication around the site of initiation by depleting the pool of available dNTPs.

For haploid cells, genomic DNA was isolated from nitrogen-starved cells with a 1C DNA content before release from nitrogen starvation (non-replicated DNA) and at 240 minutes after release from nitrogen starvation, 60 min after S-phase is completed in the absence of HU (replicated DNA, Figure 2C). Replication origins were mapped by competitive hybridization of differentially labeled replicated and non-replicated samples to a microarray containing probes that cover the fission yeast genome (Wu and Nurse, 2014). Origins were identified as peaks of increased copy number in the S-phase sample, with the copy number representing origin efficiencies (for example, a copy number of 1.5 represents 50% efficiency). A cutoff of 10% efficiency was established for origin identification (see Methods for details).

First, comparison of the replication programs of Haploid Control I and Control II strains showed almost identical profiles of origin usage (Figure 4A-B). Using a 10% efficiency cutoff for origin identification, we identified 177 origins in Control I and 186 origins in Control II. Over 90% of these sites were shared between the two backgrounds, and the average origin efficiency was very similar, with 22.56% and

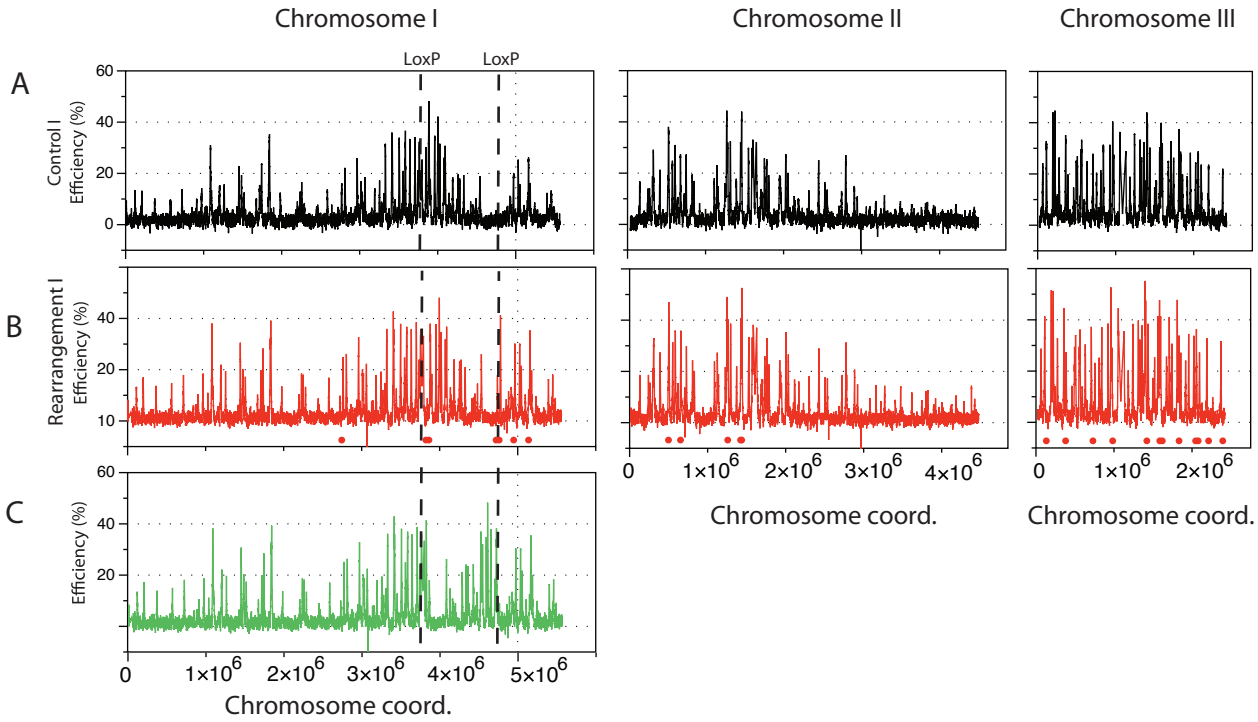

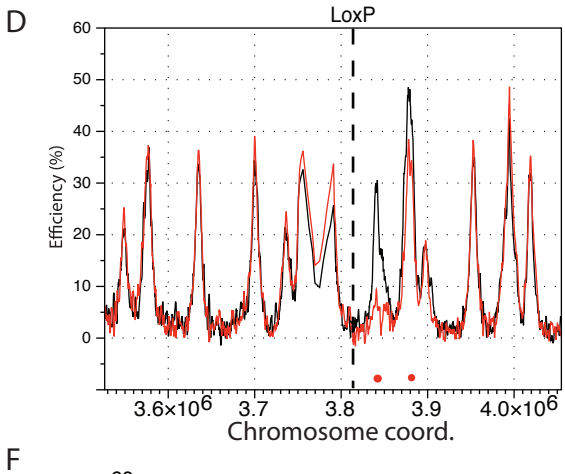

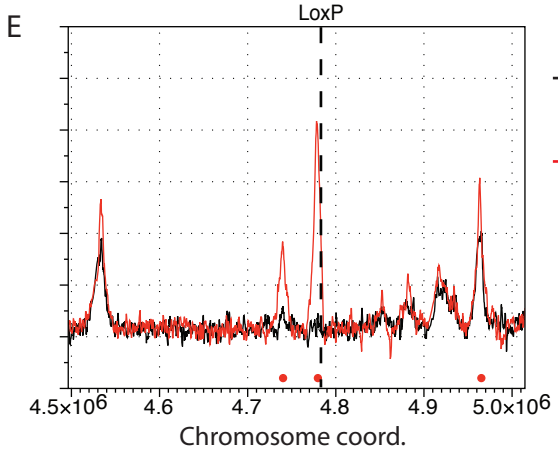

Control I

Rearrangement I

Difference ≥ 8% efficiency between the two conditions

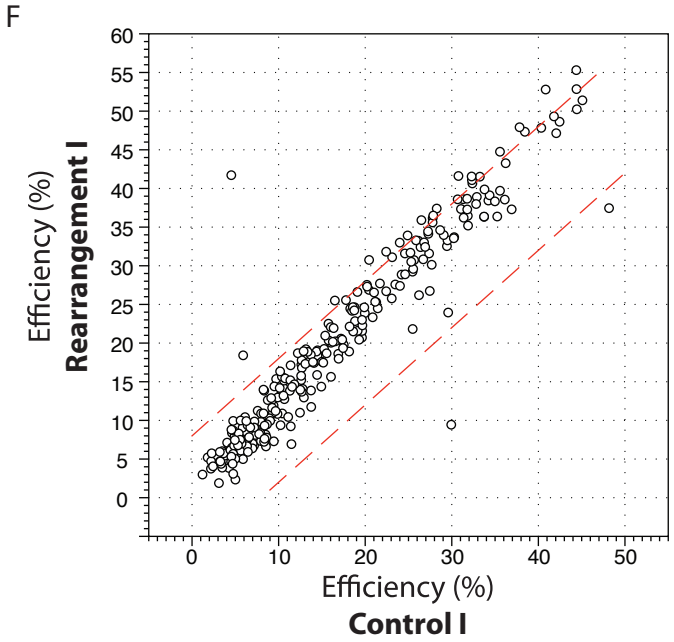

G

	Control I	Rearrangement I
Total number of origins	177	193
Average origin efficiency (%)	22.56	25.87
Number of origins in common	173	
% in common	97.74	89.64
Number of unique to each condition	4	20
% unique origin	2.03	10.15
Average efficiency of unique origins (%)	16	14
Standard deviation of efficiencies of unique origins	0.095	0.068

Figure 5: Inversion of a region of chromosome I induces local changes in origin usage within the inverted segment in mitotic S-phase.
A-B) Origin usage profiles of Haploid Control I (A, black) and Haploid Rearrangement I (B, red). The profile of the rearrangement is plotted with the original, pre-arrangement coordinates to allow direct comparison with the Control strain. Dashed lines represent the locations of the LoxP insertions at ChrI: 3810766 and ChrI: 4785016. Red dots indicate origins with ≥8% efficiency difference between the two programs. C) Profile showing origin efficiencies using the post-rearrangement chromosomal coordinates (green). X-axis: chromosome coordinates. Y-axis: origin efficiencies. Dashed lines: LoxP insertions. D-E) Detailed view of the origin usage profiles in regions surrounding the LoxP sites as in A. Black: Control I,red: Rearrangement I. Dashed lines: LoxP insertions. Red dots highlight origins that show changes of ≥8% efficiency between Control I and Rearrangement I. x-axis: chromosome coordinates, y-axis: origin efficiencies. F) Comparison of origin efficiencies in Control I vs. Rearrangement I. The efficiencies of the origins present in the compiled list of all origins (see materials and methods) are shown. X-axis: efficiency Control I, y-axis: efficiency Rearrangement I. Red dashed lines represent an 8% efficiency difference between the two strains. The 5 biggest changes in origin usage are located around the around the LoxP sites (indicated by the red dots in D and E). G) Analysis of origin usage in the Control I and Rearrangement I replication programs.

24.47% for Control I and II, respectively (Figure 4C). We then quantitatively analyzed the differences in origin usage between these two strains. We applied a cutoff of 8% absolute efficiency to define a significant change in origin efficiency between two backgrounds (see Methods for the selection of this cutoff). As shown in Figure 4A-B, origin efficiencies were highly comparable between the two strains (Figure 4D). These results demonstrate the high level of reproducibility of our assays and indicate that the integrated LoxP sites themselves do not have significant effects on the replication program.

Next, we compared each chromosomal rearrangement with its control. We found 193 origins in Haploid Rearrangement I, with an overall average efficiency of 25.87%; 88% were shared with Haploid Control I (Figure 5A-B and Figure 5G). Interestingly, when applying the 8% cutoff for changes in efficiency, we identify several origins that are clearly altered in usage (Figure 5F). Indeed, the most significant changes are located proximal to the LoxP sites in Chromosome I, within the rearranged region (Figure 5C-E). In particular, the alterations are restricted to ~100 kb regions at each end of the inversion (Figure 5C). Specifically, origins that were initially efficient became inefficient once transposed next to an inefficient region (Figure 5D), and inefficient sites that were moved into the context of an efficient region were increased in usage (Figure 5E).

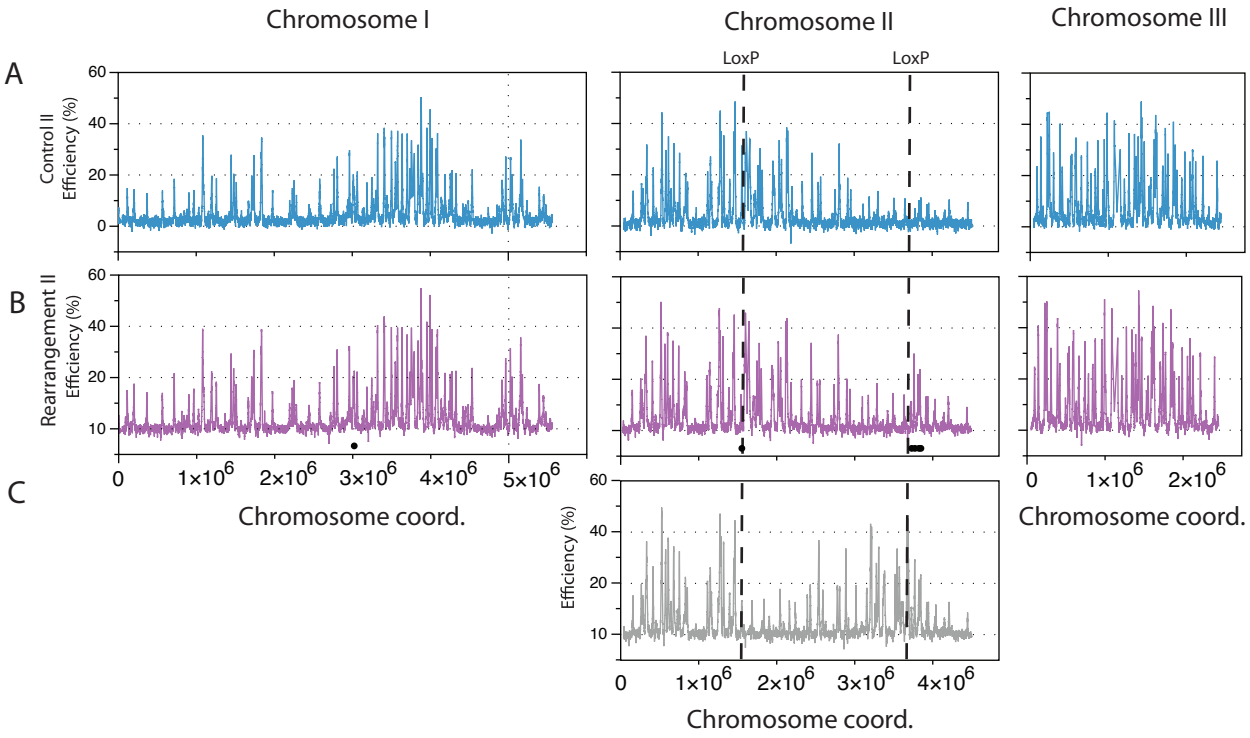

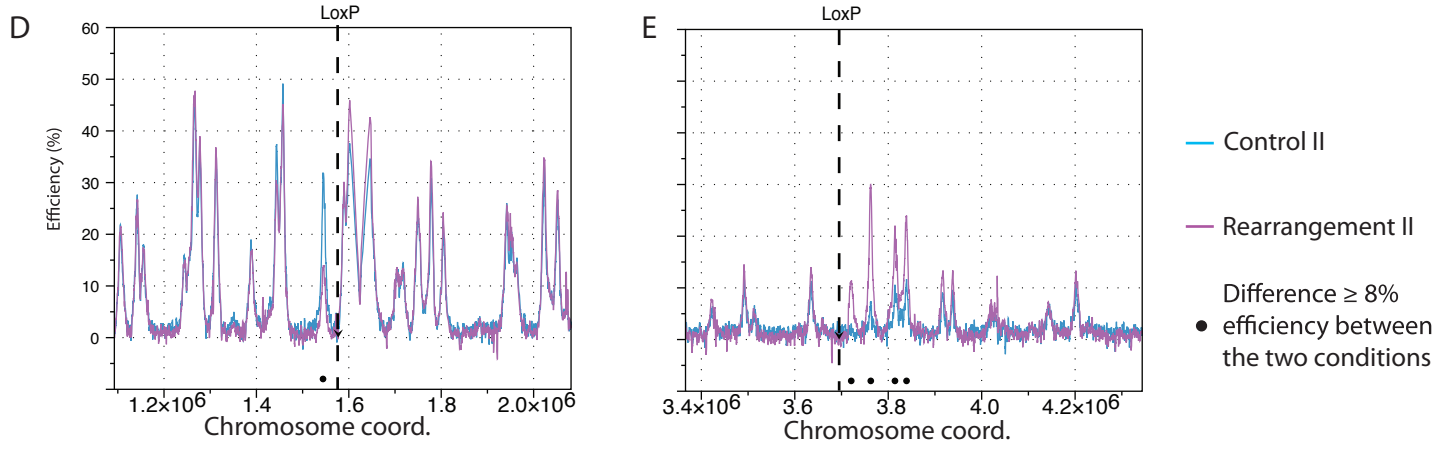

F

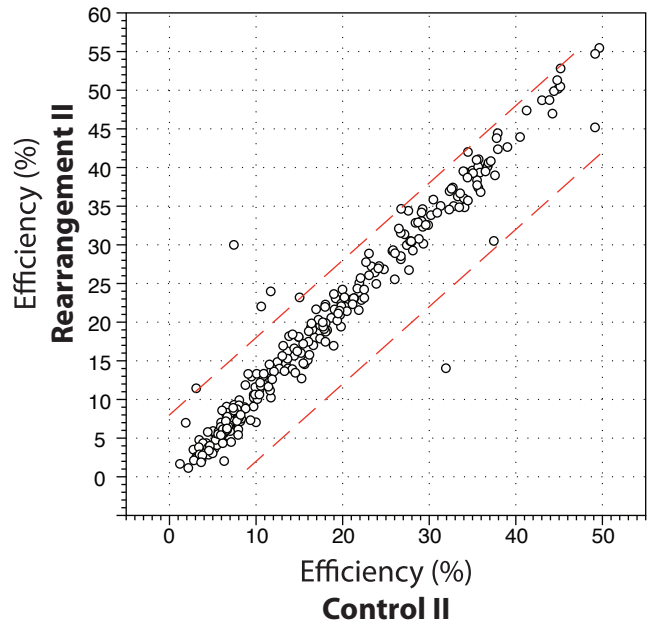

G

	Control II	Rearrangement II
Total number of origins	186	196
Average origin efficiency (%)	24.42	26.30
Number of origins in common	186	
% in common	100	89.64
Number of unique to each condition	-	10
% unique origin	-	5.1
Average efficiency of unique origins (%)	-	13
Standard deviation of efficiencies of unique origins	-	0.06

Figure 6: Inversion of a region of chromosome II induces local changes in origin usage outside of the inverted segment in mitotic S-phase.
A-B) Origin usage profiles of Haploid Control II (A, blue) and Haploid Rearrangement II (B, purple). The profile of the rearrangement is plotted with the original, pre-arrangement coordinates to allow direct comparison with the Control strain. Dashed lines represent the locations of the LoxP insertions at ChrII: 1577150 and ChrII: 3694900. Black dots indicate origins with ≥8% efficiency difference between the two programs. C) Profile showing origin efficiencies using the post-rearrangement chromosomal coordinates (gray). X-axis: chromosome coordinates. Y-axis: origin efficiencies. Dashed lines: LoxP insertions. D-E) Detailed view of origin efficiencies in the region surrounding the LoxP sites as in A. x-axis: chromosome coordinates, y-axis: Origin efficiencies. Blue: Control II, purple: Rearrangement II. Dashed lines: LoxP insertions. Black dots indicate origins with ≥8% efficiency difference between the two programs. F) Comparison of origin efficiencies in Control II vs. Rearrangement II cells. The efficiencies of the origins present in the compiled list of all origins (see materials and methods) are shown. X-axis: efficiency in the Control II program, y-axis: efficiency in the Rearrangement II program. Red dashed lines represent an 8% efficiency difference between the two strains. We identified 5 origins with a difference in efficiency higher than 8%, which are located near the LoxP sites, outside of the rearranged region (indicated by the black dots in D and E). G) Analysis of origin usage in the Control II and Rearrangement II replication programs.

For Haploid Rearrangement II, we identified 196 origins with an overall efficiency of 26.30%. Comparison with its Control II reveals that 95% of the origins were shared between the two conditions (Figure 6A-B and Figure 6G). Interestingly, we identified clear changes in origin usage due to the inversion (Figure 6C and 6F) that were localized exclusively next to the LoxP sites on Chromosome II. Similar to Rearrangement I, decreases in origin usage were found at efficient origins that were relocalized adjacent to inefficient regions (Figure 6D), while increases in efficiency resulted from bringing inefficient sites next to efficient domains (Figure 6E). Surprisingly, in contrast to Rearrangement I, the observed differences were found outside of the inverted region, within ~100-200 kb of the endpoints (Figure 6C). Thus, while the two chromosomal inversions gave similar results with regard to local changes in origin usage, the locations of these alterations differed depending on the chromosomal rearrangement.

We then performed the same analyses using the diploids Pat1 strains, and origins were mapped as described above.. In diploid Pat1 cells, non-replicated genomic DNA was isolated from nitrogen-starved cells with a 2C DNA content before release from nitrogen starvation. Replicated genomic DNA was then harvested from cells 210

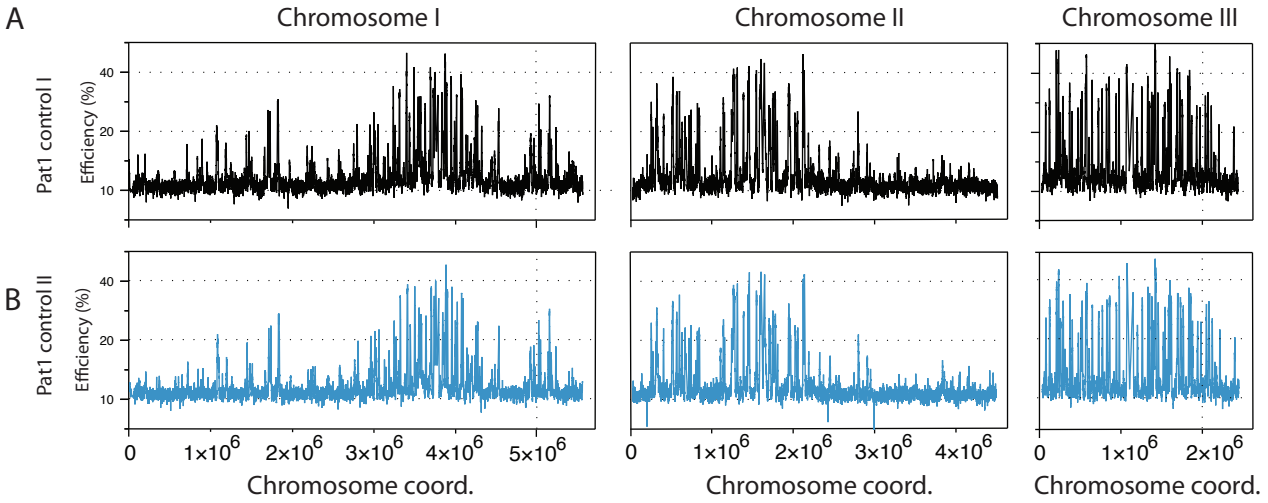

C

	Pat1 Control I	Pat1 Control II
Total number of origins	226	203
Average origin efficiency (%)	24.47	24.17
Number of origins in common	200	
% in common	88.49	98.52
Number of unique to each condition	26	3
% unique origin	11.4	1.3
Average efficiency of unique origins (%)	11	11
Standard deviation of efficiencies of unique origins	0.01	0.0015

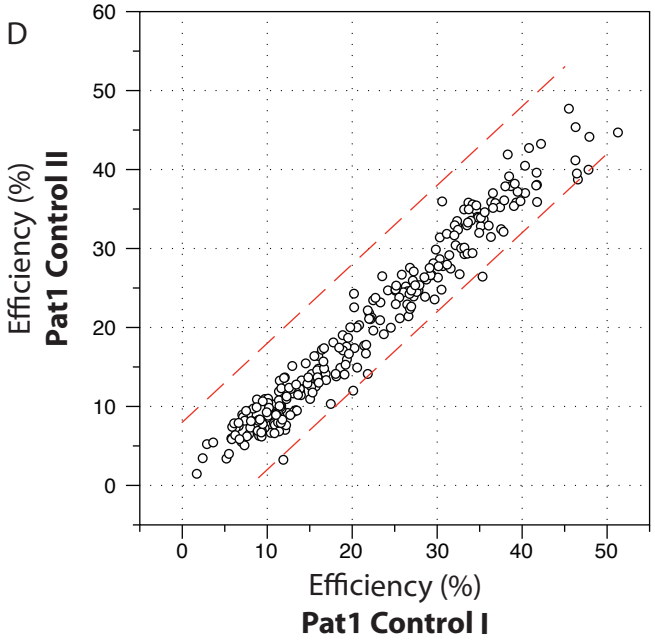

Figure 7: LoxP insertions do not change the replication program during pre-meiotic S-phase.
A-B) Origin usage profiles of Pat1 Control I (A, black) and Pat1 Control II (B, blue). X-axis: chromosome coordinates. Y-axis: origin efficiencies. C) Analysis of origin usage in the Pat1 Control I and Pat1 Control II replication program. D) Comparison of origin efficiencies in Pat1 Control I vs. Pat1 Control II cells. The efficiencies of the origins present in the compiled list of all origins (see materials and methods) are shown. X-axis: efficiency in Pat1 Control II, y-axis: efficiency in the Pat1 Control I. Red dashed lines represent a 8% difference in efficiency between the two strains.

minutes after release from nitrogen starvation (Figure 3C), 60 min after the end of S-phase in non-HU treated cells. We compared the replication programs of Pat1 Control I and Pat1 Control II strains (Figure 7). Both replication programs showed almost identical profiles of origin usage (Figure 7A-B). Using the 10% efficiency cutoff for origin identification, we identified 226 origins in Pat1 Control I and 203 origins in Pat1 Control II. Over 87% of these sites were shared between the two backgrounds, and their average origin efficiencies were very similar (24.47% and 24.17% for Pat1 Control I and II, respectively) (Figure 7C). Using the 8% cutoff in absolute efficiency, quantitative analysis of the differences in origin efficiencies between the two conditions showed no major changes in origins efficiencies (Figure 7D).

We then compared each chromosomal rearrangement with its control (Figure 8 and 9). We found 261 origins in Pat1 Rearrangement I (Figure 8A-B), with an overall average efficiency of 23.16%; 81% of them were shared with Control I (Figure 8G). Interestingly, using an 8% cutoff for changes in efficiency, we identified nine origins with significant changes in efficiencies (Figure 8D and 8F). As for Haploid Rearrangement I, the most significant changes are located within the rearranged region and proximal to the LoxP sites in chromosome I (Figure 8C-E). These alterations are restricted to ~100 kb regions at the endpoints of the inversion (Figure 8D-E), and they are similar to those observed in a mitotic S-phase. In Pat1 rearrangement II, we found 214 origins with an overall average efficiency of 24.09% (Figure 9A-B and G). Comparison with its control revealed that 88% of the origins were shared between the two conditions. We also found that nine origins were changed by more than 8% (Figure 9D-F), and all of these sites were located directly outside of the inversion on chromosome II in within ~100-200kb of the endpoints (Figure 9D-E). In these regions, we detected similar changes in origin efficiencies as in the Haploid Rearrangement II replication program. Thus, similarly to the haploid rearrangements, both chromosomal inversions locally altered the replication program during pre-meiotic S-phase in regions proximal to the LoxP sites.

All together, our results demonstrated that changes in chromosomal context induced changes in origin selection in regions adjacent to the endpoints of the

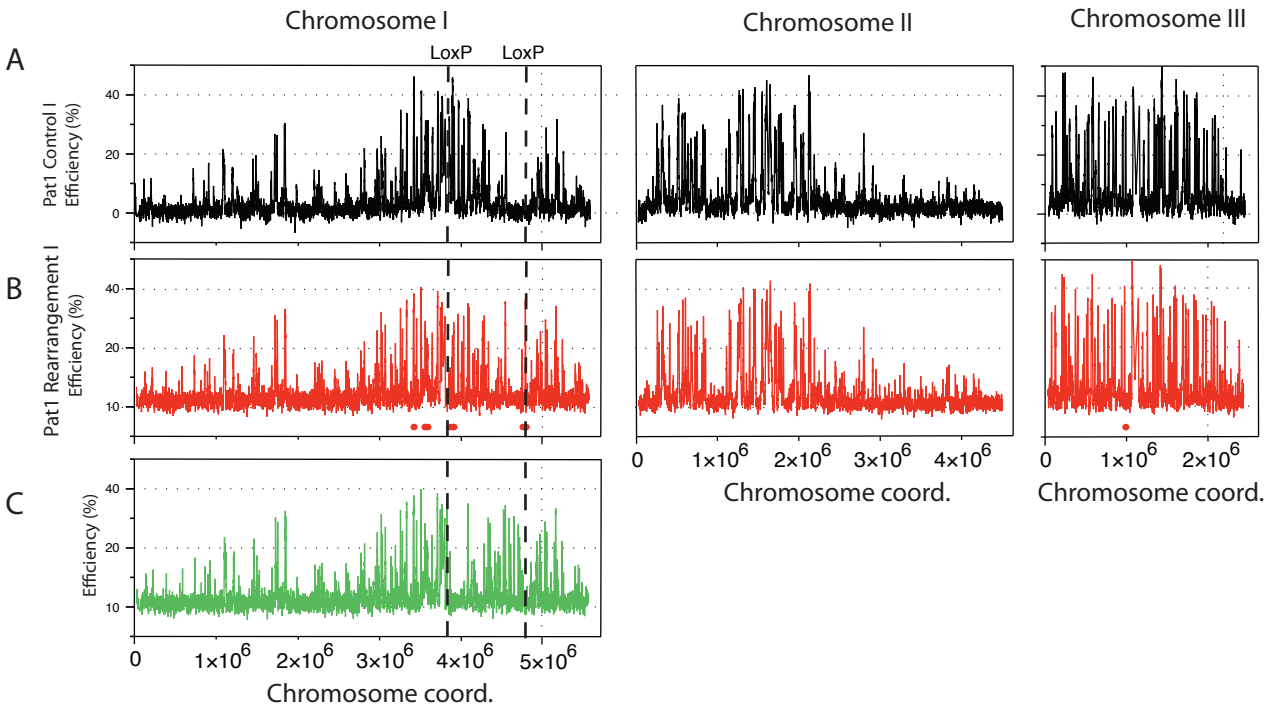

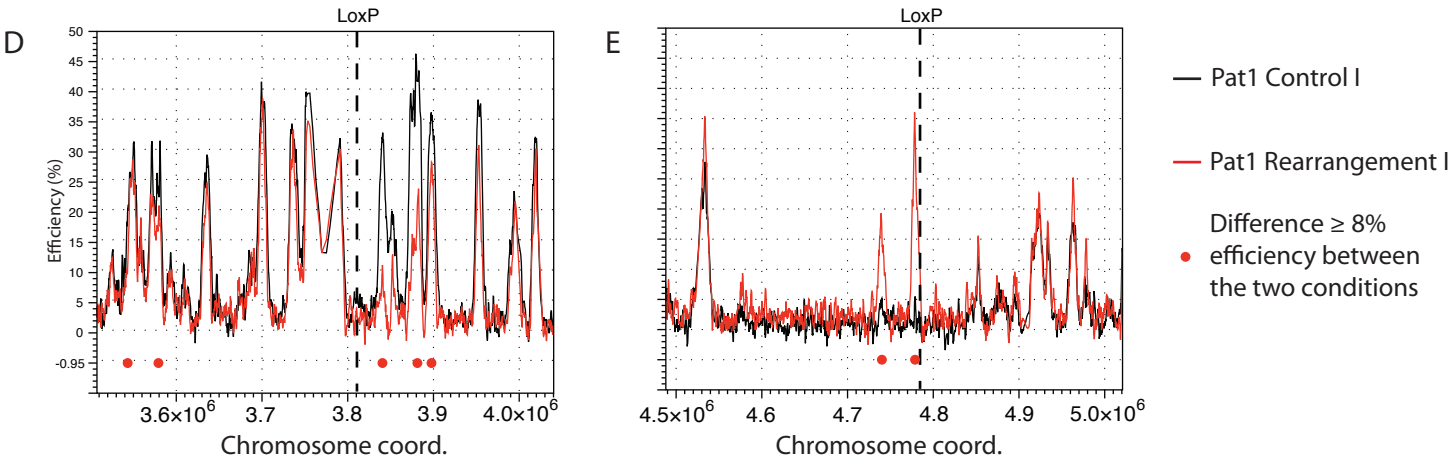

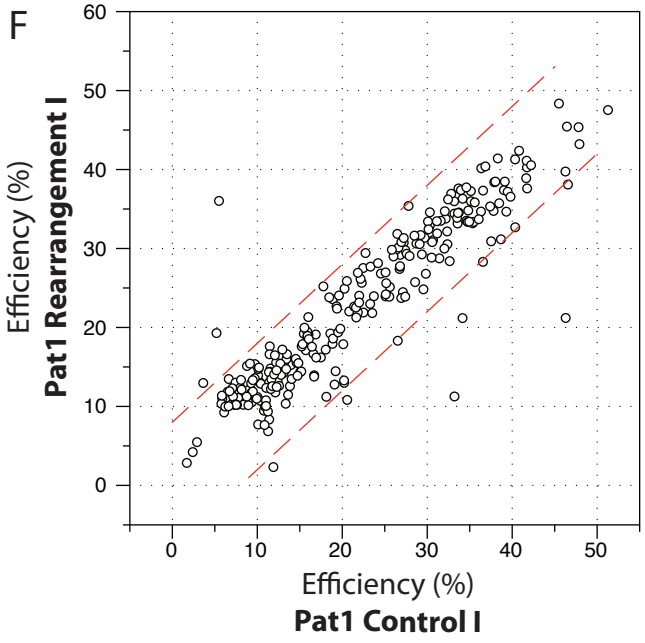

G

	Pat1 Control I	Pat1 Rearrangement II
Total number of origins	226	261
Average origin efficiency (%)	24.47	23.16
Number of origins in common	218	
% in common	96.46	83.52
Number of unique to each condition	8	43
% unique origin	2.97	15.99
Average efficiency of unique origins (%)	11	12
Standard deviation of efficiencies of unique origins	0.005	0.04

Figure 8: Inversion of a region of chromosome I induces local changes in origin usage within the inverted segment in pre-meiotic S-phase.
A-B) Origin usage profiles of Pat1 Control I (A, black) and Pat1 Rearrangement I (B, red). The profile of the rearrangement is plotted with the original, pre-arrangement coordinates to allow direct comparison with the Pat1 Control strain. Dashed lines represent the locations of the LoxP insertions at ChrI: 3810766 and ChrI: 4785016. Red dots indicate origins with ≥8% efficiency difference between the two programs. C) Profile showing origin efficiencies using the post-rearrangement chromosomal coordinates (green). X-axis: chromosome coordinates. Y-axis: origin efficiencies. Dashed lines: LoxP insertions. D-E) Detailed view of the origin usage profiles in regions surrounding the LoxP sites as in A. Black: Pat Control I, red: Pat1 Rearrangement I. Dashed lines: LoxP insertions. Red dots highlight origins that show changes of ≥8% efficiency between Pat1 Control I and Pat1 Rearrangement I. x-axis: chromosome coordinates, y-axis: origin efficiencies. F) Comparison of origin efficiencies in Pat1 Control I vs. Pat1 Rearrangement I. The efficiencies of the origins present in the compiled list of all origins (see materials and methods)are shown. X-axis: efficiency Pat1 Control I, y-axis: efficiency Pat1 Rearrangement I. Red dashed lines represent an 8% efficiency difference between the two strains. The 5 biggest changes in origin usage are located around the around the LoxP sites (indicated by the red dots in D and E). G) Analysis of origin usage in the Pat1 Control I and Pat1 Rearrangement I replication programs.

inversions. The distinct inversions bring about alterations either within or outside of the rearranged region.

Comparison of origin usage in mitotic and pre-meiotic S-phase

Although previous work has suggested that pre-meiotic S-phase does not induce a specific pattern of origin usage, we asked whether the chromosomal rearrangements might have different effects in these two conditions. Indeed, there are features of chromosomal organization that are distinct for mitotic and meiotic cycles: for instance, the Rec8 cohesin is specifically expressed during meiosis and required for proper chromosome segregation as well as meiotic recombination (Watanabe and Nurse, 1999). For these analyses, we began by comparing the overall profile of Haploid Control I vs. Pat1 Control I. We found that origin usage is very similar between the two conditions (Figure 10A-B): almost all origins in Haploid Control I are found in Pat1 Control 1, and the average efficiencies in the two strains are comparable (22.56% and 24.47% for Haploid Control I and Pat1 Control I, respectively) (Figure 10 A-B and 10E).

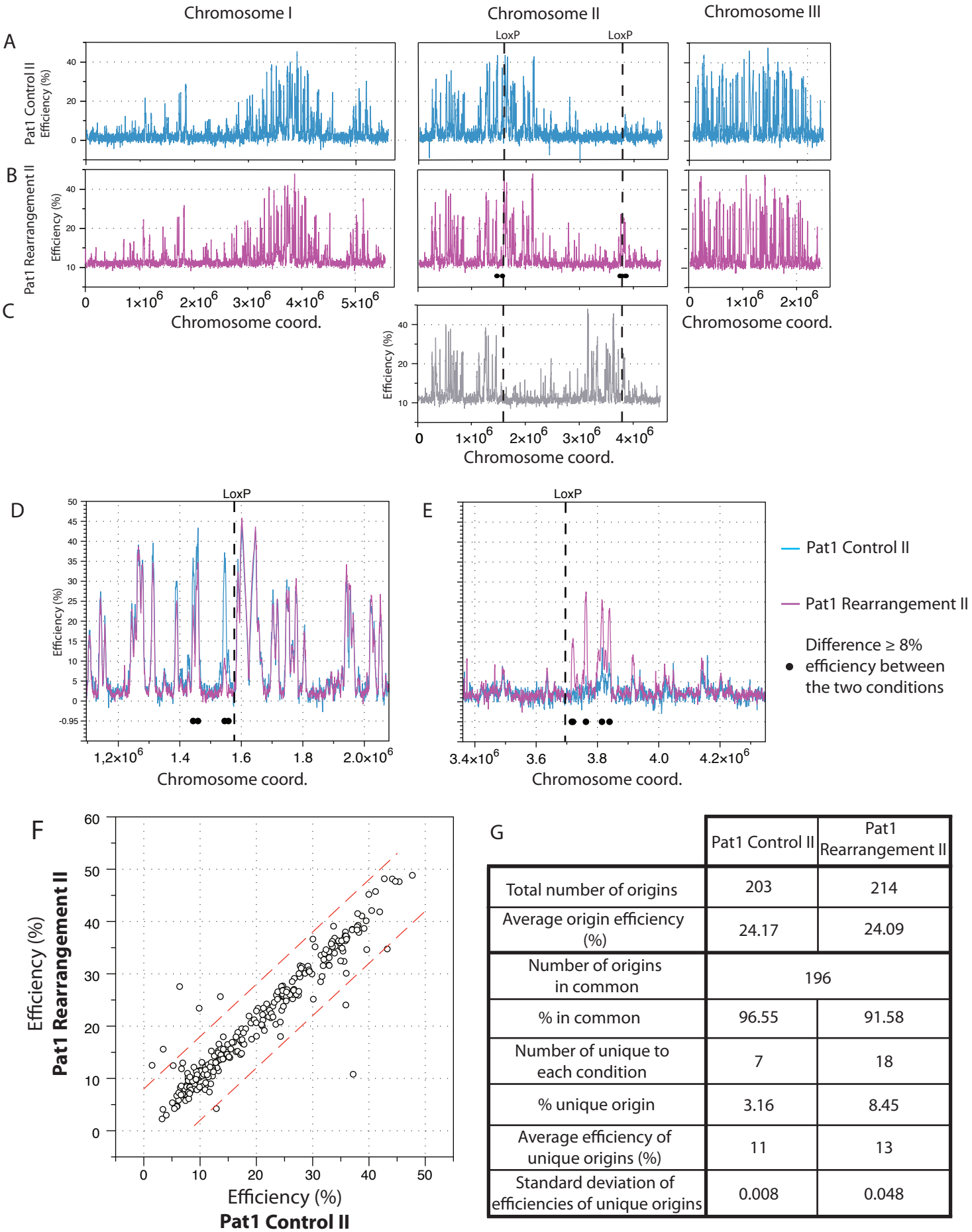

F

G

	Pat1 Control II	Pat1 Rearrangement II
Total number of origins	203	214
Average origin efficiency (%)	24.17	24.09
Number of origins in common	196	
% in common	96.55	91.58
Number of unique to each condition	7	18
% unique origin	3.16	8.45
Average efficiency of unique origins (%)	11	13
Standard deviation of efficiencies of unique origins	0.008	0.048

Figure 9: Inversion of a region of chromosome II induces local changes in origin usage outside of the inverted segment in meiotic S-phase.
A-B) Origin usage profiles of Pat1 Control II (A, blue) and Pat1 Rearrangement II (B, purple). The profile of the rearrangement is plotted with the original, pre-arrangement coordinates to allow direct comparison with the Pat1 Control II strain. Dashed lines represent the locations of the LoxP insertions at ChrII: 1577150 and ChrII: 3694900. Black dots indicate origins with ≥8% efficiency difference between the two programs. C) Profile showing origin efficiencies using the post-rearrangement chromosomal coordinates (gray). X-axis: chromosome coordinates. Y-axis: origin efficiencies. Dashed lines: LoxP insertions. D-E) Detailed view of origin efficiencies in the region surrounding the LoxP sites as in A. x-axis: chromosome coordinates, y-axis: Origin efficiencies. Blue: Pat1 Control II, purple: Pat1 Rearrangement II. Dashed lines: LoxP insertions. Black dots indicate origins with ≥8% efficiency difference between the two programs. F) Comparison of origin efficiencies in Pat1 Control II vs. Pat1 Rearrangement II cells. The efficiencies of the origins present in the compiled list of all origins (see materials and methods) are shown. X-axis: efficiency in the Pat1 Control II program, y-axis: efficiency in the Pat1 Rearrangement II program. Red dashed lines represent an 8% efficiency difference between the two strains. We identified 5 origins with a difference in efficiency higher than 8%, which are located near the LoxP sites, outside of the rearranged region (indicated by the black dots in D and E). G) Analysis of origin usage in the Pat1 Control II and Pat1 Rearrangement II replication programs.

However, we observed that there are 54 origins that are unique to Pat1 Control I and that origin usage was generally higher in this background. By applying the cutoff of 8% absolute efficiency to define significant changes, we found that 71 origins showed increases in usage in the Pat1 strain, while only 5 origins were decreased in efficiency (Figure 10E). Interestingly, we noted that most of the unique origins and increases in origin activity in Pat1 Control I are located in efficient regions of the genome. Next, comparing the overall profile of Haploid Control II vs. Pat1 Control II, we found that overall origin usage is also very similar between the two conditions (Figure 11A-B). The vast majority of sites are shared between the two backgrounds and their average efficiencies were very comparable (Figure 11E-F). However, we also identified origins that were unique to each condition as well as sites that showed significant changes in usage. Applying the cutoff of 8% absolute efficiency to define significant changes, we found that 23 origins showed increases in usage in the Pat1 Control II strain and 15 origins were decreased in efficiency (Figure 11E). Similar to what we described above, in Pat1 Control II, efficient regions contained both origins that are unique to or show increases in this background (Figure 11A-B). In contrast, the Control I strain displayed increased efficiencies and unique origins in low efficiency regions. Thus, while the

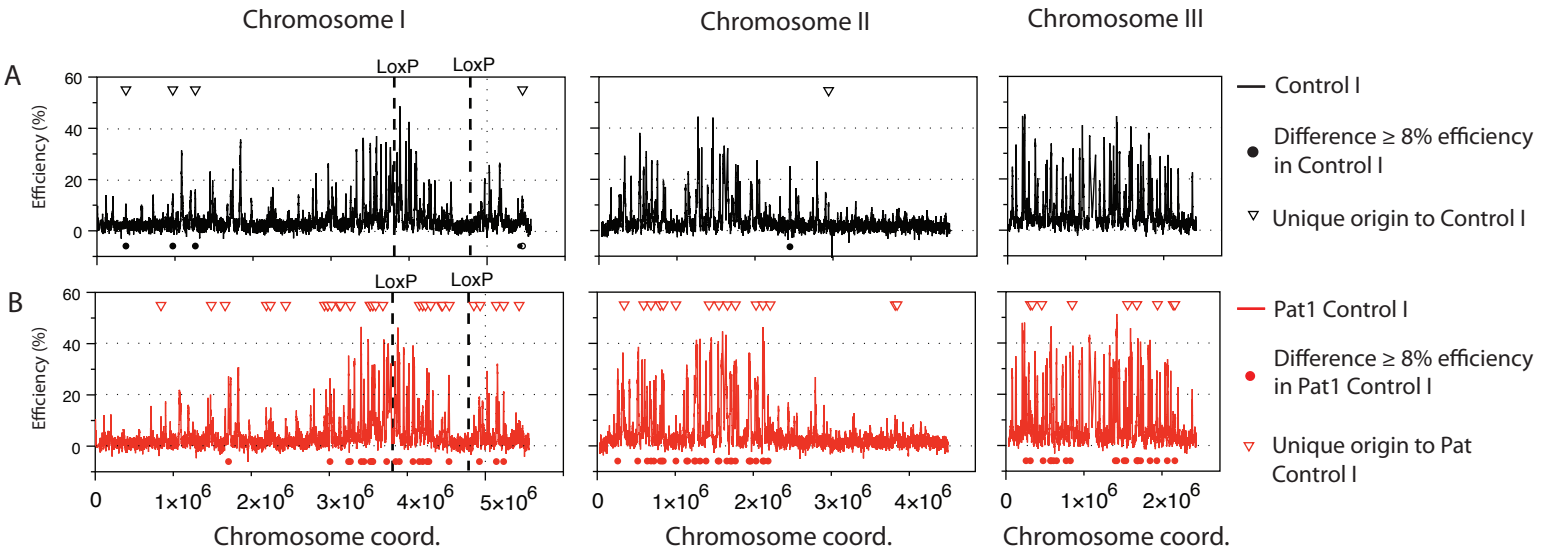

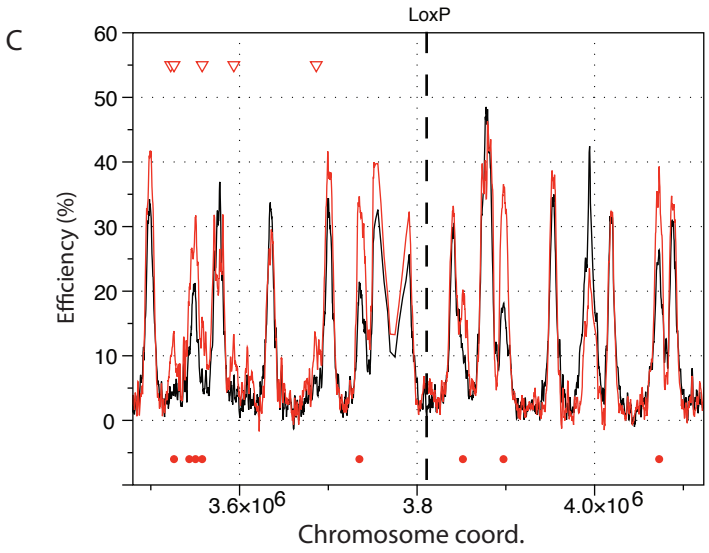

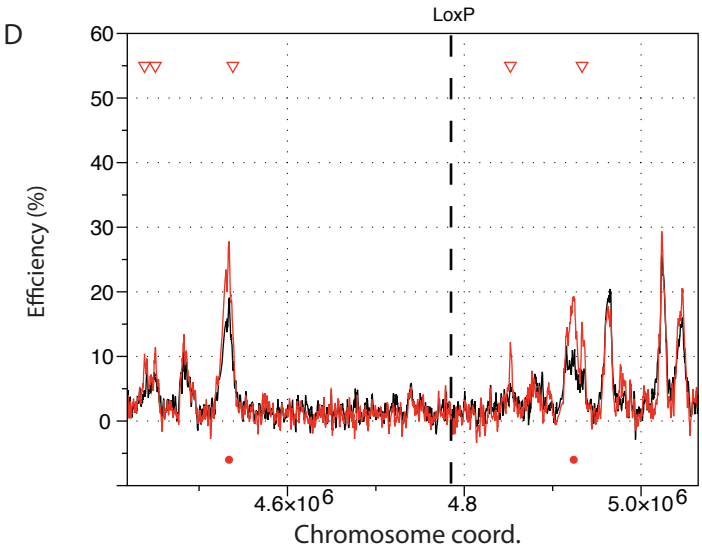

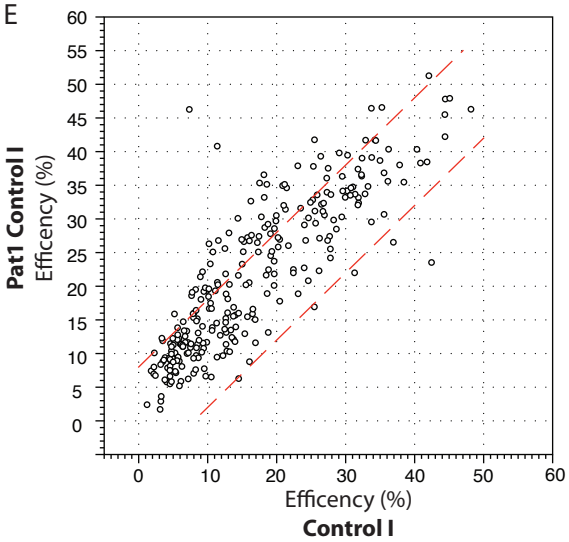

F

	Control I	Pat1 Control I
Total number of origins	177	226
Average origin efficiency (%)	22.56	24.47
Number of origins in common	172	
% in common	97.17	76.11
Number of unique to each condition	5	54
% unique origin	2.16	23.38
Average efficiency of unique origins (%)	12.9	14.18
Standard deviation of efficiencies of unique origins	0.02	0.06

Figure 10: The overall replication program remains the same between mitosis and meiosis. A) Haploid Control I (black) and B) Pat1 Control I (red) replication profiles. Dashed lines represent the location of the LoxP insertions at ChrI: 3810766 and ChrI: 4785016. Black dots: origins that show higher efficiencies (≥8%) in Haploid Control I; red dots: origins that show higher efficiencies (≥8%) in Pat1 Control I. Black triangles: origins unique to Haploid Control I; red triangles: origins unique to Pat1 Control I. C-D) Detailed view of origin efficiencies in the region surrounding the LoxP sites. x-axis: chromosome coordinates, y-axis: origin efficiencies. Red dots are as in B. E) Comparison of origin efficiencies in Haploid Control I vs. Pat1 Control I cells. The efficiencies of the origins present in the compiled list of all origins (see materials and methods) are shown. X-axis: efficiency in Haploid Control I, y-axis: efficiency in Pat1 Control I. Red dashed lines represent an 8% efficiency difference between the two strains. We identified 76 origins with a difference in efficiency ≥8% (indicated by the black and red dots in A-C). 5 origins show increases in usage in Haploid Control I, 71 show an increase in usage in Pat1 Control I. G) Analysis of origin usage in the Haploid Control I and Pat1 Rearrangement I replication programs.

overall replication pattern appears to be the same in mitotic and meiotic cells, our results suggest that there may be different alterations in origin usage in distinct genomic regions between these conditions.

We then focused on comparing strains that have chromosomal rearrangements. We first compared Haploid Rearrangement I vs. Pat1 Rearrangement I (Figure 12). Again, we found that origin usage is very similar between the two conditions (Figure 12A-B): almost all origins in Haploid Rearrangement I are found in Pat1 rearrangement I and origins showed an similar average efficiencies between the two strains (25.87% and 23.16% for Rearrangement I and Pat1 Rearrangement I, respectively) (Figure 12 A-B and 12E). However, 69 origins were identified only in Pat1 Control I, and these were enriched in high efficiency regions. Applying the cutoff of 8% absolute efficiency to define significant changes, we found that 45 origins showed increases in usage in the Pat1 strain while 22 were decreased in efficiency (Figure 10E). Interestingly, in contrast to the comparisons between the Control strains above, we found both increase and decreases in origin activity in efficient genomic regions (Figure 12A-C). We next extended these analyses and compared Haploid Rearrangement II vs. Pat1 Rearrangement II (Figure 13). Almost all of the origins present in Haploid Rearrangement II were present in the Pat1 Rearrangment II, and both strains showed similar average origin efficiencies (26.30% and 24.09% for Haploid Rearrangement II

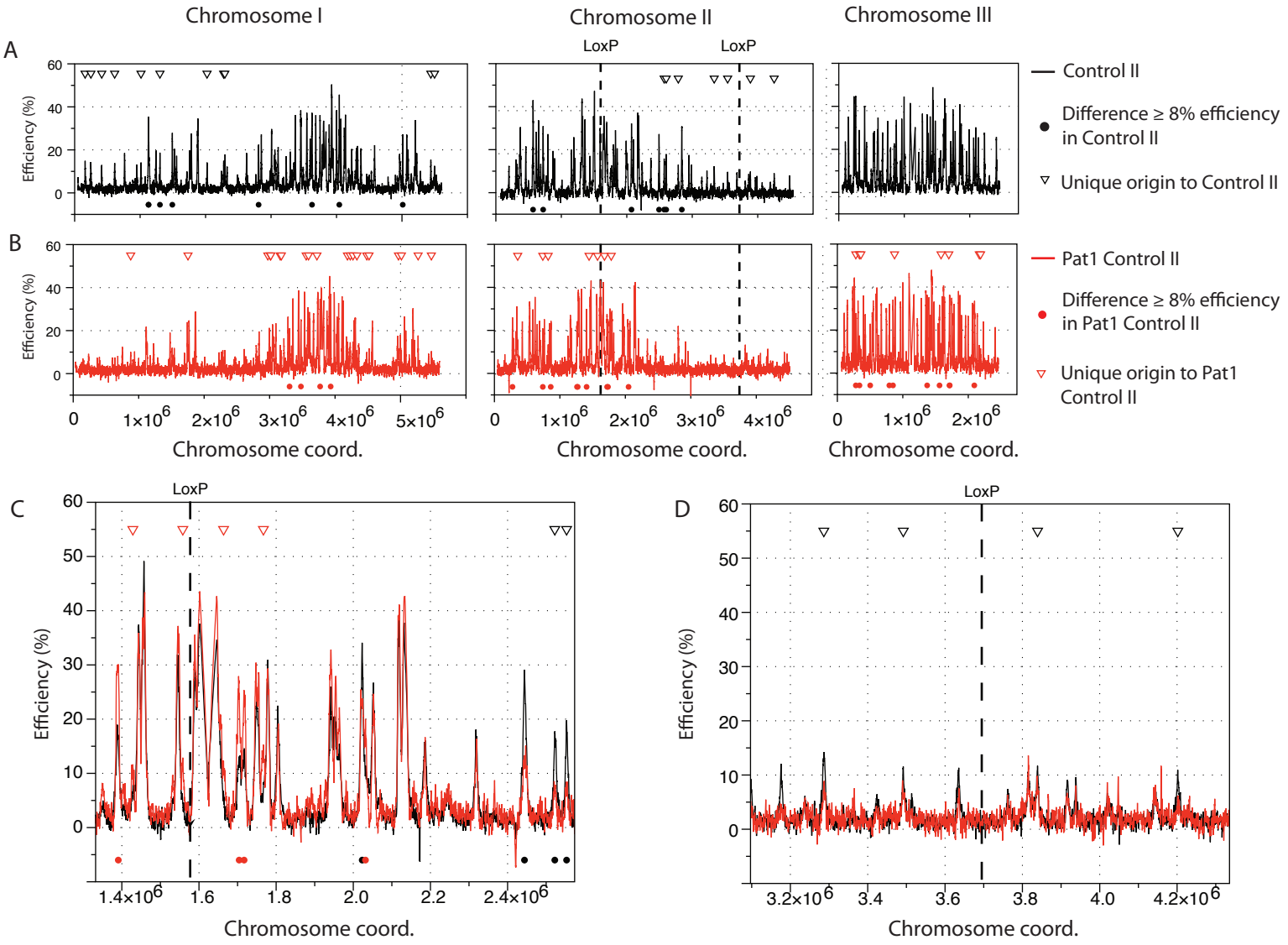

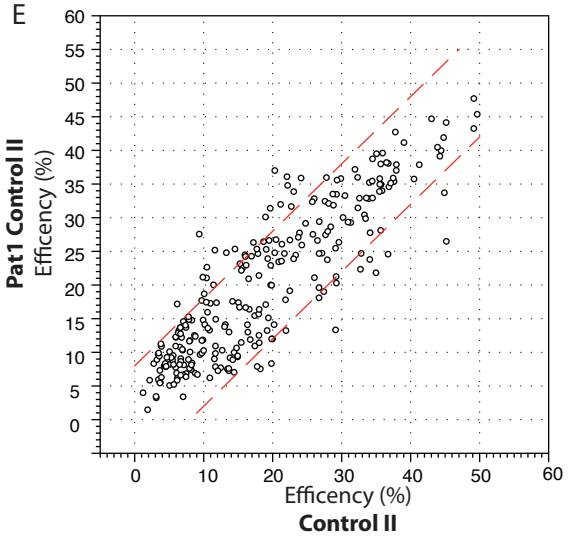

F

	Control II	Pat1 control II
Total number of origins	186	203
Average origin efficiency (%)	24.42	24.17
Number of origins in common	168	
% in common	90.32	82.76
Number of unique to each condition	18	35
% unique origin	8.14	17.24
Average efficiency of unique origins (%)	14.08	13.33
Standard deviation of efficiencies of unique origins	0.02	0.034

Figure 11: The overall replication program of Haploid Control II and Pat1 Control II remains the same between mitosis and meiosis.
A) Haploid Control II (black) and B) Pat1 Control II (red) replication profiles. Dashed lines represent the location of the LoxP insertions at ChrII: 1577150 and ChrII: 3694900. Black dots: origins that show higher efficiencies (≥8%) in Haploid Control II; red dots: origins that show higher efficiencies (≥8%) in Pat1 Control II. Black triangles: origins unique to Haploid Control II; red triangles: origins unique to Pat1 Control II. C-D) Detailed view of origin efficiencies in the region surrounding the LoxP sites at C) ChrII: 1577150 and D) ChrII: 3694900. x-axis: chromosome coordinates, y-axis: origin efficiencies. Red dots are as in B. E) Comparison of origin efficiencies in Haploid Control II vs. Pat1 Control II cells. The efficiencies of the origins present in the compiled list of all origins (see materials and methods) are shown. X-axis: efficiency in Haploid Control II program, y-axis: efficiency in the Pat1 Control II. Red dashed lines represent an 8% efficiency difference between the two strains. We identified 38 origins with a difference in efficiency ≥8% (indicated by the black and red dots in A-C). 15 origins show increases in usage in Haploid Control II, 23 show increase in Pat1 Control II. G) Analysis of origin usage in the Haploid Control II and Rearrangement II replication programs.

and Pat1 Rearrangement II, respectively; Figure 13E-F). We also noted alterations in origin usage that are different in distinct domains: for instance, most of the origins unique to or increased in Pat1 Rearrangement II are found in efficient regions, while origins that were decreased or not found in this background are preferentially located in inefficient regions (Figure 13A-B).

Therefore, our data suggest that although the replication program between mitosis and meiosis is very similar, there may be domain-related differences in origin activity between these conditions.

Local changes in meiotic DSBs formation on rearranged chromosomes

As discussed in the Introduction, earlier work has demonstrated that origin selection is a key determinant for organizing meiotic recombination (Wu and Nurse, 2014). Indeed, changing the genome-wide pattern of replication initiation during pre-meiotic S-phase has consequences for the pattern of meiotic DSBs (Wu and Nurse, 2014). Specifically, regional changes in origin efficiency were correlated with local changes in DSB formation. Given these findings, we set out to assess whether the

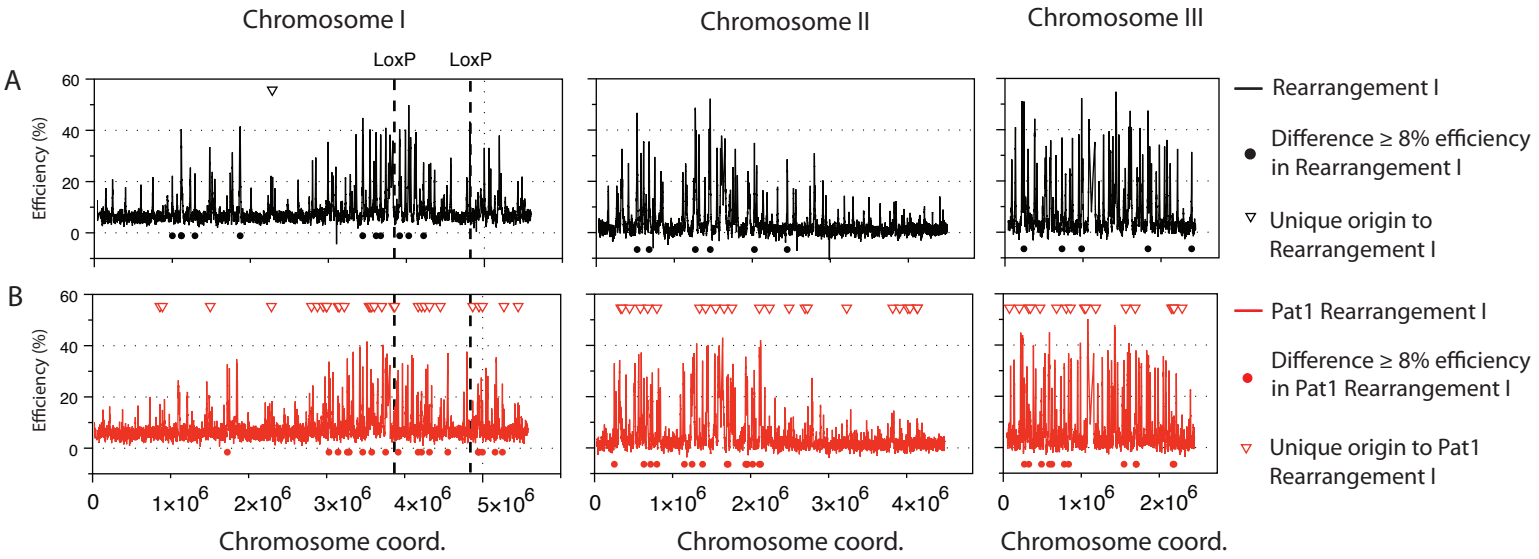

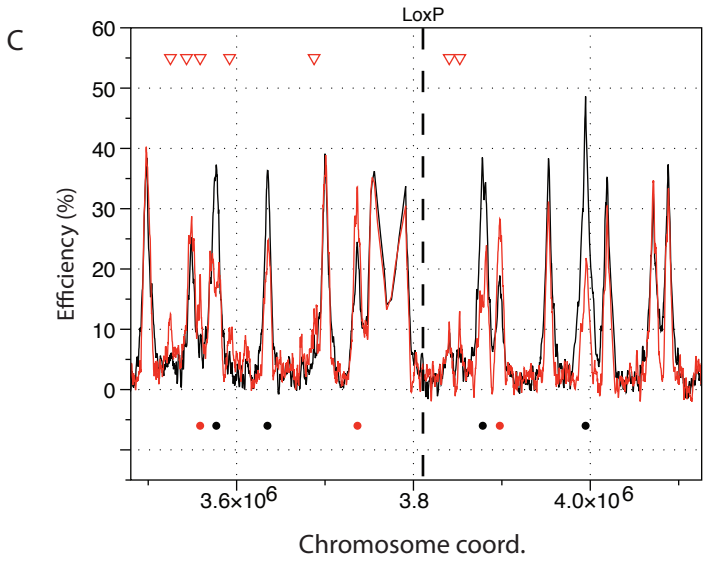

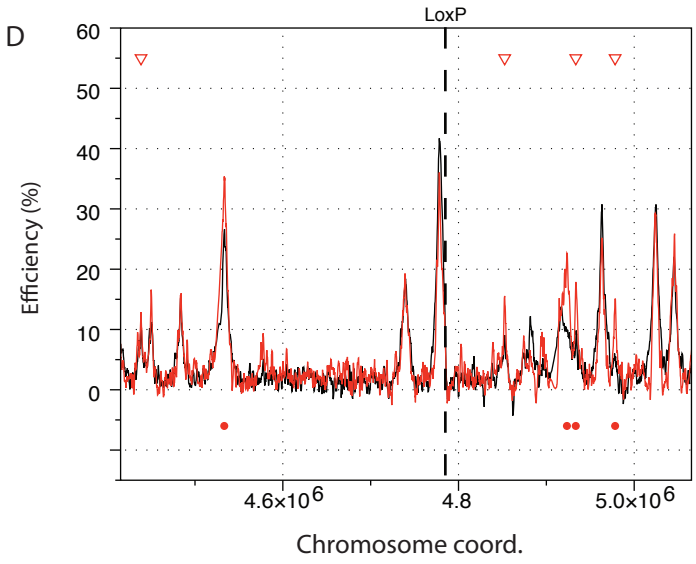

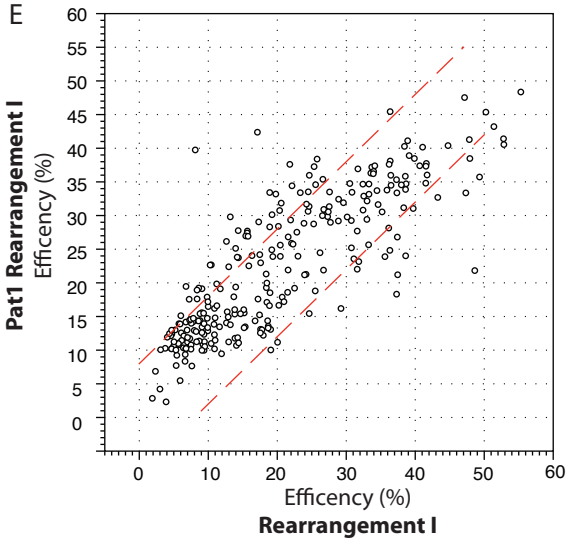

F

	Rearrangement I	Pat1 Rearrangement I
Total number of origins	193	261
Average origin efficiency (%)	25.87	23.16
Number of origins in common	192	
% in common	99.48	73.56
Number of unique to each condition	1	69
% unique origin	0.38	26.44
Average efficiency of unique origins (%)	11.9	13.53
Standard deviation of efficiencies of unique origins	-	0.04

Figure 12: The overall replication program of Rearrangement I and Pat1 Rearrangement I remains the same between mitosis and meiosis.
A) Rearrangement I (black) and B) Pat1 Rearrangement I (red) replication profiles. Dashed lines represent the location of the LoxP insertions at ChrI: 3810766 and ChrI: 4785016. Black dots: origins that show higher efficiencies (≥8%) in Rearrangement Control I; red dots: origins that show higher efficiencies (≥8%) in Pat1 Rearrangement I. Black triangles: origins unique to Haploid Rearrangement I; red triangles: origins unique to Pat1 Rearrangement I. C-D) Detailed view of origin efficiencies in the region surrounding the LoxP sites. x-axis: chromosome coordinates, y-axis: origin efficiencies. Red dots are as in B. E) Comparison of origin efficiencies in Haploid Rearrangement I vs. Pat1 Rearrangement I cells. The efficiencies of the origins present in the compiled list of all origins (see materials and methods) are shown. X-axis: efficiency in Haploid Rearrangement I, y-axis: efficiency in Pat1 Rearrangement I. Red dashed lines represent an 8% efficiency difference between the two strains. We identified 67 origins with a difference in efficiency ≥8% (indicated by the black and red dots in A-C). 22 origins show increases in usage in Haploid Control I, 45 show an increase in usage in Pat1 Control I. G) Analysis of origin usage in the Control I and Rearrangement I replication programs.

alterations in origin efficiency that arise due to the chromosomal rearrangements lead to changes in DSB formation.

For this analysis, we focused on the chromosome II inversion, which generated clear changes in origin usage in ~200 kb regions surrounding the rearranged genomic region. We began by determining the timing of DSB formation in the Pat1 Control II and Pat1 Rearranged II strains, using the binding of the recombination protein Rad51 as a marker for DSBs (Roeder, 1997; Wu and Nurse, 2014). Cells grown to exponential phase at 25ºC were depleted of nitrogen, and meiosis was induced upon addition of a nitrogen source and shift to 34°C as described above (Figure 2B). The timing of DSB formation was assessed by chromatin immunoprecipitation (ChIP) of Rad51 followed by quantitative PCR (ChIP-qPCR). We analyzed Rad51 binding at known DSBs previously identified in (Wu and Nurse, 2014) as well as at non-DSB forming sites. We will refer to these sites as Rad 51 sites and Control site respectively. Our results showed maximal levels of Rad51 association at two different DSBs 210 min after meiotic induction in both the Pat1 Control II and Pat1 Rearrangement II backgrounds, at sites that display high (Rad51 site I) or low levels (Rad51 site II) of recruitment (Figure 14B and C). We thus selected this time point for our genome-wide studies of DSBs.

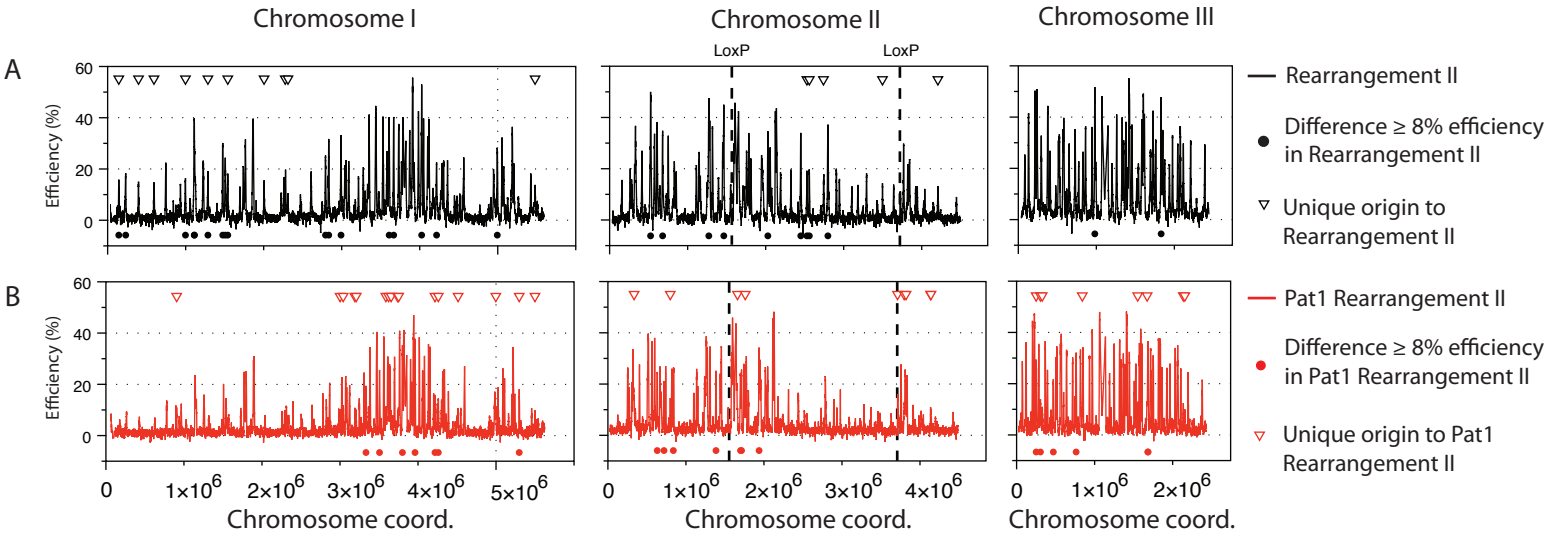

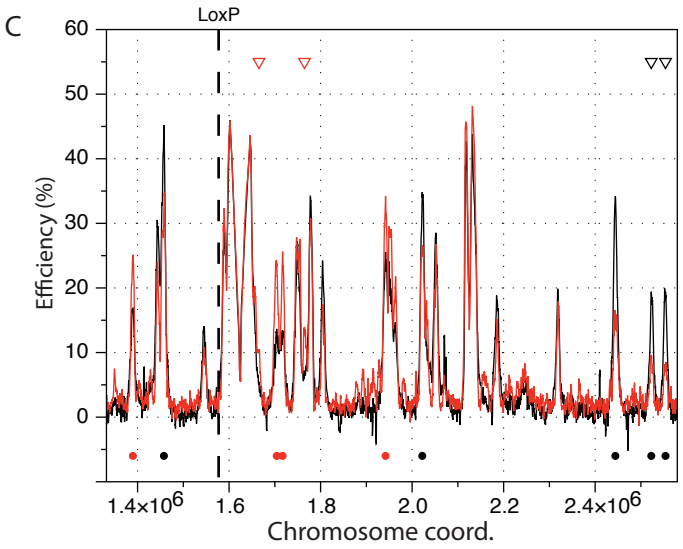

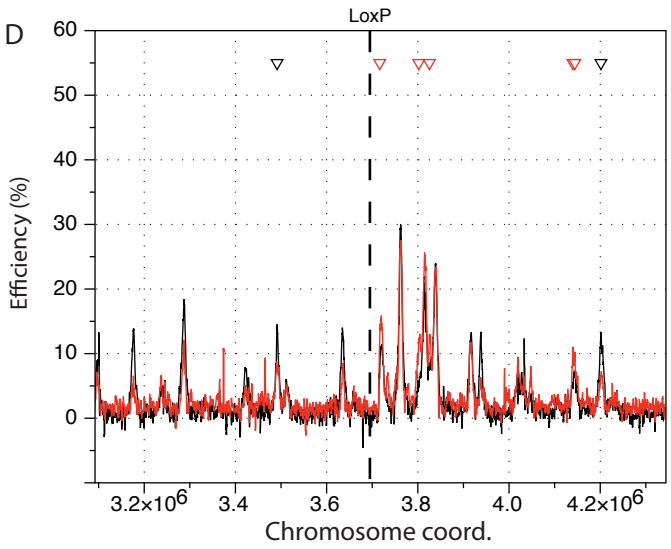

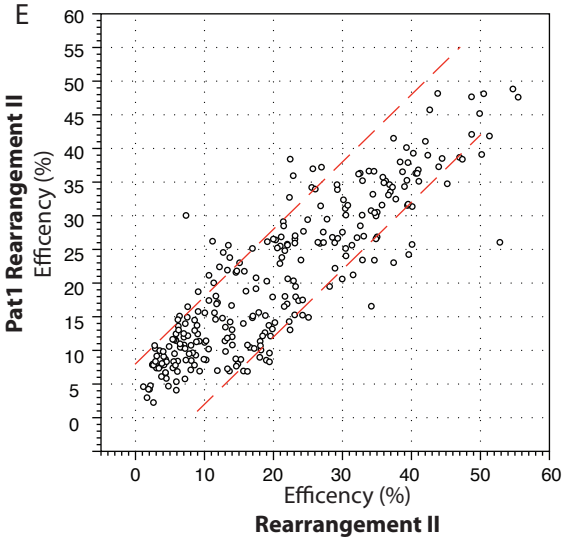

F

	Rearrangement II	Pat1 Rearrangement II
Total number of origins	196	214
Average origin efficiency (%)	26.30	24.09
Number of origins in common	181	
% in common	92.34	84.57
Number of unique to each condition	15	33
% unique origin	6.55	15.42
Average efficiency of unique origins (%)	15.27	13.12
Standard deviation of efficiencies of unique origins	0.03	0.04

<u>Figure 13:</u> The overall replication program of Rearrangement II and Pat1 Rearrangement II remains the same between mitosis and meiosis.
A) Haploid Rearrangement II (black) and B) Pat1 Rearrangement II (red) replication profiles. Dashed lines represent the location of the LoxP insertions at ChrII: 1577150 and ChrII: 3694900. Black dots: origins that show higher efficiencies (≥8%) in Haploid Rearrangement II; red dots: origins that show higher efficiencies (≥8%) in Pat1 Rearrangement II. Black triangles: origins unique to Haploid Rearrangement II; red triangles: origins unique to Pat1 Rearrangement II. C-D) Detailed view of origin efficiencies in the region surrounding the LoxP sites at C) ChrII: 1577150 and D) ChrII: 3694900. x-axis: chromosome coordinates, y-axis: origin efficiencies. Red dots are as in B. E) Comparison of origin efficiencies in Haploid Rearrangement II vs. Pat1 Rearrangement II cells. The efficiencies of the origins present in the compiled list of all origins (see materials and methods) are shown. X-axis: efficiency in Haploid Rearrangement II program, y-axis: efficiency in the Pat1 Rearrangement II. Red dashed lines represent an 8% efficiency difference between the two strains. We identified 48 origins with a difference in efficiency ≥8% (indicated by the black and red dots in A-C). 28 origins show increases in usage in Haploid Rearrangement II, 20 show increase in Pat1 Rearrangement II. G) Analysis of origin usage in the Rearrangement II and Pat1 Rearrangement II replication programs.

We then performed ChIP of Rad51 followed by microarray analysis (ChIP-on-chip) in the same conditions as above, at 210 min after meiotic induction. We found that the genome-wide profiles of Rad51 binding are very similar between the Pat1 Control II and the Pat1 Rearranged II strains (Figure 15A and 15B). To compare DSB formation between the two backgrounds, we used a cutoff of 2.0 (IP/input) to identify sites that are clearly enriched for Rad51. We found similar numbers of Rad51 sites in the Pat1 Control II and Pat1 Rearrangement II backgrounds (503 and 482, respectively), with >94% of the sites in common; the average level of binding was also highly comparable (Figure 15D). We also noted that the insertion of LoxP cassette at Chr II: 1577150 generated an ectopic DSB in both of the strains (compare of Control I (Supplementary Figure 1) with Control and Rearranged II strains). This ectopic DSB could be the result of the insertion of the cassette containing the LoxP site, which contains the constitutively active TEF promoter. Thus, this insertion may induce a change in transcription in this region, and such changes have been previously linked with DSB induction (de Castro et al., 2012).

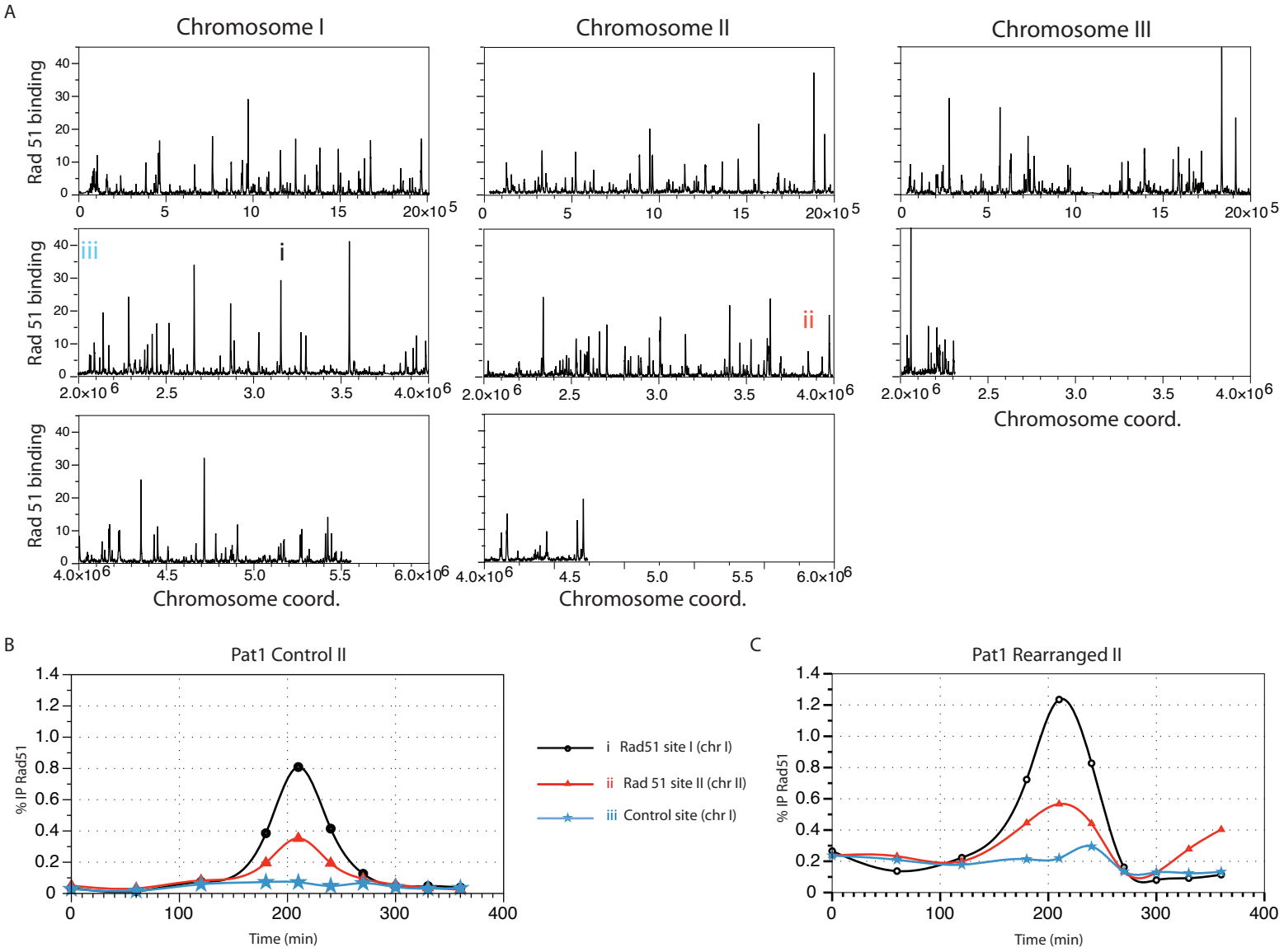

Figure 14: Time course of Rad51 binding during meiosis.
A) Genome-wide profile of Rad51 binding during meiosis after temporary nitrogen depletion (data from Wu and Nurse (2014)). The experimental conditions were comparable to those used in this study. B-C) Time courses of Rad51 binding in Pat1 Control II (B) and Pat1 Rearrangement II (C). Chromatin immunoprecipitation of Rad51 followed by qPCR analysis of three different loci chosen according to the data from Wu and Nurse (2014) are shown (see A). Cells were nitrogen-starved for 16h, re-fed with nitrogen and induced to undergo meiosis by shift to restrictive temperature. The chromosomal positions for each Rad51 site are as follows: i) Chr I: 3.15794x106 (black); ii) Chr II: 3.85804x106 (Red), iii) Chr I: 2.035805x106 (blue). iii) is a locus that shows no Rad51 binding. T = 0 represents the time of the shift to restrictive temperature. Rad51 binding reaches its maximum at 210 min.

Importantly, when we directly compared the level of Rad51 at all identified loci in the two strains, we established that they were virtually identical (Figure 15E). Using a cutoff of two in absolute IP/Input value difference between the control and the rearranged strain (see material and methods for threshold calculation), we found two sites that met this criterion (Figure 15E). Interestingly, each site was located proximal to an endpoint of the rearrangement and corresponds to the region where changes in origin efficiencies were observed (Figure 16). Surprisingly, we found that DSB formation in Pat1 Rearrangement II was reduced compared to its Control at both sites; this contrasts with the changes in origin usage that we observed (Figure 15F and 15G and Figure 16). Moreover, although they did not pass our two-fold cutoff for changes in Rad51 recruitment, we noticed additional changes in DSB formation in these regions that were not present elsewhere in the genome (Figure 15F). Our results therefore indicate that that a 2 Mb inversion of chromosome II does not produce overall changes in Rad51 binding but rather generates local alterations in Rad51 binding. Intriguingly, our data differ from what may have been expected from previous studies, potentially identifying an additional layer of regulation in meiotic recombination. This will be discussed in the next section.

Discussion

In this study, we have investigated the interplay between replication initiation and meiotic DSB formation in the context of chromosomal organization. The distinct chromosomal rearrangements that we generated induced local changes in origin selection. Using this feature, we investigated the effect of altering chromosomal context on origin usage in mitosis and meiosis and on DSB formation during meiosis. Our results showed that chromosomal context shapes the replication program: efficient origins translocated next to low efficiency regions showed a decreased in efficiency, while inefficient origins transposed adjacent to a high efficiency region increased their activity. Moreover, we also showed that a rearrangement of chromosome II leads to changes DSB formation specifically near the endpoints of the inversion. However, in contrast to what would be expected from previous studies, these alterations in Rad51 binding do not reflect the changes in origin efficiencies. Collectively, our findings bring

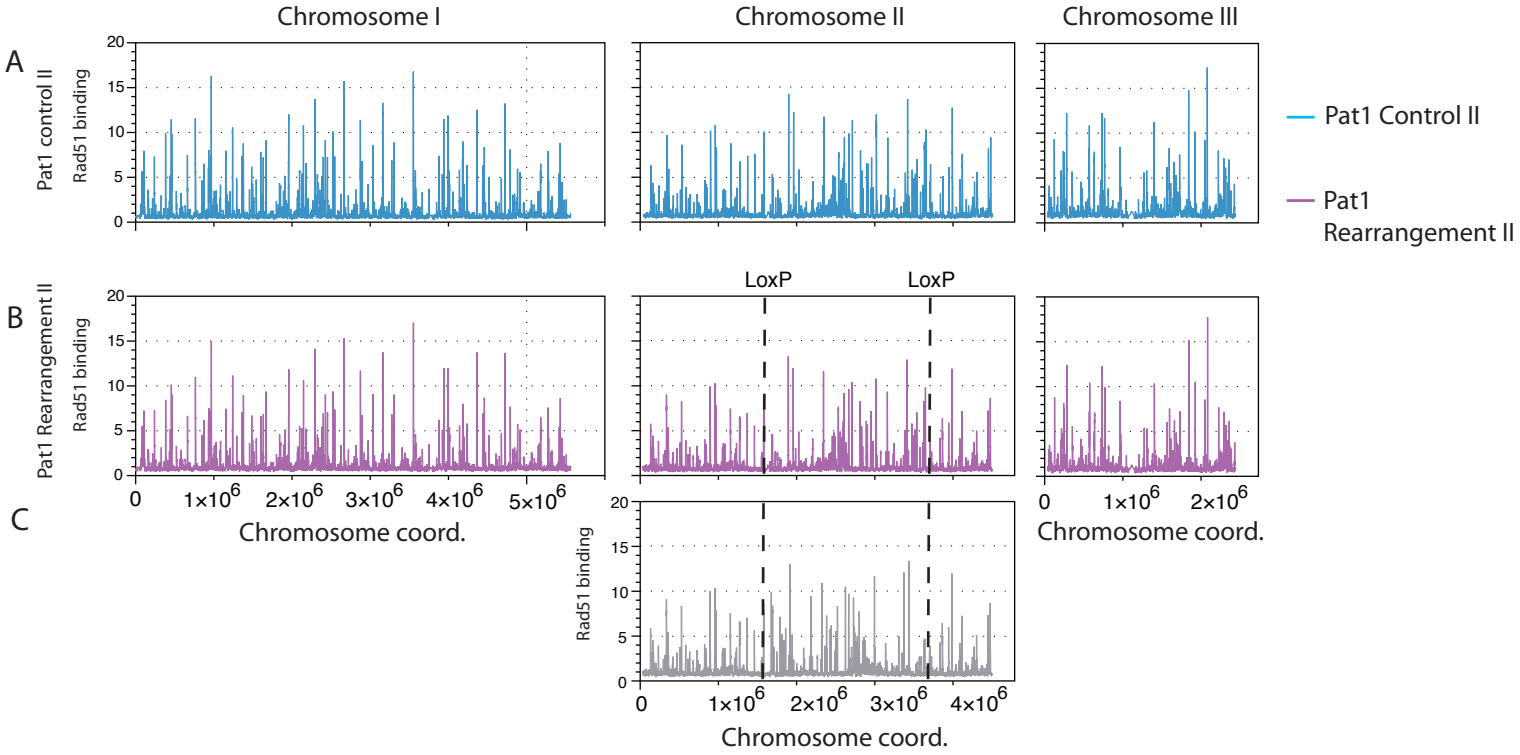

D

	Pat1 Control I	Pat1 Rearrangement
Total number of DSBs	503	482
Average intensity (IP/input)	4.8	4.6
Number of DSBs in common	475	
% in common	94.43	98.54
Number of unique DSBs to each condition	28	7
% unique DSBs	5.49	1.37
Average intensity of unique origins (IP/input)	2.16	2.13
Standard deviation of intensities of unique DSBs	0.15	0.10

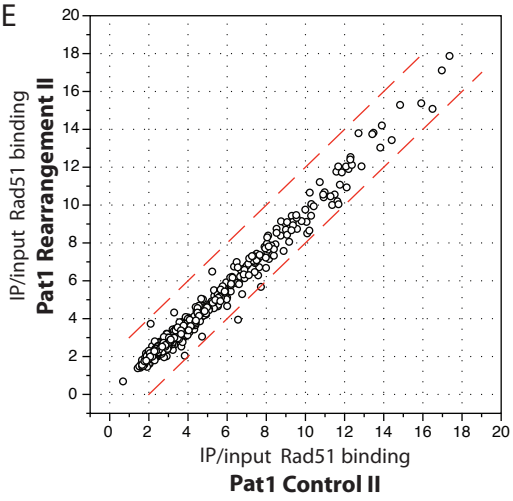

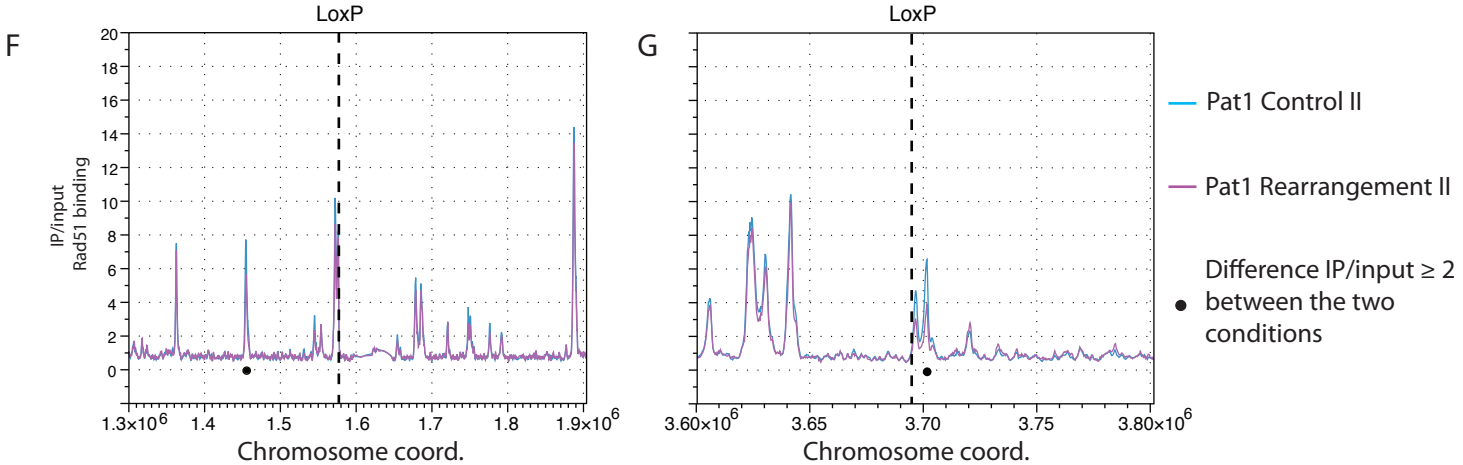

Figure 15: Chromosomal rearrangement II induces local changes in double strand breaks formation. A-C) Profiles of Rad51 along the chromosomes in Pat1 Control II (A, blue) and Pat1 Rearrangement II (B, purple). The profile of the rearrangement in B is plotted with the original, pre-arrangement coordinates to allow direct comparison with the Control strain. The profile in C shows Rad51 binding using the post-rearrangement chromosomal coordinates (gray). X-axis: chromosome coordinates. Y-axis: Rad51 binding (IP/input). Dashed lines in B and C represent the locations of the loxP sites (ChrII: 1577150 and ChrII: 3694900). D) Analysis of Rad51 binding during meiosis in Pat1 Control II and Pat1 Rearrangement II. E) Comparison of Rad51 binding between the Pat1 control II and Pat1 Rearrangement II. Rad51 sites common to the two strains were analyzed. Red dashed line: difference in absolute IP/input value of 2 between the two conditions. Loci that have a difference ≥2 are indicated by the black dots in F and G. F-G) Detailed view of the Rad51 binding profile in the region surrounding the LoxP sites. x-axis: chromosome coordinates, y-axis: Rad51 binding (IP/input).

new insights into the importance of chromosomal organization in both the establishment of the replication program and the formation of programmed DSBs for meiotic recombination.

An interesting feature of our work is the effect of chromosomal rearrangements on origin selection. In both chromosome I and II, we exchanged low efficiency regions with high efficiency domains, which resulted in local modification of the replication program at the endpoints of the rearrangement. These local changes may be due to the chromosomal context into which the origins are transposed: each chromosomal region has distinct features in DNA sequence or chromatin structure that can activate or repress the replication. The fact of moving a low efficient region to a high efficient one may modify locally the structure of the chromatin that renders it prone to transcription. For instance it has been shown that chromatin shapes DNA replication origin specificity by preventing non MCM helicase loading (Kurat et al., 2017). Thus we can think that similarly, low efficient regions may render adjacent sequences closed to replication.

However, there is likely another degree of complexity in the local regulation of the origin after translocation. While one can think that local changes may be similar between the two rearrangements, alteration of origin selection occurred within the translocated genomic fragment for the rearrangement in Chromosome I, whereas

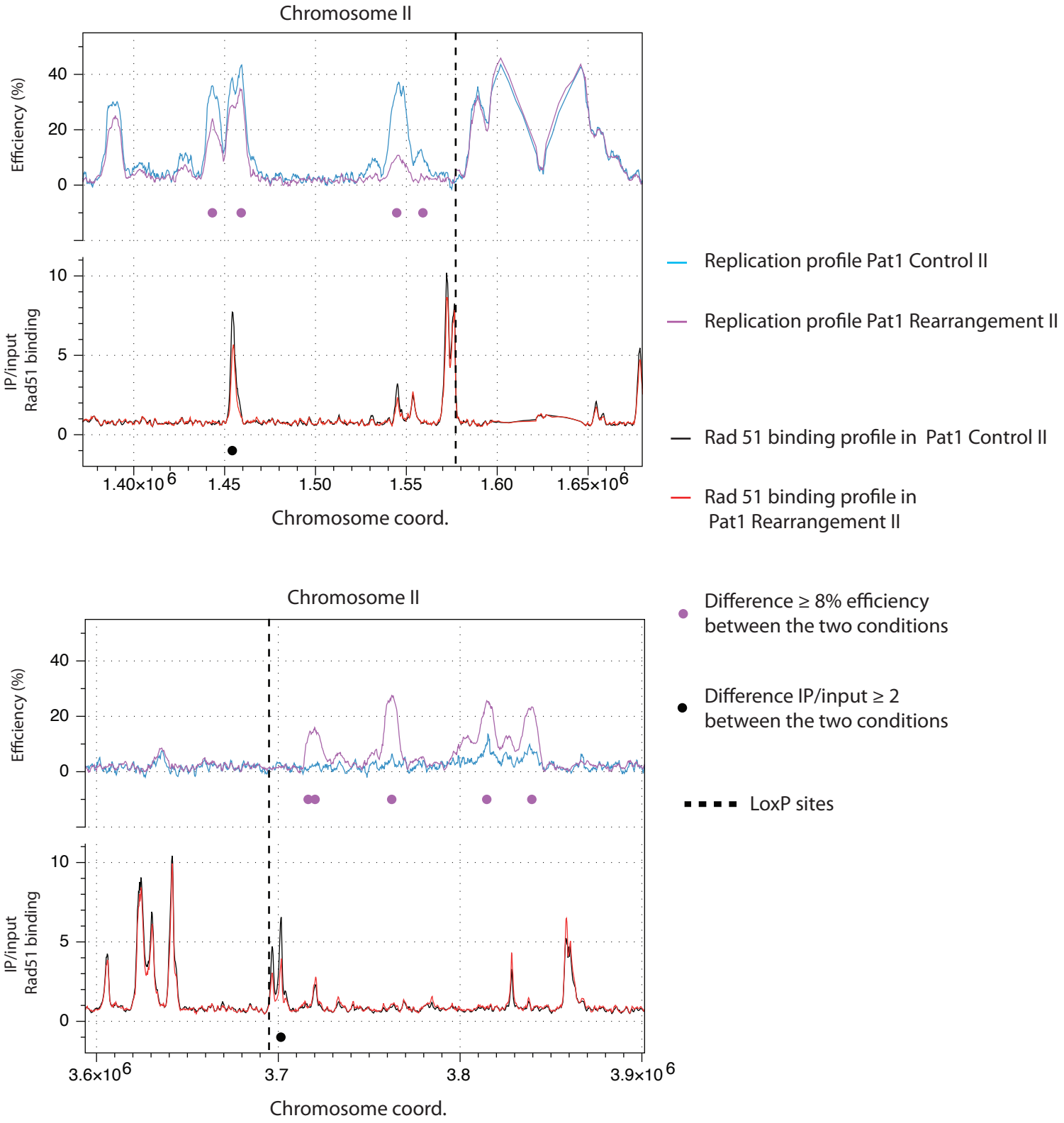

Figure 16: Comparison of the changes in origin efficiency and DSB formation in the chromosome II inversion.

Detailed views of origin efficiencies and Rad51 binding in the regions surrounding the LoxP sites at ChrII: 1577150 (Top) and ChrII: 3694900 (Bottom). Origin usage profiles of Pat1 Control II (blue) and Pat1 Rearrangment II (purple) are shown. Rad51 binding profiles of Pat1 Control II (black) and Pat1 Rearrangement II (red) are displayed. Purple dots highlight origins that show ≥8% efficiency differences between Control II and Rearrangement II. Black dots highlight differences in IP/input ≥2 between Pat1 Control II and Pat1 rearrangement II. X-axis: chromosome coordinates. Y-axis: origin efficiencies (top panels of the graphs) or Rad51 binding (IP/input, bottom panes of the graphs).

rearrangement on chromosome II resulted in changes outside the rearranged region. These differences are interesting and may be explained by the importance of the organizations of the chromosomes in the nucleus. Indeed, the genome is organized in domains called topologically associating domains (TAD) in which DNA sequences are preferentially in contact with one another, and studies have shown that the replication timing domains are associated with TADS (Dileep et al., 2015; Ryba et al., 2010). Thus it is possible that rearrangements alter the chromosomal organization of these types of domains and induce change in the replication program. This feature can explain why the chromosome I and II rearrangements do not have the same effect. One can speculate that in the case of the chromosome I, where the changes in origin usage occur within the rearrangement, the high efficiency centromeric region remains at its normal nuclear position while the inversion brings low efficiency areas in next to this locus. This may lead to increased origin usage through a greater local concentration of replication factors. In the case of the chromosome II rearrangement, it may be possible that the larger inverted fragment maintains its position within the nucleus, and it is the regions outside of the rearrangement that alter their nuclear localization.

Another interesting point of our study is the differences observed between the mitotic and the pre meiotic replication program. Previous data from our laboratory suggested that the pre-meiotic replication program does not induce a specific pattern of origin usage compared with mitosis (Wu and Nurse, 2014). While the overall replication pattern remains the same between mitotic and meiotic replication program, we observed changes in origin usage. Surprisingly, we identified differences in origin usage in pre-meiotic S-phase compared to mitotic cells. These changes appear to be different depending on the characteristics of the replication domains: for instance, in the chromosome II control and rearrangement strains, origins unique to or increased in efficiency in pre-meiotic S-phase are localized to efficient regions, while inefficient areas are enriched in sites that show increased activity or are found only in mitotic S-phase. It will be interesting to pursue these alterations in the replication program and assess whether they may be linked to the differences in chromosome organization between these conditions.

One of our most surprising results was the absence of correlation observed at the local level between origin usage and DSB formation. Previous work in the laboratory has shown that regional changes in origin selection lead to regional changes in DSB formation. Our initial hypothesis was that the changes in DSB formation reflect the changes in origin efficiency. However, our results may suggest that altering the efficiency of a few origins may not be sufficient to induce changes in meiotic recombination. This is supported by preliminary experiments performed using the Pat1 Control II and Pat1 Rearranged II strains (Supplementary Figure 1). It may then be interesting test whether a change in origin usage in lager regions would affect the pattern of DSBs. Intriguingly, our observation that there are indeed changes in DSB formation near the chromosomal inversion endpoints suggests that there may be other elements in the chromosomal context that are important for this regulation, and these possibilities may be tested in future studies using rearrangements or mutants that specifically alter the higher-order organization of the chromosomes in the nucleus.

Materials and methods

Fission yeast strains and methods

Standard media and methods for fission yeast were used (Hayles and Nurse, 1992; Moreno et al., 1991). All experiments were carried out in minimal medium plus supplements (EMM6S) at 25°C, except otherwise noted. The *Schizosaccharomyces pombe* strains used in this study are listed in Table 1.

Table 1: Strains used in this study

Strain	Genotype	Source
PN1	*h- 972*	Nurse lab
JW1073	*h-/h- 972/972*	This study
JW1044	*h+ ppi1:Pkan-loxP-LEU2:cwf7 SPBP8B7.29:loxP-ORFkanMX6-ura4:thi5 Orc1-HA Leu1-32 Ura4-D18*	This study
JW1049	*h- SPAC1F12.02c:Pkan-loxP-LEU2:SPAC1F12.04c arp2:loxP-ORFkanMX6-ura4:pvg5 Orc1-HA Leu1-32 Ura4-D18*	This study
JW1094	*h+ inversion::II:1577150<->3694900 II:1577150::loxP-KanR-Ura4 II:3694900::loxP-Leu2 Orc1-3HA Leu1-32 Ura4-294*	This study
JW1097	*h- inversion::I:3810766<->4785016 I:3810766::loxP-KanR-Ura4 I:4785016::loxP-Leu2 Orc1-HA Leu1-32 Ura4-294*	This study
JW1540	*h+/h+ SPAC1F12.02c:Pkan-loxP-LEU2:SPAC1F12.04c/ SPAC1F12.02c:Pkan-loxP-LEU2:SPAC1F12.04c arp2:loxP-ORFkanMX6-ura4:pvg5/arp2:loxP-ORFkanMX6-ura4:pvg5 Orc1-HA/Orc1-HA Leu1-32/Leu1-32 Ura4-D18/Ura4-D18 pat1-114/pat1-114*	This study
JW1541	*h+/h+ ppi1:Pkan-loxP-LEU2:cwf7/ppi1:Pkan-loxP-LEU2:cwf7 SPBP8B7.29:loxP-ORFkanMX6-ura4:thi5/SPBP8B7.29:loxP-ORFkanMX6-ura4:thi5 pat1-114/pat1-114 Leu1-32/Leu1-32 Ura4-294/Ura4-294*	This study
JW1488	*h+/h+ inversion::I:3810766<->4785016 I:3810766::loxP-KanR-Ura4 I:4785016::loxP-Leu2/ inversion::I:3810766<->4785016 I:3810766::loxP-KanR-Ura4 I:4785016::loxP-Leu2 Orc1-HA/ Orc1-HA Leu1-32/Leu1-32 Ura4-294/Ura4-294 pat1-114/ pat1-114*	This study
JW1514	*h+/h+ inversion::II:1577150<->3694900 II:1577150::loxP-KanR-Ura4 II:3694900::loxP-Leu2/ inversion::II:1577150<->3694900 II:1577150::loxP-KanR-Ura4 II:3694900::loxP-Leu2 Orc1-3HA/ Orc1-3HA Leu1-32/ Leu1-32 Ura4-294/ Ura4-294 pat1-114/ pat1-114*	This study

Cell cycle synchronization by nitrogen depletion and meiotic induction

Strains were grown at 25°C to a density of $2x10^6$ cells/mL in EMM6S. Cells were then starved of nitrogen in minimal medium (EMM-N) for 16h at 25°C. Release from starvation was carried out by feeding cells with a nitrogen source (0.05% w/v NH_4Cl) as well as adding leucine (0.225g/L) and uridine (0.225g/L); the latter allow the optimal growth of cells carrying the *LEU2* and *ura4* markers associated with the LoxP cassettes. Cells were also shifted to 34°C at this time; in strains carrying the thermosensitive mutation *pat1-114,* this results in meiotic induction.

DNA content analysis by flow cytometry

DNA content analysis was performed by flow cytometry (BD Accuri™, C6 Flow Cytometer System). Cells were first fixed with 70% cold ethanol, washed with 50mM sodium citrate and treated with RNAse A (0.1 mg/ml) overnight at 37°C. Cells were then stained with propidim iodide (2mg/ml), sonicated for 10 seconds at an amplitude of 30% using a Branson Digital Sonifier. Analysis was performed using the Flowjo analysis software.

Generation of strains containing LoxP sites

Details of the generation of the strains containing LoxP sites has been described in the first section of the results (Figure 1). Primers used for this section are listed in the table 2.

Table 2: Primers used in this study for strain generation

Primer Name	Sequence	Function
AP12	TAATTTTTGCTTCGCGCCGT	- Used with AP35: verify insertion at ChrI:3810766 - Used with AP78: verify insertion at ChrII:1577150
AP13	CACTAGTGGCCTATGCGGC	- Used with AP36: verify insertion at ChrI:3810766 - Used with AP79: verify insertion at ChrII:1577150
AP15	GTTCTTTGTTTTTATATTTTCATTTTCATTACTG TTGTTCTATGTTGTTCATTTTTTATTCACATATT TTCGGTTTCACGGCGACATGGATGTCACAAGC	Insertion at ChI: 4785016
AP16	ACCTTAAATAAATAAGAACAAATATAAAAGTGT AGTTTACGAAGACAAAATGCCTCGTGAAACCGAC AGATGAAAAACAAGGCCGCATAGGCCACTA	
AP17b	CGCCCATTTAGGGCGTTTTC	- Used with AP74: verify insertion at ChI: 4785016
AP18	TCGCGAGCCCATTTATACCC	- Used with AP20: Verify insertion at ChrI: 4785016 - Used with AP35: Verify rearrangement on ChrI - Used with AP84: verify insertion at ChrII: 3694900 - Used with AP78: Verify rearrangement on ChrII
AP20	TGAACGACAGTGGATGCAGG	- Used with AP18: verify insertion at ChrI: 4785016 - Used with AP18 after rearrangement: negative control for rearrangement on ChrI
AP33	AAAAACACTCGTTAATAAAGATATTCAGTTCAAT TAGAAAAAAAATGACAAGGTACATTTTGGTGACA AACAAAGAGTAACTGTTTAGCTTGCCTCGTCCC	Insertion at ChrI: 3810766
AP34	TTTTAATCGTTAATCCATTCCATTAAAGCGTTTT AAATTTTGGGATATTGATCGAAAATTTAATCAAC GGAAAACATTAAATAGGGAGACCGGCAGATCC	
AP35	TGAAACCATTATGATGCGTGTAAAA	-Used with AP12: verify insertion at ChrI:3810766 - Used with AP18: verify rearrangement on ChrI
AP36	TGGCTAGCCTTCCTTTGTGT	Used with AP13: verify insertion at ChrI:3810766
AP71	TATATTGACTGTTCCGTATTTCTTTAACATAGTC TTGAAGTAGCAATACTGCTGATTTTGTAATTTTA TAATGTTTTTAAGCGACATGGATGTCACAAGC	Insertion at ChrII: 3694900
AP72	AAAAAATGAATAAACTGTCATTAAAACGCTTCAT GAAACTATCAGTAACATCAATTTTGCCGTAATAA AAGTTTTGTTATGGCCGCATAGGCCACTA	
AP74	GCCAGTGGGATTTGTAGCTAAG	- Used with AP17b: verify insertion at ChI: 4785016 - Used with AP83: verify insertion at ChrII: 3694900

AP75	CATTCCTTCCGTGGTCCGAA	Verify insertion at ChrII: 3694900
AP76	AGCATATAATCAAGAAAGTACGTATTACTGAGGT TAGACAAAAAGTAACTTAGTTAAAAAATCGACGA CTTGGTTGGCCCTGTTTAGCTTGCCTCGTCCC	Insertion at ChrII:1577150
AP77	TAAGGTTAGGATTACTTTTGATAAGAGTATCCTA GTAAACAGTTAAATGTTAATACAATTACTACTAT GCGCGTTATTATATAGGGAGACCGGCAGATCC	
AP78	AACTCTGGTGCTACTCGTGC	- Used with AP12: verify insertion at ChrII:1577150 - Used with AP18: Verify rearrangement on ChrII
AP79	CGTGAAAGCCTGTTGCAGTC	Used with AP13: verify insertion at ChrII:1577150
AP83	ACGCAGCTAGGCATCTGTTT	Used with AP74: verify insertion at ChrII: 3694900
AP84	AGGAAACAGGAGACCAGACA	- Used with AP18: verify insertion at ChrII: 3694900 - Used with AP18 after rearrangement: negative control for rearrangement on ChrII

Chromatin Immunoprecipitation and quantitative PCR

Chromatin immunoprecipitation was performed as described in Wu and Nurse (2009) (Wu and Nurse, 2009). Cells were fixed with 1% formaldehyde at 25°C for 20 min and quenched with a final concentration of 125mM glycine. Cells were lysed using a FastPrep cell disruptor (MP Biomedical, USA). Chromatin extracts were then sonicated with a Bioruptor Plus (Diagenode) to generate DNA fragment around ~400-500 bp in length. Immunoprecipitations (IPs) were carried out overnight at 4°C using anti-Rad51 (Ref: sc-8349, Santa Cruz, 1µl per IP). Protein G sepharose beads (GE Helthcare) or Dynabeads (Invitrogen) were added to the sample and rotated during 4h at 4°C. IPs were then washed and eluted. Both. IP and input samples were incubated overnight at 65°C to reverse crosslinking. For quantitative PCR analysis, IPs and inputs DNA (input dilution: 1/20) were mixed Brilliant III SYBR® Master Mix/high ROX (Agilent) and run in triplicate in an Applied Biosystem 7900 HT Fast real-time PCR system. Primers used for qPCR are listed in the Table 3.

Table 3: Primers used in this study for ChIP-qPCR

Primer	Sequence	Location
OJW741 (Rad51 site I F)	ACTGTACGGGTTGGGTTTGG	Chr I: 3157500
OJW742 (Rad51 site I R)	TCTCCTTCAACGTTTCGCCTT	
LL204 (Rad51 site II F)	AACAAAGGGACAGGGATGCTA	ChrII : 3858040
LL205 (Rad51 site II R)	TCCCATTCTCGATTTGCACAC	
OJW719	AGGCTTTCAAGATTCAACGGTACT	Chr II: 1362500
OJW720	TGACACACGGACAGGCTACT	
LL0235 (Control site F)	GCACCAAACGTTACCCAGAAT	Chr I:2035783
LL0236 (Control site R)	GCTGTACCCATCTGTAATTGCA	
LL0188	ACCACCTCACCAAACAATGTG	Chr II : 1451580
LL0189	GCTGACTGTTCGTTCGTCTTT	
LL0190	ACTCAGCGTACGTACACATCT	ChrII : 1543800
LL0191	TGAAGCTAAATCGTTGCGTGT	
LL0202	CTGGGTTTTCAAGGACGCTAA	Chr II : 3700350
LL0203	ATTGGGTTCTTTCGTCTTGGC	

Origin mapping experiments and analyses

Origin mapping was performed using Agilent 4x44k *S. pombe* arrays (60-mer oligonucleotides every ~250 nucleotides, Agilent Technologies, Santa Clara, CA, USA) as previously described (Gómez-Escoda and Wu, 2017; Méchali, 2010; Wu and Nurse, 2014). Copy number was determined by comparing genomic DNA samples from non-replicating cells against cells undergoing DNA replication in hydroxyurea (HU). 12mM HU treatment limits the extension of DNA synthesis around the sites of initiation by depleting the pool of dNTP, allowing identification of replication origins. Previous studies have validated this method (Heichinger et al., 2006; Méchali, 2010; Wu and Nurse, 2014) and provides very similar origin maps to those obtained with other approaches (Aladjem, 2007; Anglana et al., 2003; Daigaku et al., 2015; Hayashi et al., 2007; Méchali, 2010). In all mapping experiments, cells in HU were harvested when S-phase would normally be completed in absence of HU, as indicated by the corresponding flow cytometry profiles (Figure 2C and Figure 3C). Non-replicated samples were taken prior to addition of 0.05%w/v NH_4Cl + 0.225g/L uridine and leucine . After addition of the nitrogen source and supplements as well as shift to 34°C, 12mM HU was immediately added to the culture. Genomic DNA was then harvested

from Haploid Control and Rearrangement cells 240 after the cell cycle re-entry and from diploid Pat1 Control and Rearrangement cells 210 min after re-entry (replicated DNA samples, HU-treated). Genomic DNA was extracted (Hiratani et al., 2008b; Hoffman and Winston, 1987) and purified using the Quiagen Genomic DNA kit. Samples were labeled using random priming method. 2µg of purified genomic DNA was used for each sample and incubated 5 minutes at 95°C with 300µg/ml of Random Primer (Invitrogen, 48190-011). Annealed primers were extended with a Klenow reaction (Klenow Fragment (3'→5' exo-) M0212S, New England BioLabs) using nucleotide mix with aha-dUTP (0.5mM dATP, 0.5mM dCTP, 0.5mM dGTP, 0.1mM dTTP, 0.4mM aha-dUTP) for two hours at 37°C. Amino-modified DNA was then purified using the Invitrogen PureLink quick PCR purification kit (K310001) according to the manufacturer's instructions. Amino-modified DNA was then precipitated using 75mM sodium acetate and 0.1µg/µl glycogen in ethanol 100% for 30 minutes at -20°C. aha-DNA was then pelleted using a cold microfuge and washed with 70% ethanol. Dried DNA pellet was then resuspended in 80µl of 0.1M sodium bicarbonate (pH 8.7). Half of the sample was incubated 90 minutes in the dark with either Cy3 or Cy5 (GE Healthcare, USA) dyes for dye coupling. Reaction was stopped using 15µl of 4M hydroxylamine for 15 minutes. Dye labeled DNA was then purified using the Invitrogen PureLink quick PCR purification kit (K310001) according to the manufacturer's instructions. 1-2 µg of differentially labeled DNA from non-replicated and replicated samples were hybridized onto the microarrays. Two independent hybidizations of the same samples were systematically performed in a dye-swap experiment, the ratios of replicated DNA to non-replicated DNA were assessed, and these datasets were averaged. To determine copy number, the geometric means over five consecutive probes were determined across the genome. For comparisons, we averaged two biological repeats for Control II vs. Rearrangement II, Pat1 Control I vs. Pat1 Rearrangement I and Pat1 Control II vs. Pat1 Rearrangement II. For Control I vs. Rearrangement I comparison, we compared two biological repeats of Control I vs. one experiment for Rearrangement I. To obtain origin efficiencies, the median of the lowest 10% of the ratios, which represents unreplicated DNA, were adjusted to a value of 1. This resulted in a correction of 0.043 for the Haploid datasets and 0.044 for Pat1 diploid datasets. The application of this correction was validated by visual inspection of the overall profiles. Copy number was converted to efficiency (for example, 1.1 = 10%).

For origin identification, we determined the moving geometric means over five consecutive probes along the chromosomes for each dataset representing the average of two biological repeats. The locations of potential origins were taken from our previously published dataset for *cdc25-22* cells treated with HU (Hyrien and Mechali, 1993; Hyrien et al., 1995; Méchali, 2010; Wu and Nurse, 2014) and peaks where the efficiency of replicated (in HU) vs. non-replicated samples was greater than 10% were identified as origins in our experiments. Their specific positions were attributed based on the coordinate of the local maximum value followed by visual confirmation. When two origins were less than 5 kb apart, they were considered as a single origin and assigned to the position with the higher copy number. The 10% cutoff for origin picking was determined by calculating the level of noise between two repeats of pat1 strains. In these conditions, we determined the difference in the value of each probe between the repeats, calculated the median of all the differences, and established a threshold at 2 standard deviations above the median value. The highest value obtained among all conditions was designed as the cutoff and applied to all experiments. Based on these criteria we established a list of origin sites that were used to compare origin efficiencies between conditions. This list was designed using Pat1 Control I, Pat1 Control II, Pat1 Rearrangement I and Pat1 Rearrangement I and II strains, and contained origins that were present in at least one of the four conditions. This list is available in supplementary table 1. To compare origin numbers and efficiencies between two experiments, peaks identified in each dataset were matched in position (Dotan et al., 2004; Wu and Nurse, 2014). When peaks in two different datasets were within a distance of 5 probes, they were considered to be the same origin.

ChIP-on-chip analysis

For ChIP-on-chip assays, we collected 100mL of cells 210min after release from nitrogen starvation, when the binding of Rad51 reaches its highest level as determined by our ChIP-qPCR experiments. We amplified and labeled ChIP material according to the protocol from (van Bakel et al., 2008; Wu and Nurse, 2014) and adapted in (Wu and Nurse, 2014). Each ChIP was then hybridized against its reciprocally labeled input

sample (IP/Input). For each sample, two biological repeats were performed for Rearrangement II, Pat1 Control II and Pat1 Rearrangement II. We analyzed one experiment for Control I. We determined the geometric means over five consecutive probes along the chromosomes for each dataset and plotted those values.

To identify peaks of Rad51 recruitment, we established a cutoff based on the values of IP/Input for all probes in each condition after calculating the dispersion of the data from the median. The data for each experiment were divided into quartiles, and we considered that significant binding occurs when the values were 1.5 times the interquartile range (IQR) above the third quartile (Q3+1.5(IQR)). The average of this value for each experiment was determined to be 1.90; we thus established a cutoff of 2.0 for identification of the sites of Rad51 binding. Moreover, we considered a locus as a Rad51 binding site when 3 consecutive probes showed values higher than our threshold.

In order to determine significant changes in DSB formation between two conditions, we established a cutoff based on the noise between two biological repeats. We determined the difference in the value of each probe between the repeats, calculated average and the standard deviation of all the differences, and established a threshold at 1.52 standard deviations around the mean value. We thus established a cutoff at 2.0 for significant changes in Rad51 binding.

Supplementary Figure 1 - Explanation

Our data showed that a 2 Mb inversion of chromosome II does not produce overall changes in Rad51 binding but rather generates local alterations in Rad51. We then wanted to determine whether similar types of alterations would be produced in a different chromosomal context. To do so we performed a preliminary experiment using the Pat1 Control I and the Pat1 Rearrangement I strains (supplementary Figure 1). Note that only one experiment for Pat1 Rearrangement I was analyzed and compared with the average of two independent repeats for Pat1 Control I. We performed ChIP-on-chip of Rad51 in the same conditions as described previously, at 210 min after meiotic induction. We found that the genome-wide profiles of Rad51 binding are very similar between the Pat1 Control I and the Pat1 Rearranged I strains (Supplementary Figure 1A and 1B). To compare DSB formation between the two backgrounds, we used a cutoff of 2.0 (IP/input) to identify sites that are clearly enriched for Rad51. We found fewer Rad51 sites in the Pat1 Control I than in the Pat1 Rearrangement I backgrounds (474 and 557, respectively). All the sites present in the Pat1 Control I were found in Pat1 Rearrangement I, which displays 83 additional Rad51 sites (Supplementary figure 1D). We also noted that the insertion of LoxP cassette at Chr II: 1577150 generated an ectopic DSB in both of the strains (Supplementary Figure 1F), consistent with our observations for the chromosome II LoxP insertions.

We then compared the level of Rad51 at all identified loci in the two strains. (Supplementary Figure 1I). We noted that the correlation were not as good as for the Rearrangement on chromosome II, likely due to the availability of only a single experiment for Pat1 Rearrangement I. Using a difference of 2 in the IP/Input as our threshold, we found 71 sites that met this criterion, all showing higher levels of Rad51 binding in Pat1 Rearrangement I. We observe changes in Rad51 binding near the LoxP sites, but these do not appear to be greater than those observed throughout the three chromosomes. These experiments need to be reproduced in order to verify the effect of this chromosomal inversion on Rad51 binding.

Supplementary Figure 1

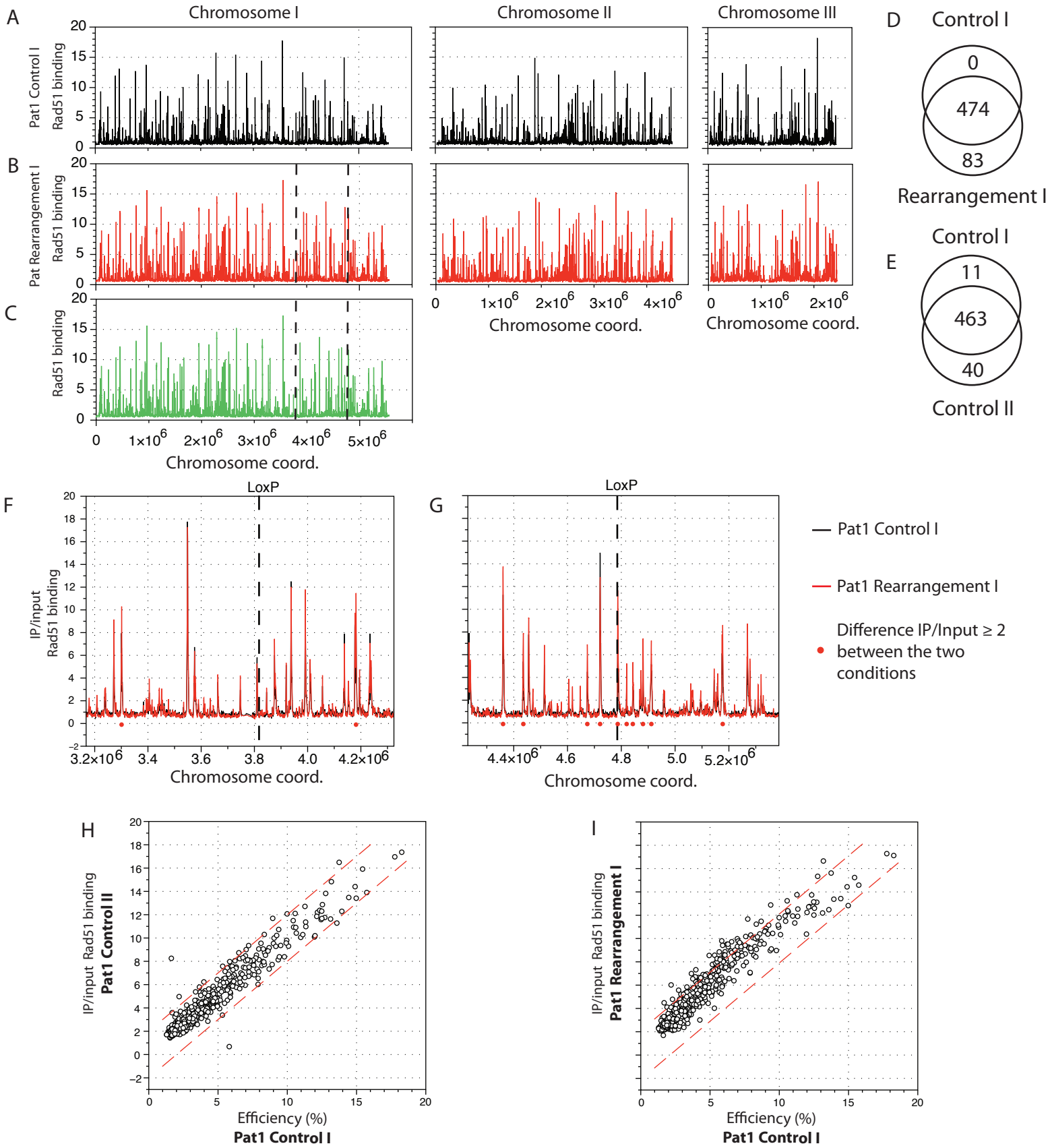

<u>Supplementary Figure 1</u>: Chromosomal rearrangement I induces local changes in double strand breaks formation

A-C) Profiles of Rad51 along the chromosomes in Pat1 Control I (A, black) and Pat1 Rearrangement I (B, red). The profile of the rearrangement in B is plotted with the original, pre-arrangement coordinates to allow direct comparison with the Control strain. The profile in C shows Rad51 binding using the post-rearrangement chromosomal coordinates (gray). X-axis: chromosome coordinates. Y-axis: Rad51 binding (IP/input). Dashed lines in B and C represent the locations of the loxP sites (ChrI: 3810766 and ChrI: 4785016). D) Venn diagram illustrating the number of common DSB to the Diploid Control II and the Diploid Rearrangement II showing difference in absolute IP/input value of 2 between the two conditions. E) Venn diagram illustrating the number of common DSB to the Diploid Control II and the Diploid Rearrangement II showing difference in absolute IP/input value of 2 between the two conditions. F-G) Detailed view of the Rad51 binding profile in the region surrounding the LoxP sites. x-axis: chromosome coordinates, y-axis: Rad51 binding (IP/input). H) Comparison of Rad51 binding between the Pat1 control II and Pat1 Control II. Rad51 sites common to the two strains were analyzed. Red dashed line: difference in absolute IP/input value of 2 between the two conditions. I) Comparison of Rad51 binding between the Pat1 control I and Pat1 Rearrangement I. Rad51 sites common to the two strains were analyzed. Red dashed line: difference in absolute IP/input value of 2 between the two conditions.

Supplementary Table 1: List of origins used for this study

Chr I		
111752.5	3008881.4	4238234.0
200574.5	3021989.4	4253835.3
365136.1	3029392.5	4276136.7
563158.1	3055491.1	4298352.1
714507	3059220.9	4326105.9
842557.7	3128158.8	4438290.7
876200.3	3144411.3	4450582.1
901315.6	3183544.7	4482955.4
966815.2	3207700.3	4533867.6
1079000.7	3246877.5	4538270.6
1083021.2	3270193.8	4740064.7
1095933.5	3299644.1	4778752.6
1191501.5	3321339.2	4852162.7
1196962.5	3406474.8	4916267.2
1255096.1	3408855	4923832.7
1444855.7	3444183.6	4933249.5
1477244.8	3499302.5	4962998.4
1487236.9	3522381.5	4976747.6
1509044.5	3526130.6	5023284.3
1664619.2	3543315.4	5046540.8
1708262.2	3550335.5	5096857.9
1719915.2	3557863	5140588.2
1734559.9	3577815.6	5154777.7
1827989.3	3593501.9	5175585.0
1833244	3635827.7	5234380.7
1973354	3673336.1	5252176.9
2193375.7	3686428.7	5393207.1
2229229.9	3699372.1	5433215.7
2244208.3	3735007.1	5447942.7
2248800.2	3840782.7	
2272207	3851634.9	
2280934.7	3879373.7	
2440132.8	3897360.1	
2577446.3	3952126.7	
2720441.5	3994172.3	
2761003.9	4019232.0	
2787299.1	4072756.3	
2803546.7	4086914.9	
2862605	4136904.0	
2937799.1	4153840.0	
2960923.3	4184183.3	
2978362.8	4196620.3	
2981426.8	4233100.4	

Chr II		
258317.5	1717856.5	4144793.1
276588.6	1751302.8	4201878.2
314304.6	1767209.3	
325146.6	1778228	
331711.7	1804513.4	
341289.1	1942241.3	
356618.1	1953305.7	
409361.3	1963543.4	
453279.6	2024386.7	
514574.1	2031375.3	
521081.7	2051864.1	
569660.5	2119123.1	
591167.8	2131264.9	
602903.3	2186196.7	
637504.5	2212730.3	
672797.9	2245896.9	
685343.5	2318492.9	
722020.8	2445210.9	
745724.9	2449628.4	
803872.7	2498421.9	
823458.7	2522381.8	
842188.9	2552136.6	
848232.9	2702353	
1003941.4	2733916.7	
1107465.9	2738012.3	
1142459.3	2791746.2	
1156159.5	2799226.4	
1242430.3	2899807.5	
1253712.1	2939969.5	
1263588.1	3237421.5	
1279715	3286824.1	
1313701.1	3490366.6	
1351037.6	3714648.5	
1390150	3722284.2	
1429648	3762656.7	
1442792.7	3802507.7	
1458167.9	3815749.5	
1545059.5	3825449.8	
1556385.5	3839190.1	
1589770.6	3916597.6	
1656249.4	4019789.9	
1665019.5	4047742.4	
1704145	4140972.4	

Chr III	
61187.8	1447917.1
75340.5	1509711.1
121614.8	1532123.3
189416.8	1553953.3
205378.9	1576589.3
233626.5	1593466.5
252669.3	1607405.3
288013.4	1672906.4
308283.9	1684875.3
332335	1686424.6
368771.2	1720703.7
399092.1	1753162
453823.9	1820674.3
471702.3	1842479.2
504630.3	1868471.1
520026.2	1929453.6
566763.8	1937725.5
574524.1	1967872.3
604880.7	2035766.1
644162.8	2063186.2
666595.9	2066627.8
721219	2107468.9
766690.9	2139313
790573.1	2160022.0
821291.7	2169403.4
827165.7	2201673.9
844305.5	2277047.5
852572.9	2383388.1
937797.1	
972445.4	
975076.4	
1024421.1	
1039782.5	
1167389	
1192631.4	
1251376.6	
1324041.8	
1343658.4	
1371514.3	
1396674.5	
1409796.4	
1415472.8	
1422051.9	

References

Aladjem, M.I. (2007). Replication in context: dynamic regulation of DNA replication patterns in metazoans. Nat Rev Genet *8*, 588–600.

Anglana, M., Apiou, F., Bensimon, A., and Debatisse, M. (2003). Dynamics of DNA replication in mammalian somatic cells: nucleotide pool modulates origin choice and interorigin spacing. Cell *114*, 385–394.

Bähler, J., Schuchert, P., Grimm, C., and Kohli, J. (1991). Synchronized meiosis and recombination in fission yeast: observations with pat1-114 diploid cells. Curr Genet.

Bähler, J., Wu, J.Q., Longtine, M.S., Shah, N.G., McKenzie, A., Steever, A.B., Wach, A., Philippsen, P., and Pringle, J.R. (1998). Heterologous modules for efficient and versatile PCR-based gene targeting in Schizosaccharomyces pombe. Yeast *14*, 943–951.

Berezney, R., Dubey, D.D., and Huberman, J.A. (2000). Heterogeneity of eukaryotic replicons, replicon clusters, and replication foci. Chromosoma *108*, 471–484.

Borde, V., Goldman, A.S., and Lichten, M. (2000). Direct coupling between meiotic DNA replication and recombination initiation. Science *290*, 806–809.

Daigaku, Y., Keszthelyi, A., Müller, C.A., Miyabe, I., Brooks, T., Retkute, R., Hubank, M., Nieduszyski, C.A., and Carr, A.M. (2015). A global profile of replicative polymerase usage. Nat. Struct. Mol. Biol. *22*, 192–198.

de Castro, E., Soriano, I., Marín, L., Serrano, R., Quintales, L., and Antequera, F. (2012). Nucleosomal organization of replication origins and meiotic recombination hotspots in fission yeast. Embo J. *31*, 124–137.

Dileep, V., Ay, F., Sima, J., Vera, D.L., Noble, W.S., and Gilbert, D.M. (2015). Topologically associating domains and their long-range contacts are established during early G1 coincident with the establishment of the replication-timing program. Genome Res. *25*, 1104–1113.

Dotan, Z.A., Dotan, A., Ramon, J., and Avivi, L. (2004). Altered mode of allelic replication accompanied by aneuploidy in peripheral blood lymphocytes of prostate cancer patients. Int. J. Cancer *111*, 60–66.

Gilbert, D.M., and Cohen, S.N. (1990). Position effects on the timing of replication of chromosomally integrated simian virus 40 molecules in Chinese hamster cells. Molecular and Cellular Biology *10*, 4345–4355.

Gómez-Escoda, B., and Wu, P.-Y.J. (2017). Roles of CDK and DDK in Genome Duplication and Maintenance: Meiotic Singularities. Genes *8*.

Hayashi, M., Katou, Y., Itoh, T., Tazumi, A., Tazumi, M., Yamada, Y., Takahashi, T., Nakagawa, T., Shirahige, K., and Masukata, H. (2007). Genome-wide localization of pre-RC sites and identification of replication origins in fission yeast. Embo J. *26*, 1327–1339.

Hayles, J., and Nurse, P. (1992). Genetics of the fission yeast Schizosaccharomyces pombe. Annu. Rev. Genet. *26*, 373–402.

Heichinger, C., Penkett, C.J., Bähler, J., and Nurse, P. (2006). Genome-wide characterization of fission yeast DNA replication origins. Embo J. *25*, 5171–5179.

Hiratani, I., Ryba, T., Itoh, M., Yokochi, T., Schwaiger, M., Chang, C.-W., Lyou, Y., Townes, T.M., Schübeler, D., and Gilbert, D.M. (2008a). Global reorganization of replication domains during embryonic stem cell differentiation. PLoS Biol *6*, e245.

Hiratani, I., Ryba, T., Itoh, M., Yokochi, T., Schwaiger, M., Chang, C.-W., Lyou, Y., Townes, T.M., Schübeler, D., and Gilbert, D.M. (2008b). Global reorganization of replication domains during embryonic stem cell differentiation. PLoS Biol *6*, e245.

Hoffman, C.S., and Winston, F. (1987). A ten-minute DNA preparation from yeast efficiently releases autonomous plasmids for transformation of Escherichia coli. Gene *57*, 267–272.

Hyrien, O., and Mechali, M. (1993). Chromosomal replication initiates and terminates at random sequences but at regular intervals in the ribosomal DNA of Xenopus early embryos. Embo J. *12*, 4511–4520.

Hyrien, O., Maric, C., and Mechali, M. (1995). Transition in specification of embryonic metazoan DNA replication origins. Science *270*, 994–997.

Jackson, D.A., and Pombo, A. (1998). Replicon clusters are stable units of chromosome structure: evidence that nuclear organization contributes to the efficient activation and propagation of S phase in human cells. J. Cell Biol. *140*, 1285–1295.

Katou, Y., Kanoh, Y., Bando, M., Noguchi, H., Tanaka, H., Ashikari, T., Sugimoto, K., and Shirahige, K. (2003). S-phase checkpoint proteins Tof1 and Mrc1 form a stable replication-pausing complex. Nature *424*, 1078–1083.

Kiang, L., Heichinger, C., Watt, S., Bähler, J., and Nurse, P. (2010). Specific replication origins promote DNA amplification in fission yeast. J. Cell. Sci. *123*, 3047–3051.

Kurat, C.F., Yeeles, J.T.P., Patel, H., Early, A., and Diffley, J.F.X. (2017). Chromatin Controls DNA Replication Origin Selection, Lagging-Strand Synthesis, and Replication Fork Rates. Molecular Cell *65*, 117–130.

Méchali, M. (2010). Eukaryotic DNA replication origins:many choices for appropriate answers. Nature Publishing Group *11*, 728–738.

Miyoshi, T., Ito, M., Kugou, K., Yamada, S., Furuichi, M., Oda, A., Yamada, T., Hirota, K., Masai, H., and Ohta, K. (2012). A central coupler for recombination initiation linking chromosome architecture to S phase checkpoint. Molecular Cell *47*, 722–733.

Moreno, S., Klar, A., and Nurse, P. (1991). Molecular genetic analysis of fission yeast Schizosaccharomyces pombe. Meth. Enzymol. *194*, 795–823.

Murakami, H., and Keeney, S. (2014). Temporospatial Coordination of Meiotic DNA

Replication and Recombination via DDK Recruitment to Replisomes. Cell *158*, 861–873.

Murakami, H., Borde, V., Shibata, T., Lichten, M., and Ohta, K. (2003). Correlation between premeiotic DNA replication and chromatin transition at yeast recombination initiation sites. Nucleic Acids Research *31*, 4085–4090.

Pichugina, T., Sugawara, T., Kaykov, A., Schierding, W., Masuda, K., Uewaki, J., Grand, R.S., Allison, J.R., Martienssen, R.A., Nurse, P., et al. (2016). A diffusion model for the coordination of DNA replication in Schizosaccharomyces pombe. Sci. Rep. *6*, 18757.

Pope, B.D., Hiratani, I., and Gilbert, D.M. (2010). Domain-wide regulation of DNA replication timing during mammalian development. Chromosome Res. *18*, 127–136.

Rivera-Mulia, J.C., and Gilbert, D.M. (2016). Replicating Large Genomes: Divide and Conquer. Molecular Cell *62*, 756–765.

Roeder, G.S. (1997). Meiotic chromosomes: it takes two to tango. Genes & Development *11*, 2600–2621.

Ryba, T., Hiratani, I., Lu, J., Itoh, M., Kulik, M., Zhang, J., Schulz, T.C., Robins, A.J., Dalton, S., and Gilbert, D.M. (2010). Evolutionarily conserved replication timing profiles predict long-range chromatin interactions and distinguish closely related cell types. Genome Res. *20*, 761–770.

Sternberg, N., and Hamilton, D. (1981). Bacteriophage P1 site-specific recombination. I. Recombination between loxP sites. J. Mol. Biol. *150*, 467–486.

Valentin, G., Schwob, E., and Seta, Della, F. (2006). Dual role of the Cdc7-regulatory protein Dbf4 during yeast meiosis. J. Biol. Chem. *281*, 2828–2834.

van Bakel, H., van Werven, F.J., Radonjic, M., Brok, M.O., van Leenen, D., Holstege, F.C.P., and Timmers, H.T.M. (2008). Improved genome-wide localization by ChIP-chip using double-round T7 RNA polymerase-based amplification. Nucleic Acids Research *36*, e21.

Wan, L., Niu, H., Futcher, B., Zhang, C., Shokat, K.M., Boulton, S.J., and Hollingsworth, N.M. (2008). Cdc28-Clb5 (CDK-S) and Cdc7-Dbf4 (DDK) collaborate to initiate meiotic recombination in yeast. Genes & Development *22*, 386–397.

Watanabe, Y., and Nurse, P. (1999). Cohesin Rec8 is required for reductional chromosome segregation at meiosis. Nature *400*, 461–464.

Watson, A.T., Garcia, V., Bone, N., Carr, A.M., and Armstrong, J. (2008). Gene tagging and gene replacement using recombinase-mediated cassette exchange in Schizosaccharomyces pombe. Gene *407*, 63–74.

Werler, P.J.H., Hartsuiker, E., and Carr, A.M. (2003). A simple Cre-loxP method for chromosomal N-terminal tagging of essential and non-essential Schizosaccharomyces pombe genes. Gene *304*, 133–141.

Wu, P.-Y.J., and Nurse, P. (2009). Establishing the Program of Origin Firing during S Phase in Fission Yeast. Cell *136*, 852–864.

Wu, P.-Y.J., and Nurse, P. (2014). Replication origin selection regulates the distribution of meiotic recombination. Molecular Cell *53*, 655–662.

Chapter III

Construction of a system for evaluating the local requirement for DNA replication in DSB formation

Introduction

The formation of programmed double-stranded DNA breaks (DSBs) is one of the key features of meiosis. These DSBs allow genetic shuffling (Handel and Schimenti, 2010; Székvölgyi and Nicolas, 2010) as well as proper chromosome segregation during meiosis I (Murakami and Keeney, 2008). Meiotic DSB formation requires the conserved Spo11 protein (Rec12 in the fission yeast), which is a type II topoisomerase-like enzyme (Keeney, 2008) that cleaves DNA. In addition, the core proteins involved in DSB formation have homologs throughout eukaryotes and are organized in different groups. The SFT (Seven-Fifteen-Twenty-four) subcomplex binds to DNA as well as to DSBC (DSB catalytic core complex), which contains Spo11 (De Veaux et al., 1992; Keeney, 2001). Ultimately, Spo11 cleaves DNA to generate DSBs, which are then resolved by subsequent recombination events and repair events.

As described in the previous chapters, diverse studies have identified a relationship between replication and DSBs during meiosis (Borde et al., 2000; Murakami and Nurse, 2001; Murakami and Keeney, 2014; Wu and Nurse, 2014). Early evidence was provided by Borde et al. in 2000, which showed that delaying replication of a region of a chromosome during pre-meiotic S phase affects the timing of DSB formation in that region (Borde et al., 2000). More recently, work from our laboratory has demonstrated that changes in the replication program during pre-meiotic S phase result in changes in the pattern of DSB formation along the chromosome (Wu and Nurse, 2014). More precisely, this study found that increasing the efficiency of origin firing in a region resulted in an increase the frequency DSB formation in this same region. Thus, these data suggest a coupling between the program of origin selection and meiotic recombination. However, the mechanisms that link these processes remain to be elucidated. Recent studies in the budding yeast have shown that the DDK kinase Cdc7/Hsk1, which functions in origin activation, phosphorylates factors required for meiotic recombination (Murakami and Keeney, 2014). The recruitment of DDK to the replisome has been proposed to play an important role in the regulation of DSB formation (Murakami and Keeney, 2014). Nevertheless, we still do not understand key aspects of this control. For instance, higher levels of origin activation in a region may simply increase the local concentration of replication factors that interact with recombination components. This may also create an environment that allows or impairs

the deposition of potential marks that determine DSB sites. Alternatively, interactions that are crucial for DSB formation may require progression of the replication machinery along the DNA and would therefore rely on duplication of the region containing the DSB.

In the present study, we propose to investigate these possibilities by assessing the direct relationship between the progression of the replication machinery and the establishment of DSB sites in the fission yeast *S. pombe*. For this, we constructed and inserted an inducible replication fork barrier to determine whether the replication machinery must progress through a DSB site before breaks are formed or whether origin activation is sufficient to induce the formation of DSB. In this chapter, we will present preliminary results of this work.

Results

Characterization of a genetic background for inducing synchronous meiosis

In order to test whether the initiation of replication is sufficient for inducing the formation of a nearby DSB or whether a region containing potential DSB sites have to be duplicated before breaks are made, we decided to use and characterize a new genetic background that allows for synchronous progression through meiosis. In our previous study, we used the well-characterized temperature sensitive mutation of the *pat1* kinase (*pat1-114*) which induces meiotic entry after a shift to restrictive temperature (34°C) (Bähler et al., 1991; Iino and Yamamoto, 1985). While this allele has been widely used, the high temperature necessary for entering meiosis in a *pat1-114* background presents a number of disadvantages. For instance, chromosomes missegregate more frequently during meiosis I, spore viability is reduced compared with wild-type cells and nuclear positioning of the centromeres is aberrant (Bähler et al., 1991; Chikashige et al., 2004; Yamamoto and Hiraoka, 2003). We thus decided to use another method of Pat1 inactivation that allows meiotic induction at a lower and more physiological temperature. Moreover, the reduced temperatures slow the progression of the replication machinery, which may provide us with greater time resolution for our experiments (Aparicio et al., 1997). Interestingly, mutations of *pat1* have been generated that render it sensitive to nhibition by a non-hydrolysable ATP analog

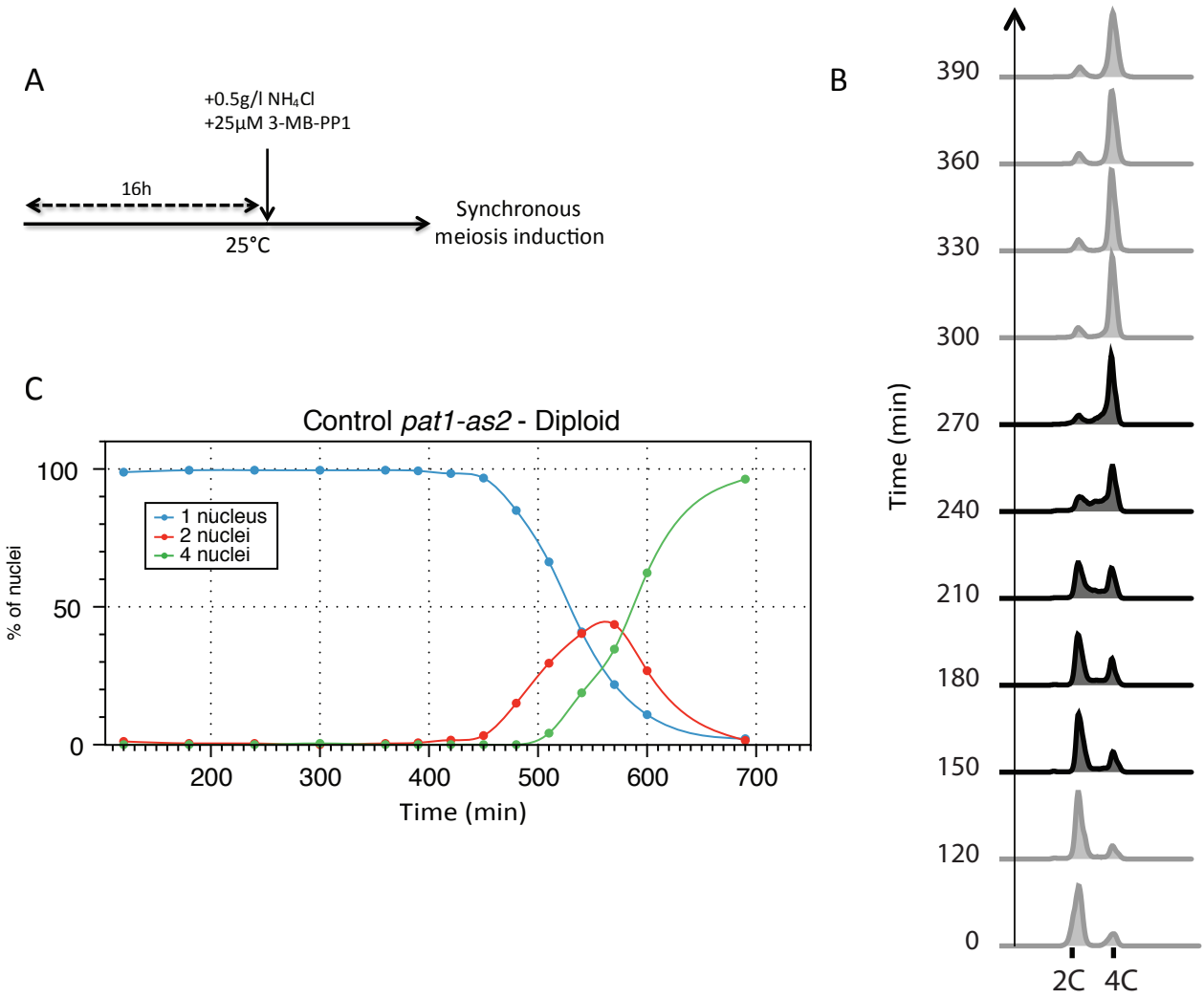

Figure 1: Meiotic cell cycle characterization and meiotic progression in Pat1-as2. A) Experimental design for initiating synchronous meiosis. B) Flow cytometry analysis of the pre-meiotic S-phase after nitrogen starvation. t = 0 corresponds to the time at which nitrogen and the non hydrolysable ATP analog (3-MB-PP1) were added to the medium. Duration of the pre-meiotic S-phase is indicated in black. C) Time course of meiotic progression of diploid pat1-as2 strains induced to undergo meiosis. Ethanol-fixed cells were stained with DAPI to detect nuclei. The number of nuclei per cell was counted every 30 or 60 minutes to determine the kinetics of meiosis I and II after nitrogen depletion (n > 300). Most of the cells have proceeded through meiosis I and meiosis II around 5h and 7h respectively after release from nitrogen starvation.

(3-MB-PP1) (Cipak et al., 2012; Guerra-Moreno et al., 2012). We therefore characterized and optimized the use of the *pat1–as2* mutant (Cipak et al., 2012) for our experiments.

First, we characterized meiotic induction and progression in the *pat1-as2* background. Diploid *pat1-as2* cells were grown to exponential phase at 25°C and depleted of nitrogen during 16 h for G0/G1 arrest. Cultures were then released into the cell cycle upon addition of the nitrogen source 0.05%w/v and 25µM of the 3-MB-PP1 inhibitor at 25°C (Figure 1A). Flow cytometry analysis showed that pre-meiotic S phase starts 150 min after release from G0/G1 and takes 120 min to be completed (Figure 1B). We then analyzed the timing and the execution of meiosis I and II following DNA replication (Figure 1B). Completion of meiosis I occurs when cells harboring two nuclei, and cells with four nuclei are observed when meiosis II has finished. Our results showed that the majority of cells have completed meiosis I and II around five and seven hours after S phase completion, respectively. These data indicate a high level of synchrony and are consistent with previous studies (Cipak et al., 2012; Guerra-Moreno et al., 2012). Moreover, unpublished studies in the lab have shown that the program of origin efficiencies in *pat1-as2* is virtually identical to our previous observations using the *pat1-114* mutant in similar experimental contexts. Taken together, these findings suggest that *pat1-as2* is an ideal background to use for our study.

Construction of a system that generates inducible replication fork barriers during pre-meiotic S-phase

The relationship between origin selection and DSB formation may be intimately linked to the progression of the replication machinery along the DNA. In this case, we would hypothesize that a region containing DSBs must be duplicated before breaks are made. To test this possibility, we designed a system in which replication fork barriers are induced to block the progression of the replisome through a region that contains a DSB hotspot. We took advantage of the well-characterized site-specific terminator of replication RTS1 in the fission yeast (Dalgaard and Klar, 2001). RTS1 is a DNA sequence present in the genome of *S. pombe* that serves as a polar replication fork barrier (RFB) when bound by the Rtf1 protein, and it regulates imprinting at *mat1* locus

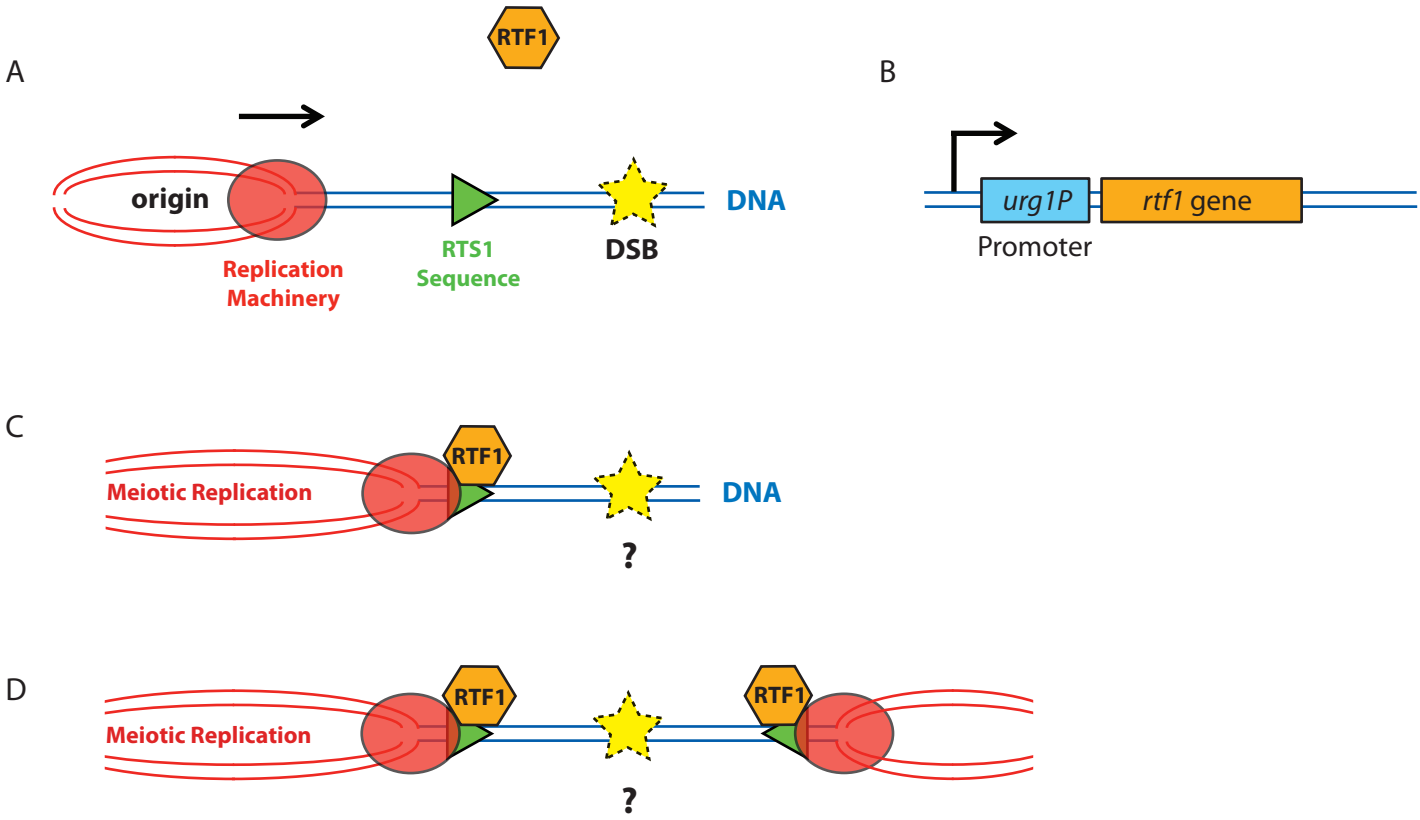

Figure 2: Strategy to generate an inducible replication fork blockage.
A) After identification of a DSB hotspot, the S. pombe RTS1 DNA sequence is inserted between a replication origin and a DSB. The RTS1 sequence act as a polar replication barrier when bound by the RTF1 protein. B) The barrier will be made inducible by putting the RTF1 gene under the control of the urg1 uracil-regulatable promoter. C) After RTF1 induction and meiotic entry, the replication machinery is blocked at the RTS1 sequence. Moreover, D) in order to completely isolate the DSB hotspot from replication, a second RTS1 sequence can be inserted in the opposite side of the DSB hotspot. The presence of DSB formation is assessed by chromatin immumoprecipitation follow by q-PCR of Rad51.

(Dalgaard and Klar, 2001). Our strategy consists in generating strains containing one or two RTS1 sequences for either delaying (one insertion) or preventing (two insertions) the duplication of a region containing a DSB site. More precisely, we integrated RTS1 sequence near sites of mapped DSBs, separating these sites from the proximal origins (Figure 2A). In addition, to construct an inducible barrier, we have 1) deleted the endogenous *rtf1* gene and 2) integrated *rtf1* at the *urg1* locus to place it under the control of this uracil-regulatable promoter (Watson et al., 2013) (Figure 2B), which allows strong and rapid expression upon addition of uracil (Watt et al., 2008). Thus, after *rtf1* induction, its binding to RTS1 sequence would serve to arrest the replication fork when it reaches this site, resulting in a delay in replication in that region; the locus would then be replicated passively from the other side of the DSB (Figure 2C). Moreover, insertion of a second RTS1 sequence on the other side of the DSB would significantly inhibit replication through this region (Figure 2D).

The combination of the above constructions with the *pat1-as2* background enables us to test our hypothesis. DSB formation can be assessed using chromatin immunoprecipitation of the recombination protein Rad51 (Roeder, 1997) followed by quantitative PCR. Moreover, in order to confirm that potential effects on DSBs formation are linked with meiotic recombination, the same constructions will be generated in a *rec12 Δ* mutant. Thus, this approach allows us to determine whether the initiation of replication is sufficient to promote DSB formation or whether a region containing potential DSB sites must be duplicated before DNA breaks are generated.

Integration of inducible replication fork barriers

Prior to the generation of the strains containing inducible replication fork barriers, we selected the sites of RTS1 insertion to minimalize potential side effects of integrating this sequence in the genome. We identified target sites that are located in intergenic regions and away from essential genes or annotated tRNAs and ncRNAs. Based on these parameters, we chose to evaluate the impact on DSB hotspots in different origin contexts, based on published meiotic recombination and replication

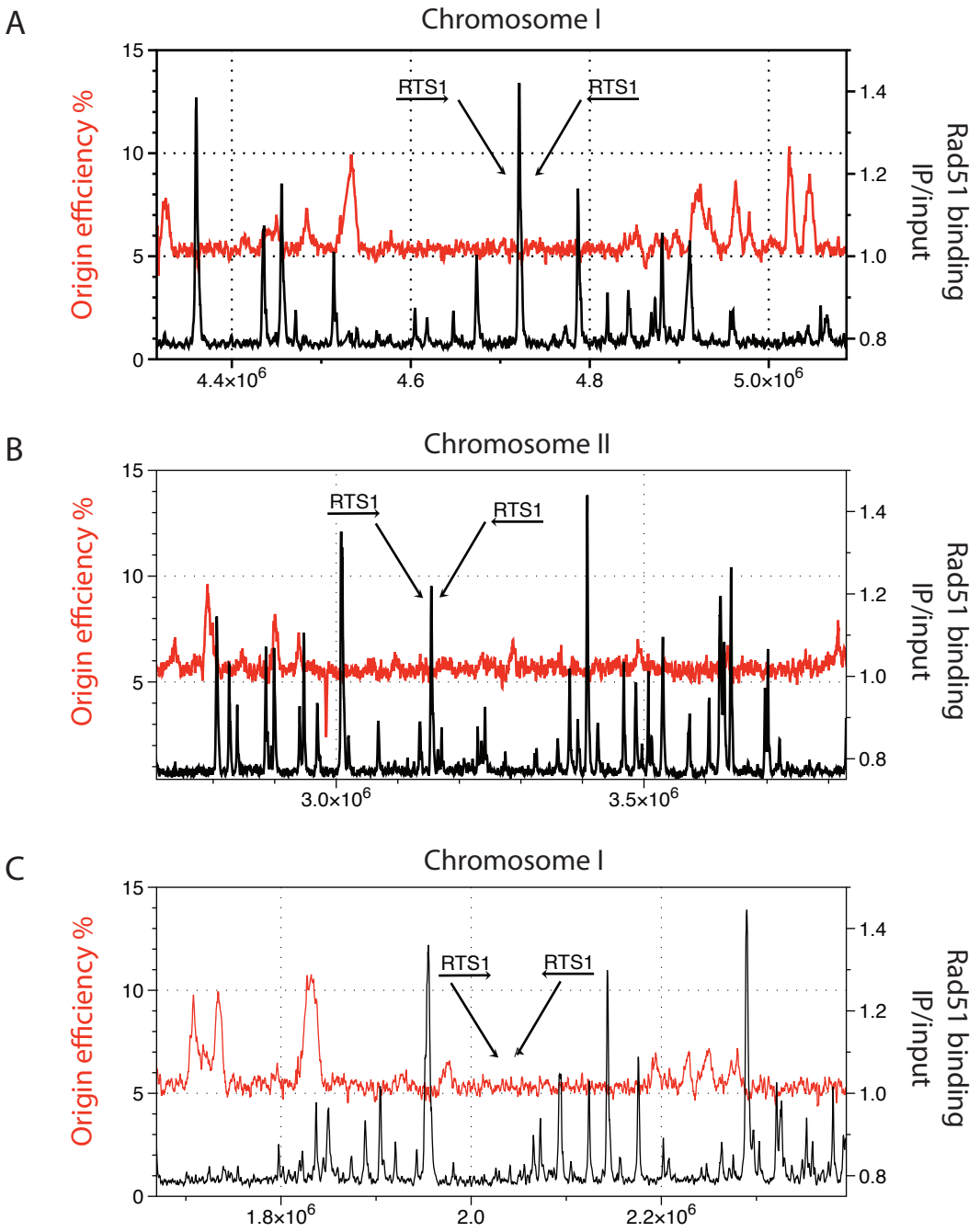

Figure 3: Location of RTS1 DNA sequence in the genome.
A) Location of RTS1 insertions on chromosome I. B) Location of RTS1 insertion on chromosome II. C) Location of RTS1 insertions on chromosome I in a site where no DSB hotspot wasdetected. In all the cases, strains contain the RTS1 sequence either 5' or 3' of the DSB hotspot or in both side of the hotspot. Red, origin usage in meiosis after nitrogen starvation and pat1as2 inactivation through 3-MB-PP1 inhibitor. Black, Rad51 binding to DNA after nitrogen starvation and meiosis induction. The abscissa represents the chromosome coordinates, and the ordinateshows the level of Rad51 binding (right) and the origin ef□ iciency (left). RTS1 DNA sequencesnext to DSB sites were inserted at ChrI : 4709252, ChrI : 4739524, ChrII : 3149658 and ChrII :3168415. For the control, RTS1 sequences were inserted at ChrI: 2029213 and ChrI : 2058827.

initiation data from our laboratory (Wu and Nurse, 2014) These include 1) a DSB located between two efficient origins in a high-efficiency region (Figure 3A) and 2) a DSB flanked by an efficient origin on one side and an inefficient region on the other side (Figure 3B). For each site, the RTS1 barrier was integrated on either one or both sides of the selected DSBs, between the DSB and the adjacent origin (Figure 3A-B). As a control, we also chose a region that does not contain DSBs (Figure 3C). Haploid version of these integrations in the *pat1-as2* background were first generated, followed by diploidization of these strains. The list of constructed strains can be found in the material and methods.

Characterization of RTS1-containing strains

Next, we characterized the diploid *pat1-as2* strains containing RTS1 to assess whether they show any phenotypes. For these assays, we analyzed strains that contain the RTS1 sequence inserted in either one side or the other of the DSB. We characterized the control strains as well as the insertions in chromosome II (Figure 3B-C). Cells were grown to exponential phase at 25°C, depleted of nitrogen during 16 h for G0/G1 arrest, and released into the cell cycle upon addition of a nitrogen source (NH_4Cl) and 3-MB-PP1 inhibitor at 25°C (Figure 4A). Flow cytometer analysis showed that cell cycle progression was identical for the 4 tested strains (Figure 4B). We noted that pre-meiotic S-phase was advanced by 30 min compared with a *pat1-as2* background without the RTS1 insertions (compare Figure 1B and Figure 4B).

Next, we analyzed the timing and execution of meiosis I and II following the completion of DNA replication (Figure 4C). We counted the number of nuclei during meiotic progression to assess meiosis I and II. Comparison of these data with a *pat1-as2* background showed that while meiosis begins ~30 min earlier in all RTS1-insertion strains, the relative timings of meiotic events are not affected. Indeed, cells have completed meiosis I and II around 5 h and 7h after the end of the pre-meiotic S phase, respectively.

Thus, the insertion of RTS1 sequences at ectopic sites does not significantly affect the progression of meiotic events.

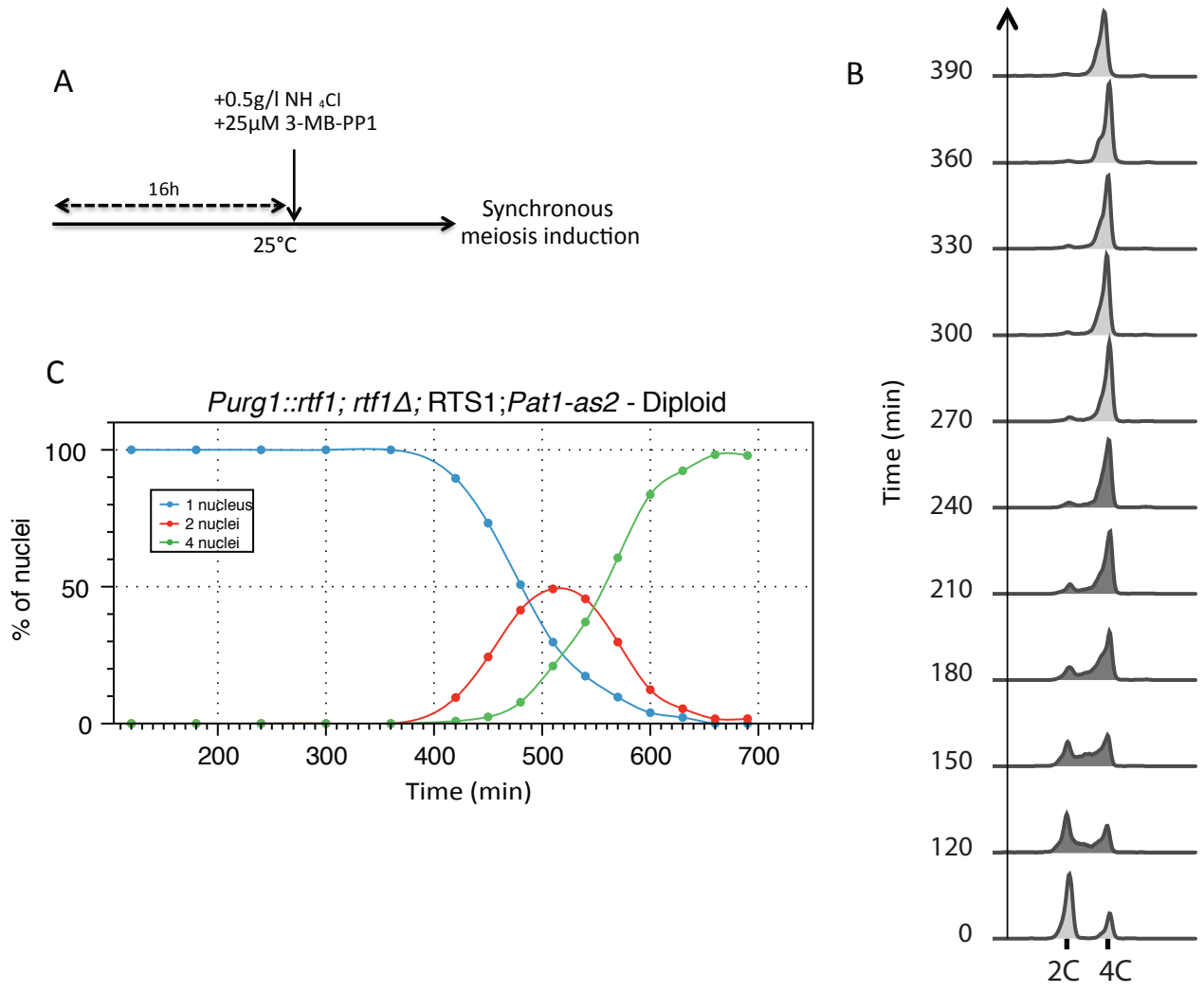

Figure 4: Meiotic cell cycle characterization and meiotic progression in RTF1 strains.
A) Experimental design for initiating synchronous meiosis. B) Flow cytometry analysis of the pre-meiotic S-phase after nitrogen starvation. This pro□ile is representative of the different strains generated in that study. t = 0 corresponds to the time at which nitrogen and the non hydrolysable ATP analog (3-MB-PP1) were added to the medium. Duration of the pre-meiotic S-phase is indicated in black. C) Time course of meiotic progression of diploid pat1-as2 strains induced to undergo meiosis. Ethanol-□ixed cells were stained with DAPI to detect nuclei. The number of nuclei per cell was counted every 30 or 60 minutes to determine the kinetics of meiosis I and II after nitrogen depletion (n > 300). Most of the cells have proceeded through meiosis I and meiosis II at around 4h30 and 6h30 respectively after release from nitrogen

Characterization of the control of rtf1 gene expression by the urg1 promoter

The binding of the Rtf1 protein to the RTS1 sequence is required for blocking the replication fork at this site. In our strains, the endogenous rtf1 gene was deleted, and we integrated a copy of it was placed under the control of the uracil-regulatable promoter urg1 promoter. This construction renders its transcription dependent to the addition of uracil, and we assayed the induction of *rtf1* after uracil addition in our system.

We first determined the induction of *rtf1* gene expression in an otherwise wild-type haploid backround (Strain: LL042) (Figure 5A). Cells were grown asynchronously. For *urg1* induction, cells were grown in exponential phase in EMM liquid medium, and we then added 0.25 mg/ml of uracil (Watson et al., 2013; Watt et al., 2008). We monitored *rtf1* expression at different time points after uracil addition by quantitative PCR using primers specific to the spliced version of the *rtf1* mRNA (Figure 5A). Consistent with previous data (Watt et al., 2008), our results showed that *rtf1* was induced 30 min after uracil addition, resulting in a 100-fold increase compared to t = 0 that is sustained for at least 40 min (Figure 5B). We next tested these induction conditions in *pat1-as2* diploid cells containing *urg1-rtf1* and RTS1 on chromosome II. Using the same conditions as above and normalized our data to the t = 0, our results showed a high level of expression of the spliced *rtf1* mRNA 30 min after uracil addition that is maintained for at least 90 min (Figure 5D). Thus we confirmed that upon uracil addition, *rtf1* is highly expressed in vegetatively growing RTS1 diploid cells.

Finally, we tested the induction of *rtf1* during meiosis. To this end, cells were grown to exponential phase and then depleted of nitrogen during 16 h for G0/G1 arrest. Cells were then allowed to re-enter the cell cycle through the addition of NH_4Cl, and meiosis was induced using 3-MB-PP1 treatments. As S phase starts ~2 h after cell cycle re-entry, we induced *rtf1* expression 60 min after the addition of nitrogen to permit sufficient for cells to express *rtf1* prior to DNA replication (Figure 4B). Levels of *rtf1* were assessed by quantitative PCR, and data were normalized to the *atg22* gene, whose mRNA level does not vary during meiosis (Mata et al., 2002). We determined the time course of *rtf1* expression without and with uracil in the conditions described above; this was compared with exponentially growing cells in the absence of uracil (Figure 5F).

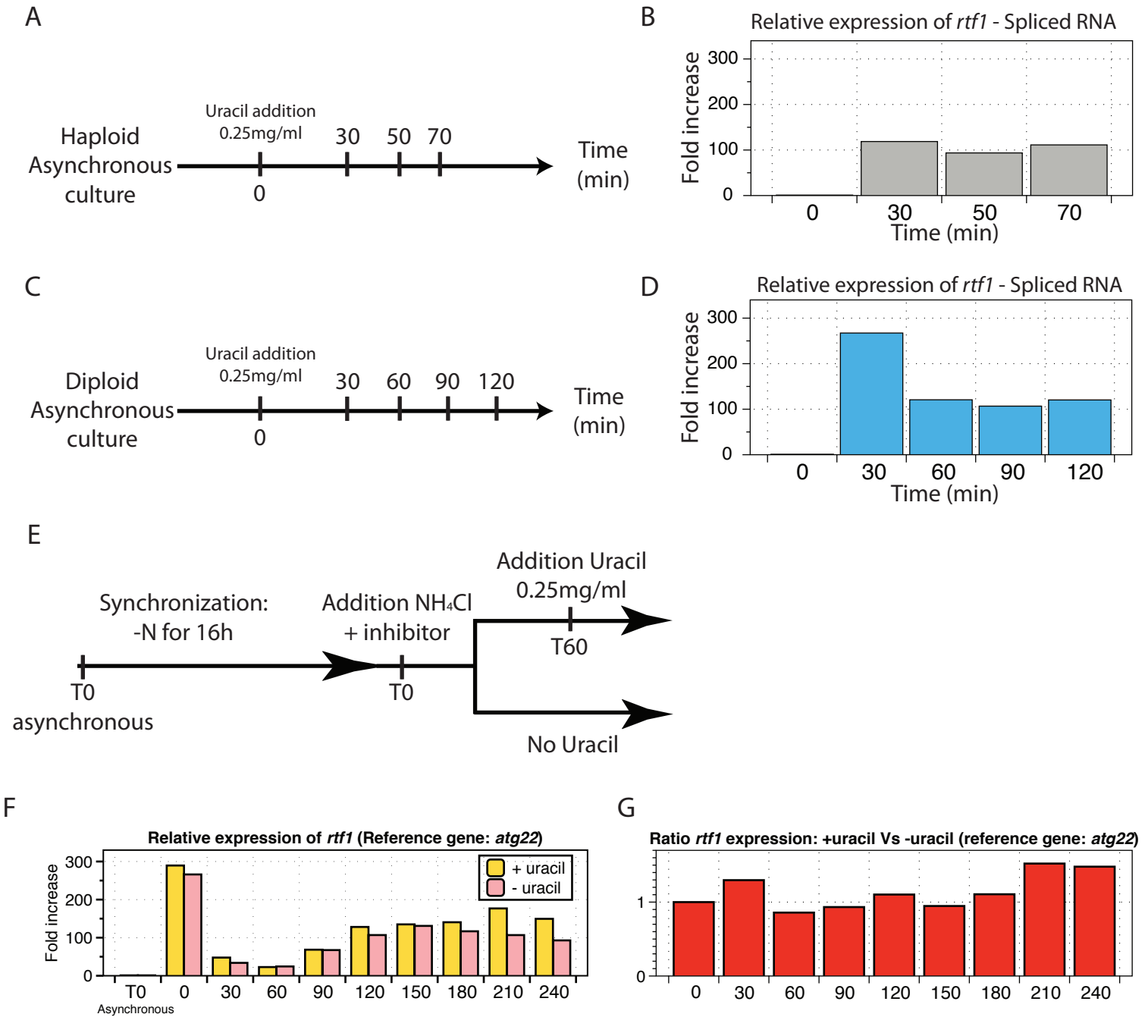

Figure 5: Induction of purg1::rtf1 is dependent of uracil addition in vegetatively growing cells but independent during meiosis.

A) Experimental design to induce rtf1 under the control of the urg1 promoter in haploid vegetatively growing cells. B) Quantitative PCR analysis of purg1::rtf1. Haploid RTS1 cells were grown exponentially and rtf1 was induced at T = 0 by addition of 0.25mg/ml of uracil. Data were normalized to T = 0. x-axis time (min), y-axis fold increase in rtf1 mRNA. C) Experimental design to induce rtf1 under the control of the urg1 promoter in diploid vegetatively growing cells. D) Quantitative PCR analysis of purg1::rtf1. Diploid RTS1 cells were grown exponentially and rtf1 was induced at T = 0 by addition of 0.25mg/ml of uracil. Data were normalized to T = 0. x-axis time (min), y-axis fold increase in rtf1 mRNA. E) Experimental design to induce synchronous meiosis and rtf1 induction. Cells were grown to exponential phase at 25°C, depleted of nitrogen during 16 h for G0/G1 arrest an released to induced meiosis by addition of nitrogen source NH4Cl and 3-MB-PP1 at 25°C. Uracil was then added or not to the media after 60 minutes. F) Quantitative PCR analysis of purg1::rtf1 expression during meiosis. Data were normalized to atg22 that does not vary during meiosis and to rtf1 in vegetatively growing cells (T0 assynchronous). Yellow bars represent the condition when uracil was added to the media 60min after release from G0/G1 (+ uracil). Purple bars represent the condition when uracil was not added to the media (- uracil). x-axis time (min), y-axis fold increase in rtf1 mRNA. G) Ratio between + uracil and – uracil (data in F).

Interestingly, we observed that *rtf1* was highly induced by nitrogen depletion; this is consistent with previous observations indicating that the *urg1* gene is induced by nitrogen starvation (Mata and Bähler, 2006; Mata et al., 2002; 2007). This level then decreases dramatically 30 min after the addition of nitrogen. Surprisingly, our data showed that its expression increases as cells continue to proliferate, regardless of the presence of uracil in the medium (Figure 5F); however, we do find modestly higher *rts1* levels in cells treated with uracil (Figure 5G). These findings suggest that the *urg1* promoter induces transcription both in nitrogen depletion conditions as well as during meiotic progression. Relevant to our experiments, our results indicate that significant *rts1* expression is observed ~90 min after the release from nitrogen starvation and meiotic induction and that these levels are modestly enhanced by the addition of uracil.

Characterization of the levels of Rtf1 protein in our system

To determine the levels of of RTF1 protein during the course of our experiments, we generated both haploid and diploid containing HA-tagged versions of RTF1 (RTF1-3HA) under the control of the *urg1* promoter. We first assessed RTF1-3HA by Western blot during a time course of *urg1* induction in asynchronous cultures. For this, cells were grown to exponential phase at 25°C in EMM liquid medium, and 0.25mg/ml uracil was then added for the induction. Cells were harvested every 30 min, and whole cell extracts were analyzed using an anti-HA antibody (Figure 6A). In the absence of uracil, we detected no RTF1-3HA protein. RTF1-3HA level began to increase 90 min after the addition of uracil and continued for at least 3 h after uracil addition. We then performed these experiments during a synchronous meiosis. Diploid *pat1-as2* cells containing RTS1 in chromosome II (LL098, see material and methods) were grown to exponential phase at 25°C, depleted of nitrogen during 16 h for G0/G1 arrest, and released to undergo meiosis by addition of NH_4Cl and 3-MB-PP1. Uracil was then added to the media after 60 minutes for *urg1::rtf1-3HA* induction. Cells were harvested every 30 min, and whole cell extracts were analyzed by Western blot using an anti-HA antibody. Consistent with our observations for the transcript levels of *urg1-rtf1*, we found that RTF1-HA was present after nitrogen depletion (T0 Mei, Figure 6B) and that its level decreased after cell cycle re-entry. Nevertheless, we detected an increase in RTF1-3HA 120 min following uracil addition (180 min, Figure 6B); these levels further increase

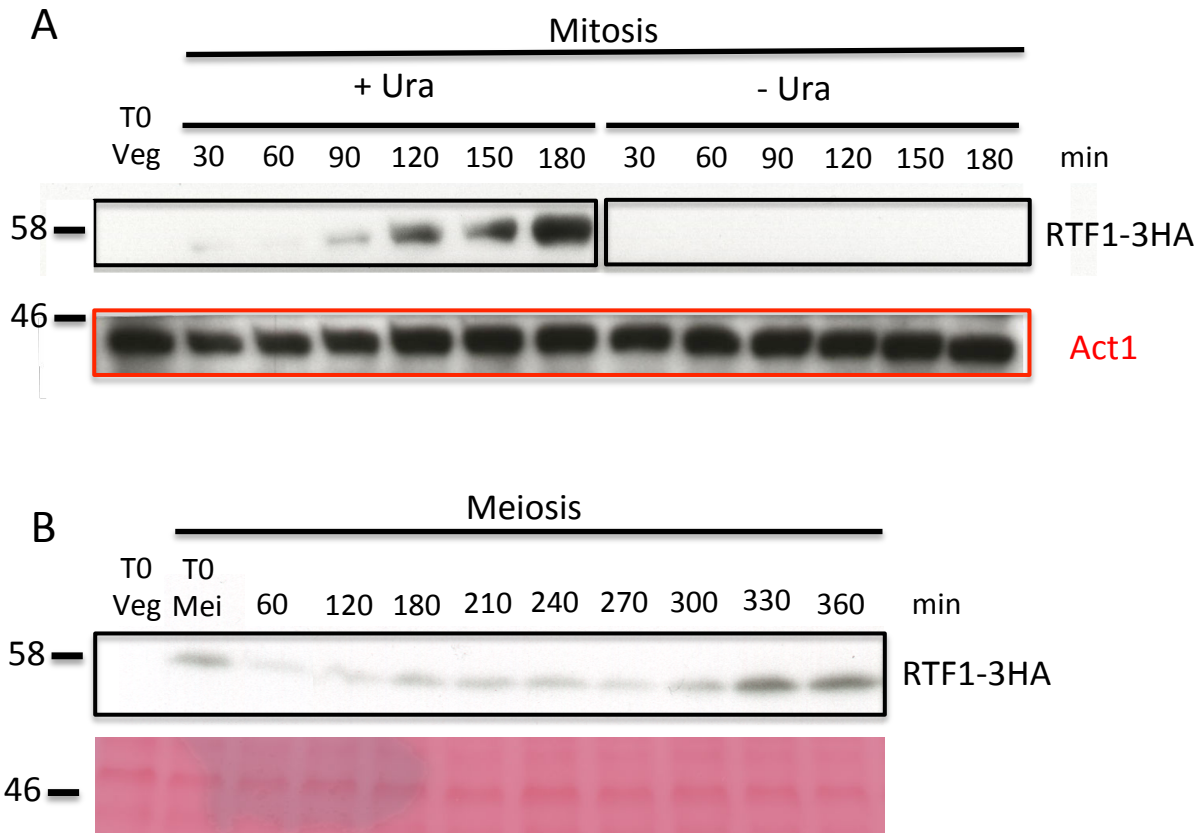

<u>Figure 6</u>: Dynamic of RTF1 induction in RTS1 mitotic and meiotic strains.
A) Immunoblot of RTF1-3HA induction after addition of uracil (left panel) or without addition of uracil (right panel) during mitosis. Act1 was used as loading control. T0 Veg represent the time when uracil was added to the media in + uracil condition. B) Immunoblot of RTF1-3HA induction after addition of uracil. Uracil were added at T = 60 to the cells. Ponceau was uses as loading control.

until at least 360 min after release from G0/G1. Thus, while we detect RTF1-HA in our experimental context, its levels remain relatively modest during pre-meiotic S phase. It ability to block DNA replication at the ectopically inserted RTS1 sequences therefore remains to be evaluated.

Discussion and perspectives

In this chapter, we have described our efforts to set up an experimental system that aims to investigate the relationship between the progression of the replication machinery and the establishment of DSB sites during meiosis in *S. pombe.* For this purpose, we designed a system in which the progression of the replication machinery through a DSB site can be controlled using an inducible RTS1-RTF1 replication fork barrier. This was integrated in the genetic background of the *pat1-as2* mutant for the analysis of two DSB sites located in different origin contexts. We have generated a number of the strains required for our assays, and we have performed critical characterization of our system. In particular, we showed that the ectopic RTS1 insertions do not significantly perturb synchronous meiotic progression in diploid *pat1-as2* strains, with a similar relative timing of pre-meiotic S phase, meiosis I, and meiosis II. Moreover, we evaluated the induction of the Rtf1 protein, which is essential for the replication fork barrier activity of RTS1. Our results showed that *rtf1* RNA and protein levels are induced shortly after the addition of uracil in vegetatively growing cells. However, *rtf1* expression is induced by nitrogen depletion, and its RNA levels increased during meiotic progression; this occurred independently of the presence of uracil in the medium. Nevertheless, as Rtf1 is present during a synchronous meiosis, it is possible that even these low levels may be sufficient for blocking replication at RTS1. To test this, a preliminary chromatin immunoprecipitation experiment of the Swi1 factor was performed in our experimental conditions (data not shown); Swi1 is a component of the replication fork protection complex that is important for RTS1 function (Dalgaard and Klar, 2001; Noguchi et al., 2004). However, our initial data do not indicate a blockage of the replication fork at RTS1. To optimize the system, it may be possible to induce *rtf1* at an earlier time point or with higher levels of uracil. Alternatively, we may consider using another inducible promoter such as the thiamine-repressible *nmt1* promoter;

Table 1: Strains used for this study

Strain	Genotype	Source
LL042	*h+ ; urg1Δ::RTF1 ; RTF1Δ::KanMX6*	This study
LL084	*h-/h- SPAC17H9.13c:RTS1:Pdi2/SPAC17H9.13c:RTS1:pdi2 urg1Δ::RTF1/urg1Δ::RTF1 rtf1Δ::KanMX6/rtf1Δ::KanMX6 pat1::clonNatR pat1-as (L95A) HphR/pat1::clonNatR pat1-as (L95A) HphR*	This study
LL088	*h-/h- vma11:RTS1:CPAC732.02c/vma11:RTS1:CPAC732.02c urg1Δ::RTF1/urg1Δ::RTF1 rtf1Δ::KanMX6/rtf1Δ::KanMX6 pat1::clonNatR pat1-as (L95A) HphR/pat1::clonNatR pat1-as (L95A) HphR*	This study
LL091	*h-/h- atg16:RTS1:Xbj1/atg16:RTS1:Xbj1 urg1Δ::RTF1/urg1Δ::RTF1 rtf1Δ::KanMX6/rtf1Δ::KanMX6 pat1::clonNatR pat1-as (L95A) HphR/pat1::clonNatR pat1-as (L95A) HphR*	This study
LL095	*h-/h- caf5:RTS1:pob3/caf5:RTS1:pob3 urg1Δ::RTF1/urg1Δ::RTF1 RTF1Δ::KanMX6/RTF1Δ::KanMX6 pat1::clonNatR pat1-as (L95A) HphR/pat1::clonNatR pat1-as (L95A) HphR*	This study
LL140	*h- urg1Δ::RTF1 RTF1Δ::KanMX6 pat1::clonNatR pat1-as (L95A) HphR klp3:RTF1:mak1*	This study
LL131	*h+ ura4-D18 urg1Δ::RTF1 RTF1Δ::KanMX6 caf5RTS1:pob3 atg16:RTS1:xbj1 pat1::clonNatR pat1-as (L95A) HphR*	This study
LL132	*h+ ura4-D18 urg1Δ::RTF1 RTF1Δ::KanMX6 SPAC17H9.13c :RTS1:pdi2 vma11:RTS1:CPAC732.02c pat1::clonNatR pat1-as (L95A) HphR*	This study
LL133	*h+ SPAC17H9.13c:RTS1:Pdi2 urg1Δ::RTF1 RTF1Δ::KanMX6 pat1::clonNatR pat1-as (L95A) HphR rec12Δ::BSD*	This study
LL134	*h+ vma11:RTS1:CPAC732.02c urg1Δ::RTF1 RTF1Δ::KanMX6 pat1::clonNatR pat1-as (L95A) HphR rec12Δ::BSD*	This study
LL134	*h+ vma11:RTS1:CPAC732.02c urg1Δ::RTF1 RTF1Δ::KanMX6 pat1::clonNatR pat1-as (L95A) HphR rec12Δ::BSD*	This study
LL135	*h+ atg16:RTS1:xbj1 urg1Δ::RTF1 RTF1Δ::KanMX6 pat1::clonNatR pat1-as (L95A) HphR rec12Δ::BSD*	This study

however, *nmt1* has a long induction time (~12 h), which is one of the reasons that we chose the *urg1* promoter for our studies.

Once full complement of the strains containing the RTS1 insertions are generated and our system properly optimized, we will be able to determine the requirement for DNA replication in the regulation of meiotic DSB formation. Blocking the passage of the replication fork may have no effect on DSB formation, which would suggest that the assembly of replication complexes at origins or the initiation of replication might be sufficient to modulate the sites of meiotic recombination. To analyze this latter possibility, we could target specific factors involved in different steps of replication to particular sites and assess whether this alters DSB formation. To do so, the LacI / LacO system can be used to recruit LacI-replication factor fusions to LacO sites integrated in different regions of interest. Alternatively, if blocking the passage of the replication machinery through a DSB site impairs break formation, this may suggest that the genomic region has to be duplicated prior the generation of a DSB. A complementary method for evaluating this possibility would be to allow only a portion of the genome to be duplicated using either hydroxyurea treatment or mutations in genes encoding for replication factors. A genome-wide assessment of DSB formation would then reveal whether breaks are confined to duplicated regions of the genome. Taken together, these approaches will elucidate the mechanisms by which DNA replication modulates DSB formation.

Materials and Methods

Fission yeast strains and methods

Standard media and methods for fission yeast were used (Hayles and Nurse, 1992; Moreno et al., 1991). All experiments were carried out in minimal medium plus supplements (EMM6S) at 25°C, except where otherwise noted. For experiments assessing the induction of *urg1-rtf1*, EMM medium was used. The *Schizosaccharomyces pombe* strains constructed for this study are listed in Table 1.

Cell cycle synchronization by nitrogen depletion and meiotic induction

Strains were grown at 25°C to a density of $2x10^6$ cells/mL in EMM6S. Cells were then starved of nitrogen in minimal medium (EMM-N) for 16h at 25°C. Release from G0/G1 induced by nitrogen starvation was carried out by feeding cells with a nitrogen source (0.05%w/v NH_4Cl). Meiosis was induced by adding the 3-MBPP1 inhibitor (A602960, Toronto Research Chemicals Inc.) to a final concentration of 25μM. A stock 10 mM solution of 3-MBPP1 was prepared by dissolving the inhibitor in DMSO.

DNA content analysis by flow cytometry

DNA content analysis was performed by flow cytometry (BD Accuri™, C6 Flow Cytometer System). Cells were first fixed with 70% cold ethanol, washed with 50mM sodium citrate and treated with RNAse A (0.1 mg/ml) overnight at 37°C. Cells were then stained with propidim iodide (2mg/ml), sonicated for 10 seconds at an amplitude of 30% using a Branson Digital Sonifier. Analysis was performed using the Flowjo analysis software.

RNA extraction and RT-qPCR analysis

RNA was extracted using the hot acid phenol method and treated with DNAse (Ambion™ TURBO™ DNase). 400ng RNA was used for the reverse transcription reaction using the QuantiTect Reverse Transcription Kit (QUIAGEN). cDNA synthesis was performed at 42°C for 15 minutes. Quantiscript Reverse Transcriptase was heat inactivated at 95°C for 3 minutes. Samples were analyzed by qPCR (Applied Biosystems 7900 HT Fast real time PCR system). For qPCR, cDNA samples were mixed with Brilliant III SYBR® Master Mix/high ROX (Agilent Technologies) and run in triplicate. Primers used to assess the splicing of RTF1 are as follows: LL0145: CGCGACTACATTCAACCTGG; LL0146: GGGATGAAGGATTGCTTTGC. Data acquisition was performed using the SDS 2.4 software.

Protein purification and western blot

Whole cell extracts for Western analysis were prepared by washing the harvested cell pellets twice with 20% (w/v) trichloroacetic acid (TCA) and then breaking the cells with glass beads using a FastPrep cell disruptor (MP Biomedical). The supernatant was recovered by centrifugation. Beads were washed 4 times with 5% TCA and quickly centrifuged. Supernatants were pooled to the same tube. Precipitated proteins were recovered by centrifugation and then suspended in SDS-PAGE sample buffer. After adjusting the pH to 8.8, samples were sonicated 5 seconds at 20% power with a Bioruptor Plus (Diagenode) and boiled 5 minutes at 95°C. Extracts were subjected to SDS-PAGE and transferred to PVDF membranes. The following antibodies were used: anti-HA (12CA5, mouse; Sigma ; 1:8000 dilution), and anti-Act1 (mouse; Sigma ; 1:1000 dilution), and anti-mouse HRP-conjugated antibody (Molecular Probes ; 1:250).

References

Aparicio, O.M., Weinstein, D.M., and Bell, S.P. (1997). Components and dynamics of DNA replication complexes in S. cerevisiae: redistribution of MCM proteins and Cdc45p during S phase. Cell *91*, 59–69.

Bähler, J., Schuchert, P., Grimm, C., and Kohli, J. (1991). Synchronized meiosis and recombination in fission yeast: observations with pat1-114 diploid cells. Curr Genet.

Borde, V., Goldman, A.S., and Lichten, M. (2000). Direct coupling between meiotic DNA replication and recombination initiation. Science *290*, 806–809.

Chikashige, Y., Kurokawa, R., Haraguchi, T., and Hiraoka, Y. (2004). Meiosis induced by inactivation of Pat1 kinase proceeds with aberrant nuclear positioning of centromeres in the fission yeast Schizosaccharomyces pombe. Genes Cells *9*, 671–684.

Cipak, L., Hyppa, R.W., Smith, G.R., and Gregan, J. (2012). ATP analog-sensitive Pat1 protein kinase for synchronous fission yeast meiosis at physiological temperature. Cell Cycle *11*, 1626–1633.

Dalgaard, J.Z., and Klar, A.J. (2001). A DNA replication-arrest site RTS1 regulates imprinting by determining the direction of replication at mat1 in S. pombe. Genes & Development *15*, 2060–2068.

De Veaux, L.C., Hoagland, N.A., and Smith, G.R. (1992). Seventeen complementation groups of mutations decreasing meiotic recombination in Schizosaccharomyces pombe. Genetics *130*, 251–262.

Guerra-Moreno, A., Alves-Rodrigues, I., Hidalgo, E., and Ayté, J. (2012). Chemical genetic induction of meiosis in Schizosaccharomyces pombe. Cell Cycle *11*, 1621–1625.

Handel, M.A., and Schimenti, J.C. (2010). Genetics of mammalian meiosis: regulation, dynamics and impact on fertility. Nat Rev Genet *11*, 124–136.

Hayles, J., and Nurse, P. (1992). Genetics of the fission yeast Schizosaccharomyces pombe. Annu. Rev. Genet. *26*, 373–402.

Iino, Y., and Yamamoto, M. (1985). Negative control for the initiation of meiosis in Schizosaccharomyces pombe. Proc. Natl. Acad. Sci. U.S.a. *82*, 2447–2451.

Keeney, S. (2001). Mechanism and control of meiotic recombination initiation. Curr. Top. Dev. Biol. *52*, 1–53.

Keeney, S. (2008). Spo11 and the Formation of DNA Double-Strand Breaks in Meiosis. Genome Dyn Stab *2*, 81–123.

Mata, J., and Bähler, J. (2006). Global roles of Ste11p, cell type, and pheromone in the control of gene expression during early sexual differentiation in fission yeast. Proc. Natl. Acad. Sci. U.S.a. *103*, 15517–15522.

Mata, J., Lyne, R., Burns, G., and Bähler, J. (2002). The transcriptional program of meiosis and sporulation in fission yeast. Nat. Genet. *32*, 143–147.

Mata, J., Wilbrey, A., and Bähler, J. (2007). Transcriptional regulatory network for sexual differentiation in fission yeast. Genome Biol. *8*, R217.

Moreno, S., Klar, A., and Nurse, P. (1991). Molecular genetic analysis of fission yeast Schizosaccharomyces pombe. Meth. Enzymol. *194*, 795–823.

Murakami, H., and Nurse, P. (2001). Regulation of premeiotic S phase and recombination-related double-strand DNA breaks during meiosis in fission yeast. Nat. Genet.

Murakami, H., and Keeney, S. (2008). Regulating the formation of DNA double-strand breaks in meiosis. Genes & Development *22*, 286–292.

Murakami, H., and Keeney, S. (2014). Temporospatial Coordination of Meiotic DNA Replication and Recombination via DDK Recruitment to Replisomes. Cell *158*, 861–873.

Noguchi, E., Noguchi, C., McDonald, W.H., Yates, J.R., and Russell, P. (2004). Swi1 and Swi3 Are Components of a Replication Fork Protection Complex in Fission Yeast. Molecular and Cellular Biology *24*, 8342–8355.

Roeder, G.S. (1997). Meiotic chromosomes: it takes two to tango. Genes & Development *11*, 2600–2621.

Székvölgyi, L., and Nicolas, A. (2010). From meiosis to postmeiotic events: homologous recombination is obligatory but flexible. FEBS Journal *277*, 571–589.

Watson, A.T., Daigaku, Y., Mohebi, S., Etheridge, T.J., Chahwan, C., Murray, J.M., and Carr, A.M. (2013). Optimisation of the Schizosaccharomyces pombe urg1 Expression System. PLoS ONE *8*, e83800.

Watt, S., Mata, J., López-Maury, L., Marguerat, S., Burns, G., and Bähler, J. (2008). urg1: a uracil-regulatable promoter system for fission yeast with short induction and repression times. PLoS ONE *3*, e1428.

Wu, P.-Y.J., and Nurse, P. (2014). Replication origin selection regulates the distribution of meiotic recombination. Molecular Cell *53*, 655–662.

Yamamoto, A., and Hiraoka, Y. (2003). Monopolar spindle attachment of sister chromatids is ensured by two distinct mechanisms at the first meiotic division in fission yeast. Embo J. *22*, 2284–2296.

Chapter IV

General discussion

General discussion

During meiosis, DNA replication is followed by double-strand break (DSB) formation, a process that is a key contributor to the exchange of genetic material during sexual reproduction. Over the past decades, a number of studies have suggested a link between DNA replication and meiotic DSB formation. However, the mechanisms linking these two processes are still not fully understood. My thesis has taken two approaches to try to decipher the crosstalk between genome duplication and meiotic recombination.

Effect of chromosomal context on DNA replication

As presented in earlier sections, DNA replication follows a program that is organized in time and efficiency along the chromosomes (Heichinger et al., 2006; Wu and Nurse, 2009). In addition, regions that replicate at the same time tend to be localized in close proximity in the nucleus (Berezney et al., 2000; Pichugina et al., 2016). Thus, chromosomal context is likely to play a critical role in regulating origin selection during S-phase. In Chapter 2, I have described the generation of chromosomal inversions and assessed their impact on the replication program. We have demonstrated that these rearrangements do not have effects on cell proliferation and meiotic progression. Importantly, our results demonstrated that these inversions trigger context-dependent changes in origin usage. Indeed, efficient origins translocated next to low efficiency regions showed decreases in efficiency, while inefficient origins transposed next to a high efficiency region increased their activities; the changes observed in this context were restricted to a ~100kb region of the endpoints of the inversion. The observation that only a restricted region is affected may indicate the possible importance of cis-regulatory elements that regulate origin usage. For instance, epigenetic modifications extending into or out of the rearranged fragment may render a region permissive or inhibitory of origin activity. However, while we observed changes in origin selection, the chromosome I and II rearrangements do not have the same effects: changes in the inversion on chromosome I were observed within the inverted fragment, while changes in chromosome II are outside of the rearranged region. The

different effects of distinct chromosomal rearrangements on origin selection may imply a more complex regulation that does not depend only on cis-regulatory elements. One possibility is that the chromosomal rearrangements affect the arrangement of the chromosomes in the nucleus. For example, in fission yeast, telomeres tend to be located next to the nucleolus while centromeres are at the spindle pole body (Rodriguez and Bjerling, 2013). Moreover, regions with similar timing and efficiencies tend to co-localize in the nucleus. Thus, one can speculate that chromosomal inversions may re-position genomic regions in the nucleus. In the case of the chromosome II rearrangement, which inverts a large part of the right arm of the chromosome, this may result in the centromere bringing the region just outside of the rearrangement near other centromeric loci, which are early-replicating in *S. pombe*.

In our study, we also compared the meiotic and the mitotic replication programs. Previous work from our lab had suggested that pre-meiotic S phase does not induce a specific pattern of origin usage (Wu and Nurse, 2014). Our results showed that while the overall replication program is conserved between mitosis and meiosis, some changes are detectable when comparing the two programs. These differences can due to several factors. First, mitosis and meiosis are two processes that require different transcription programs and regulators, and this may have an effect on origin usage. In addition, there are specific features of chromosomal context that may be different in these two conditions: epigenetic marks/chromatin configuration may interact with replication and modify the replication program to a certain extent. Moreover, it is also possible that higher-order chromosome conformation is different during pre-meiotic S phase compared to mitotic S phase.

Chromosomal context and DSB formation

One interesting finding of our work come from the analysis of DSB formation on rearranged chromosomes. Previous work in our laboratory has shown that origin selection is a key determinant in the organization of meiotic recombination (Wu and Nurse, 2014). More precisely, regional changes in origin efficiency were correlated with local changes in DSB formation. In addition, Murakami and Kenney (2014) proposed a model in which the DDK Cdc7, a kinase important for DNA replication (Valentin et al.,

2006; Wan et al., 2006), is recruited to the replication machinery and subsequently phosphorylates the critical recombination factor Mer2 (Murakami and Keeney, 2014). From this model, one hypothesis would be that local increases in origin usage could recruit recombination factors that promote DSBs. In our study, our expectation was to observe changes in DSB formation accordingly to the changes in origin efficiency induced by the chromosomal rearrangements. Interestingly, while we found that the rearrangement of chromosome II led to changes in DSB formation, they did not correspond with the alterations in origin usage. However, we note that the changes in DSB formation were limited to the regions in which origin efficiency was altered, suggesting that local changes in chromosome context may locally modify DSB formation. The analysis of additional chromosomal rearrangements, including those that do not induce changes in origin usage, may clarify our findings.

Investigation of the steps in DNA replication that are important for DSB formation

In Chapter 3, we have described preliminary work aiming to investigate the relationship between the progression of the replication machinery and the establishment of DSB sites during meiosis. We designed and constructed a system in which the progression of the replication fork through a DSB site can be controlled using an inducible replication fork barrier that relies on RTS1/Rtf1. The initial characterization of our system showed that ectopic RTS1 insertions did not perturb meiosis progression. However, induction of *Rtf1* expression remains problematic in our experimental conditions. The uracil inducible promoter we used to induce *Rtf1* was activated by nitrogen depletion and increases in activity during meiosis even in the absence of uracil. While this could be sufficient to trigger the replication fork barrier activity of RTS1, preliminary experiments showed that no blockage was detected at RTS1 sites. Thus, further optimizations of the system are necessary.

Ultimately, we aim to determine whether the blockage of the replication machinery have an effect on the formation of nearby DSBs. If no change in DSB formation is detected, this would suggest that replication initiation is sufficient to promote the formation of proximal DSBs. To test this possibility, the lacO/lacI system can be used to target replication factors to specific sites in the genome and asses

whether this alter DSB formation. Alternatively, if the blockage of the replication machinery prior to its passage through a DSB site impairs break formation, this would imply that a locus must be duplicated before a DSB can be made. A complementary method for evaluating this possibility would be to allow only a portion of the genome to be duplicated using either hydroxyurea treatment or mutations in genes encoding for replication factors. The restriction of DSB in duplicated regions would provide evidence toward this model. Taken together, these approaches will elucidate the mechanisms by which DNA replication modulates DSB formation.

A single molecule method to analyze the relationship between DNA replication and meiotic recombination

So far, studies aiming to decipher the link between replication and recombination have been carried out using a population of cells (Borde et al., 2000; Miyoshi et al., 2012; Murakami and Keeney, 2014; Wu and Nurse, 2014). While the replication pattern in a cell population is clearly defined, at the single cell level, origin selection and exhibits a high level of stochasticity (Patel et al., 2006). The same may be the case for DSB formation during meiosis. It therefore remains unknown how these processes interact in a given cell at the single molecule level. Thus, and complementary to our studies, we initiated the development of a single-molecule approach to visualize replication and DSB formation along individual chromosome. Chromatin stretching is a technique that allows the visualization of DNA fibers containing proteins (Green et al., 2009). We aimed to combine nucleotide analog incorporation into DNA with immunofluorescence in order to visualize DNA replication and sites of DSB formation, respectively. In this context, we already have successfully used EdU incorporation to label DNA synthesis. However, protein detection using immunofluorescence has been more difficult to achieve. At this point, we are able to detect histone H3 and the DSB binding protein Rad52, two proteins that are tightly bound to DNA, but this is only observed when multiple fibers are found together. We are working on amplifying the signal using both antibody and enzyme based approaches in order to detect these events in individual chromatin fibers. The development of this technique, in combination with the other approaches described above, will allow the identification of the molecular links between pre-meiotic S phase and DSB formation.

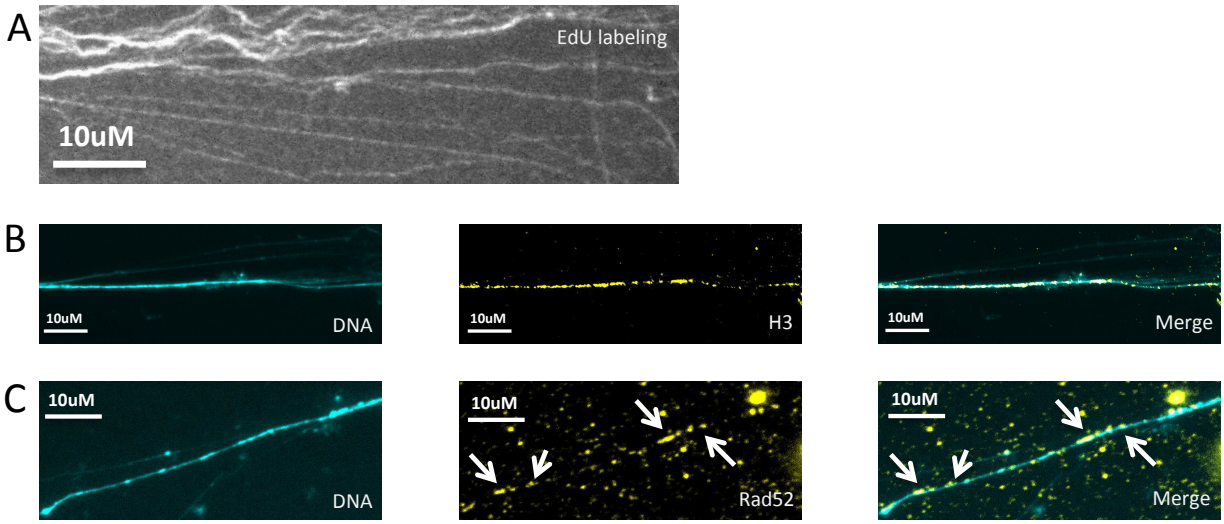

Chromatin fiber stretching.
A) EdU staining of stretched chromatin fibers. Asynchronous population of *S. pombe* cells was labeled with EdU (thymidine analog) during the entire S-phase. After stretching, EdU is revealed using a click-chemistry reaction. EdU staining allows better detection of single chromatin fiber compared with DAPI. B) Stretched chromatin fiber stained for DNA (DAPI, Left panel) and immunostained for histone H3 (Center panel) shows colocalization of the signals along chromatin fibers (Right panel). C) Stretched chromatin fiber from asynchronous population of *S. pombe* cells stained for DNA (DAPI, left panel) and immunostained for the DSB associated protein Rad51 (Center panel) shows Rad51 localization on DNA (Right panel). Cells were synchronized in G2 using a *cdc25-22; rad3Δ* mutant. Cells were then shifted to permissive temperature, and hydroxyurea (HU) was added. During S-phase, presence of HU in *rad3Δ* (checkpoint defective) background leads to an accumulation of DSBs.

In this thesis, we have provided evidence that the genomic context is important in the establishment of DNA replication program. We also found that a targeted modification of origin usage may not be sufficient to induce changes in DSB formation. Moreover, we initiated work to construct a system for deciphering the complex relationship between replication and recombination during meiosis as well as to develop single-molecule methods to address this question. Our results open new directions for investigating the interplay between chromosomal organization, DNA replication, and meiotic recombination

References

Berezney, R., Dubey, D.D., and Huberman, J.A. (2000). Heterogeneity of eukaryotic replicons, replicon clusters, and replication foci. Chromosoma *108*, 471–484.

Borde, V., Goldman, A.S., and Lichten, M. (2000). Direct coupling between meiotic DNA replication and recombination initiation. Science *290*, 806–809.

Green, M.D., Sabatinos, S.A., and Forsburg, S.L. (2009). Microscopy techniques to examine DNA replication in fission yeast. Methods Mol. Biol. *521*, 463–482.

Heichinger, C., Penkett, C.J., Bähler, J., and Nurse, P. (2006). Genome-wide characterization of fission yeast DNA replication origins. Embo J. *25*, 5171–5179.

Miyoshi, T., Ito, M., Kugou, K., Yamada, S., Furuichi, M., Oda, A., Yamada, T., Hirota, K., Masai, H., and Ohta, K. (2012). A central coupler for recombination initiation linking chromosome architecture to S phase checkpoint. Molecular Cell *47*, 722–733.

Murakami, H., and Keeney, S. (2014). Temporospatial Coordination of Meiotic DNA Replication and Recombination via DDK Recruitment to Replisomes. Cell *158*, 861–873.

Patel, P.K., Arcangioli, B., Baker, S.P., Bensimon, A., and Rhind, N. (2006). DNA replication origins fire stochastically in fission yeast. Mol. Biol. Cell *17*, 308–316.

Pichugina, T., Sugawara, T., Kaykov, A., Schierding, W., Masuda, K., Uewaki, J., Grand, R.S., Allison, J.R., Martienssen, R.A., Nurse, P., et al. (2016). A diffusion model for the coordination of DNA replication in Schizosaccharomyces pombe. Sci. Rep. *6*, 18757.

Rodriguez, A., and Bjerling, P. (2013). The links between chromatin spatial organization and biological function. Biochm. Soc. Trans. *41*, 1634–1639.

Valentin, G., Schwob, E., and Seta, Della, F. (2006). Dual role of the Cdc7-regulatory protein Dbf4 during yeast meiosis. J. Biol. Chem. *281*, 2828–2834.

Wan, L., Zhang, C., Shokat, K.M., and Hollingsworth, N.M. (2006). Chemical inactivation of cdc7 kinase in budding yeast results in a reversible arrest that allows efficient cell synchronization prior to meiotic recombination. Genetics *174*, 1767–1774.

Wu, P.-Y.J., and Nurse, P. (2009). Establishing the Program of Origin Firing during S Phase in Fission Yeast. Cell *136*, 852–864.

Wu, P.-Y.J., and Nurse, P. (2014). Replication origin selection regulates the distribution of meiotic recombination. Molecular Cell *53*, 655–662.

ABSTRACT

DNA replication is a highly conserved and regulated step of the cell cycle. Defects in genome duplication have severe consequences for cell proliferation and have been linked to different pathologies, including cancer. Replication initiates at discrete sites along the chromosomes known as origins. For a population of cells, the program of replication is defined by the distribution and activation of origins across the genome. However, cells within the same population display plasticity in origin usage, and the subset of origins activated during S-phase varies from one cell cycle to the next. While changes in the replication program have been observed during development and differentiation as well as in cancer, the functional importance of these alterations remained unknown. Our laboratory previously demonstrated in the fission yeast that the program of origin selection during pre-meiotic S phase regulates the sites of double-strand break (DSB) formation during meiosis, providing the first evidence for the functional consequences of genome-wide changes in origin usage. Building on this work, my thesis takes two approaches to investigate the crosstalk between genome duplication and meiotic recombination, using the fission yeast *Schizosaccharomyces pombe* as a model system.

First, we explored the impact of chromosomal organization on the program of DNA replication and meiotic recombination. To this end, we engineered chromosomal rearrangements that exchange the positions of replication domains with different efficiency and timing characteristics. Our results demonstrated that this induced local changes in origin efficiency near the endpoints of the rearranged region during both mitotic and pre-meiotic S phase. Interestingly, while genome-wide analysis of the DSB profile showed alterations near the rearranged ends, these differences did not reflect the changes in origin usage. This unexpected finding suggests a complex regulation of DSB formation during meiosis that hints at a potential role for chromosomal context in this process.

In addition, we aimed to investigate the steps in DNA replication that are important for promoting DSB formation. Specifically, we focused on evaluating whether the replication machinery must progress through a DSB site before breaks are formed or whether origin activation is sufficient to induce nearby DSBs. For these studies, we constructed and characterized a system for inducing a replication fork barrier during pre-meiotic S phase.

Taken together, my thesis work provides new directions for investigating the interplay between chromosomal organization, DNA replication and meiotic recombination.

Résumé

La réplication de l'ADN est une étape essentielle du cycle cellulaire. Elle permet de dupliquer l'information génétique afin que les deux cellules filles issues de la division cellulaire héritent chacune d'une copie identique du génome. La duplication du génome est contrôlée et régulée de manière spécifique par différents mécanismes conservés au sein des eucaryotes. Un des aspects de ce contrôle est la spécification d'un programme de réplication de l'ADN. Au sein d'une cellule, la synthèse de l'ADN s'initie à partir de sites, appelés origines de réplication, distribués sur l'ensemble du génome. Sur l'ensemble de ces sites potentiels, seule une partie est utilisée à chaque phase S. De plus, cet ensemble varie d'une cellule à une autre ainsi que d'un cycle cellulaire à l'autre. A l'échelle d'une population cellulaire, le programme de réplication est défini par le moment auquel chaque origine est activée ainsi que par la fréquence d'usage de chaque origine dans une population cellulaire, appelée efficacité. Ces propriétés sont modulées par différents paramètres tels que le niveau de nucléotides, les modifications de la chromatine, la transcription génique ou encore la régulation du cycle cellulaire, suggérant que l'activation des origines de réplication est fortement régulée. Bien que des altérations du programme de réplication aient été observées dans les cellules souches embryonnaires de souris en différentiation, durant le développement chez le Xénope et la Drosophile ainsi que dans les cellules cancéreuses, l'importance de ces changements sur les fonctions cellulaires reste peu caractérisée.

Dans le but d'en savoir plus sur ce dernier point, des travaux effectués sur la levure de fission *Schizosaccharomyces pombe* ont cherché à déterminer si la réplication a des fonctions importantes durant la méiose. La méiose est une division cellulaire spéciale qui génère quatre gamètes pour la reproduction sexuée et dont les mécanismes sont conservés chez les eucaryotes. Durant ce procédé, la réplication de l'ADN pré-méiotique est suivie par la formation de cassures double brin de celui-ci. La réparation de ces cassures résulte en un échange du matériel génétique entre les chromosomes homologues, ce qui promeut la diversité génomique. Bien que chez la levure de fission, le programme de réplication mitotique soit très similaire au

programme de réplication méiotique lorsque ceux-ci sont effectués en milieu de culture riche en nutriments, des études ont montré que ce dernier change significativement lorsque la méiose est effectuée dans un milieu pauvre en nutriments. En prenant avantage de ces différences, ces études ont montré que le changement du programme de réplication pré-méiotique entre les conditions de cultures riches et pauvres en nutriments, correspondait à des changements dans la génération des cassures doubles brins dans le génome. Plus précisément, Wu et Nurse en 2014 ont observé que les régions du génome montrant une augmentation de l'usage des origines de réplication présentent aussi une augmentation des cassures doubles brins de l'ADN. Par conséquent, ces résultats montrent pour la première fois qu'un changement du programme de réplication à l'échelle du génome a des conséquences sur les fonctions cellulaires. Ainsi, il est possible que l'environnement chromatinien ou encore le contexte chromosomique puissent être des acteurs clef dans la sélection des origines de réplication et la distribution des cassures doubles brins de l'ADN.

Pertinentes pour notre hypothèse, de nombreuses études récentes montrent que le génome est organisé en domaines de régulation. Par exemple, chez les eucaryotes, il a été montré l'existence de régions de l'ADN qui se dupliquent à des temps précis durant la phase S. De plus il a été aussi montré que la réplication de l'ADN est spatio-temporellement organisée au sein du noyau, avec les régions qui se dupliquent au même moment, localisées les unes à coté des autres. Enfin, des travaux effectués sur la levure de fission montrent que l'insertion d'une origine de forte efficacité dans une région de faible activité baisse son activité. Ainsi, ces travaux suggèrent que l'environnement chromatinien et le contexte chromosomique joueraient un rôle dans la sélection des origines durant la phase S. Basés sur ces résultats, mes travaux de thèse visent à comprendre le lien existant entre la réplication du génome et la recombinaison méiotique via deux approches.

Dans un premier temps, nous avons exploré l'impact de l'organisation chromosomique sur la réplication de l'ADN et la recombinaison méiotique. Pour cela nous avons généré des réarrangements chromosomiques qui échangent les positions de domaines de réplication possédant différents efficacités et timing de réplication en utilisant la technique Cre-Lox. En utilisant cette approche nous avons pu déplacer de

larges régions contenant des domaines de réplication et ainsi conserver les caractéristiques des origines et les régions régulatrices qui les entourent, pouvant être importantes pour une activation correcte de ces dernières. Nous avons inséré des sites LoxP dans le génome de *S. pombe* afin de générer des inversions chromosomiques sur le chromosome I et sur le chromosome II. L'insertion a été faite de sorte à positionner une région de faible efficacité à coté d'une région de forte efficacité après recombinaison induite via l'expression de la Cre-recombinase. Les réarrangements chromosomiques générés nous ont permis d'étudier l'effet que peut avoir une altération du contexte chromosomique sur l'utilisation des origines de réplication durant la mitose et la méiose ainsi que la génération de cassures doubles brins durant la méiose. En utilisant une puce à ADN afin de déterminer le programme de réplication mitotique et pré-méiotique, nos analyses montrent des résultats similaires. Dans les deux cas, nous avons observé que ces réarrangements induisaient des changements de l'efficacité des origines situés spécifiquement de part et d'autre des extrémités des régions réarrangées. Une explication possible à ce phénomène serait que le nouvel environnement chromatinien dans lequel ces origines se trouvent, pourrait jouer un rôle dans l'activation ou la répression de ces régions. Par exemple, une région hétérochromatique (origines inefficaces) mise à coté d'une région efficace pourrait rendre cette dernière plus réfractaire à l'initiation de la réplication. Alternativement, ces changements pourraient être dus à une désorganisation de régions associées topologiquement.

Nous avons, par la suite, analysé la distribution des cassures doubles brins de l'ADN généré sur l'ensemble du génome suite à la réplication pré-méiotique. En nous appuyant sur les travaux de Wu et Nurse en 2014, nous nous attendions à observer des changements dans la formation des cassures doubles brins reflétant les changements de l'efficacité des origine dans la même région. L'immumoprécipitation de la protéine de recombinaison Rad51 suivie d'une analyse sur puce à ADN (ChIP-on-Chip) a montré des changements dans la formation des cassures doubles brins localisés aux extrémités de la région réarrangée. Toutefois, contrairement à nos attentes, ces changement ne reflètent pas les changements du programme de réplication. Ces résultats inattendus suggèrent que le contrôle des cassures doubles brins de l'ADN durant la méiose est régulé de manière complexe et que le contexte chromosomique pourrait jouer un rôle dans ce procédé. De plus il est possible que le

changement de l'efficacité de quelques origines ne serait pas suffisant pour induire des changements correspondants dans la génération des cassures doubles brins.

En parallèle, nous nous sommes intéressés à déterminer quelles étaient les étapes importantes de la réplication de l'ADN pour la formation des cassures doubles brins. Du fait du lien existant entre la réplication et la recombinaison, nous nous sommes spécifiquement concentrés à déterminer si la machinerie de réplication doit passer par un site de cassure avant que celle-ci soit faite ou si l'initiation de la réplication est suffisante pour induire les cassures doubles brins adjacentes. Pour cela nous avons construit un système dans lequel il est possible d'induire une barrière de réplication durant la phase S de méiose appelée RTS1. Cette séquence, présente naturellement dans le génome de *S. pombe*, exerce sa fonction de barrière lorsqu'elle est liée à la protéine RTF1. Ainsi, en mettant la séquence codante de RTF1 sous le contrôle d'un promoteur inductible, il est possible d'induire une barrière de réplication spécifiquement à l'endroit où la séquence RTS1 est insérée. Nous avons caractérisé ce système et avons déterminé que l'ARN d'Rtf1 était produit indépendamment de son induction durant la méiose et reste présent durant cette dernière. Toutefois, la protéine RTF1 est présente en faible quantité, ce qui ne semble pas être suffisant pour induire le blocage de la machinerie de réplication sur le site RTS1. Notre système reste encore à être optimisé pour être fonctionnel. Notamment, nous étudions la possibilité d'induire Rtf1 via un autre promoteur que celui utilisé jusqu'alors. Une fois optimisé, il sera possible de déterminer l'implication de la réplication dans la formation des cassures doubles brins.

Ces deux approches complémentaires permettront de comprendre l'interaction existant entre la réplication du génome et la recombinaison méiotique. Toutefois, ces études utilisent une population cellulaire pour répondre à ces questions. Dans le futur, il serait intéressant de déterminer comment la réplication et la recombinaison sont couplées en analysant la coordination existant au niveau d'une seule molécule d'ADN.